MECHANISMS AND ENERGETICS OF ALKANE ACTIVATION

BY TRANSITION METAL IONS IN THE GAS PHASE

Thesis by

Margaret A. Tolbert

In Partial Fulfillment of the Requirements

for the Degree of

Doctor of Philosophy

California Institute of Technology

Pasadena, California

1986

(Submitted Dec. 23, 1985)

TO MY PARENTS

ACKNOWLEDGMENTS

The work presented in this thesis would not have been possible without the help of many people. I especially thank my research advisor, Jack Beauchamp, for his constant encouragement and support. I have benefited greatly from his vast chemical knowledge and intuition.

I also thank the past and present members of the Beauchamp group for their help and fellowship. I am grateful to Mary Mandich for introducing me to the ion-beam machine used in this work. I am also lucky to have worked with Bruce Schilling. Bruce provided moral support, a helpful hand and was always available to discuss the theoretical aspects of this work. I was fortunate in sharing my office with a group of diverse and interesting personalities. Maureen Hanratty, Gary Kruppa, Dave Dearden and Heonin Kang were always available for conversation, coffee and assistance. Thanks also go to the members of the Janda group for their friendship, especially Sally Hair.

I would also like to thank the staff of the Caltech shops, particularly Tom Dunn, Tony Stark and Guy Duremberg. The support that they provided was invaluable. Roberta Penska deserves thanks for typing portions of this thesis.

Above all, I thank my family for the support and encouragement they have given me. I especially thank my husband, Steve, for his constant help, support and cheerful assistance during the course of this work.

ABSTRACT

The mechanisms and energetics of alkane activation by transition metal ions in the gas phase are studied using an ion beam apparatus. These investigations concentrate on the reactivity of several early first row transition metal ions (Sc^+, Ti^+, V^+) and the second row group 8-10 metal ions (Ru^+, Rh^+, Pd^+). The reaction mechanisms are probed using deuterium labelled alkanes. Experimental and theoretical metal-ligand bond dissociation energies are used to help interpret the observed metal ion reactivities.

Chapter II provides a detailed study of the reactions of Ru^+, Rh^+ and Pd^+ with alkanes. The reactivity observed is contrasted to that of their first row congeners Fe^+, Co^+ and Ni^+.

Chapter III presents a determination of the heterolytic, M^+-H^-, and homolytic, M-H, bond dissociation energies for the first and second row group 8-10 metals. A correlation is found between the homolytic bond energies and the metal atom promotion energy to a state derived from an s^1d^n electronic configuration.

Chapter IV examines the reactions of Ti^+ and V^+ with alkanes and deuterium labelled alkanes. Dehydrogenation mechanisms and deuterium isotope effects are explored.

Chapter V reports the unusual reactivity of Sc^+ with alkanes. The ability of Sc^+ to form two strong metal-ligand sigma bonds results in alkane activation processes which are not observed for most other transition metal ions.

TABLE OF CONTENTS

CHAPTER I

INTRODUCTION

Recent studies have shown that transition metal ions in the gas phase can activate the C-H and C-C bonds of saturated hydrocarbons.[1-6] The complex mechanisms of alkane activation have been studied using a variety of complementary techniques. These include labelling studies,[1c,3,4] product structural analysis using collision-induced dissociation,[7-9] and measurements of kinetic energy release distributions.[10] The bulk of this previous work has centered on the reactions of the first row group 8-10 metal ions. From these studies, a picture of hydrocarbon activation at Fe^+, Co^+ and Ni^+ centers is emerging. In the present work, the activation of alkanes by early first row and group 8-10 second row transition metal ions are investigated using an ion beam apparatus. These studies extend our understanding of alkane activation at a variety of first and second row transition metal centers.

In Chapter II, the reactions of the second row metal ions Ru^+, Rh^+ and Pd^+ with alkanes are reported. Deuterium labelled alkanes are used to help unravel the complicated reaction mechanisms. The reactivity observed for Ru^+ and Rh^+ is vastly different than for the corresponding first row metal ions Fe^+ and Co^+. Whereas competitive C-C bond insertions and/or B-alkyl transfers occur at Fe^+ and Co^+ centers, the corresponding processes do <u>not</u> occur competitively for Ru^+ and Rh^+. These differences are explained in terms of the electronic configurations of the metal ions and the orbitals used for bonding to the metal ions. The uniquely high Lewis acidity of Pd^+ is proposed to account for the distinct reactivity observed

in the reactions of this metal ion with alkanes.

The ability to understand and ultimately predict metal reactivity at carbon-hydrogen bonds is based on the knowledge of M-H and M-alkyl bond strengths. The ionic bond strengths $D(M^+-H)$ and $D(M^+-CH_3)$ have been reported previously for a number of metal ions.[11-13] In Chapter III, the homolytic bond energies, $D(M-H)$, and the heterolytic bond energies, $D(M^+-H^-)$, are reported for the first and second row group 8-10 metals. Knowledge of these bond dissociation energies is important for an understanding of the reactivity observed at transition metal centers. With the exception of PdH, a correlation is found between the homolytic metal hydrogen bond energies and the promotion energy necessary to excite the metal atom to a state derived from an s^1d^n configuration. This suggests that the bonding in the metal hydrides utilizes a metal orbital that is predominantly s-like in character. The lack of correlation observed for PdH is proposed to be due to participation of d electrons in the bonding due to the stable d^{10} configuration of ground state Pd.

Recent condensed phase studies of bond activation at early transition metal centers have revealed a rich chemistry associated with these metals.[14-16] In Chapter IV, the reactions of the early transition metal ions Ti^+ and V^+ with alkanes and deuterium labelled alkanes are presented. The reactivity of these metal ions is much more similar to the reactivity of Ru^+ and Rh^+ than to the other first row transition metal ions. There are important differences, however, in the reactions of V^+. These are exemplified by the observation of large deuterium

isotope effects in the reactions of V^+ with alkanes. The reactivity of Ti^+ and V^+ are interpreted from an examination of the bonding to these metal ions.

In Chapter V, the gas phase reactivity of Sc^+ is reported. The reaction of Sc^+ with n-butane and larger alkanes results in the abundant formation of products of the general form $Sc(C_nH_{2n+2})^+$. It is postulated that these products, which are not observed in abundance for any other metal ion studied to date, are dialkylscandium ions. The unique reactivity observed for Sc^+ is proposed to be a result of the formation of two strong sigma bonds to the metal center. The electronic configuration of ground state Sc^+, s^1d^1, is ideally suited to the formation of two strong sigma bonds with only a minimal loss of electron exchange energy.

Selected References

1. (a) Halle, L. F.; Armentrout, P. B.; Beauchamp, J. L.
    <u>Organometallics</u> **1982**, <u>1</u>, 963.

    (b) Armentrout, P. B.; Beauchamp, J. L. <u>J. Am. Chem. Soc.</u>
    1981, <u>103</u>, 784.

    (c) Houriet, R.; Halle, L. F.; Beauchamp, J. L.
    <u>Organometallics</u> **1983**, <u>2</u>, 1818.

2. Jacobson, D. B.; Freiser, B. S. <u>J. Am. Chem. Soc.</u> **1983**, <u>105</u>,
    5197.

3. Halle, L. F.; Houriet, R.; Kappes, M. M.; Staley, R. H.;
    Beauchamp, J. L. <u>J. Am. Chem. Soc.</u> **1982**, <u>104</u>, 6293.

4. Tolbert, M. A.; Beauchamp, J. L. <u>J. Am. Chem. Soc.</u> **1984**, <u>106</u>,
    8117.

5. (a) Byrd, G. D.; Freiser, B. S. <u>J. Am. Chem. Soc.</u> **1982**, <u>104</u>,
    5944.

    (b) Byrd, G. D.; Burnier, R. C.; Freiser, B. S. <u>J. Am. Chem.
    Soc.</u> **1982**, <u>104</u>, 3565.

6. Allison, J.; Freas, R. B.; Ridge, D. P. <u>J. Am. Chem. Soc.</u>
    1979, <u>101</u>, 1332.

7. Jacobson, D. B.; Freiser, B. S. <u>J. Am. Chem. Soc.</u> **1983**, <u>105</u>,
    736.

8. Larson, B. S.; Ridge, D. P. <u>J. Am. Chem. Soc.</u> **1984**, <u>106</u>,
    1912.

9. Peake, D. A.; Gross, M. L.; Ridge, D. P. <u>J. Am. Chem. Soc.</u>
    1984, <u>106</u>, 4307.

10. Hanratty, M. A.; Beauchamp, J. L.; Illies, A. J.; Bowers, M.
    T. <u>J. Am. Chem. Soc.</u> **1985**, <u>107</u>, 1788.

11. Armentrout, P. B.; Halle, L. F.; Beauchamp, J. L. <u>J. Am.
    Chem. Soc.</u> **1981**, <u>103</u>, 6501.

12. Mandich, M. L.; Halle, L. F.; Beauchamp, J. L. <u>J. Am. Chem.
    Soc.</u> **1984**, <u>106</u>, 4403.

13. Elkind, J. L.; Ervin, K. M.; Aristov, N.; Armentrout, P. B.,
    submitted.

14. McAlister, D. R.; Erwin, D. K.; Bercaw, J. E. <u>J. Am Chem. Soc.</u> **1978**, <u>100</u>, 5966.

15. McDade, C.; Green, J. C.; Bercaw, J. E. <u>Organometallics</u> **1982**, <u>1</u>, 1629.

16. Thompson, M. E.; Bercaw, J. E.; <u>Pure Appl. Chem.</u> **1984**, <u>56</u>, 1.

CHAPTER II

ACTIVATION OF ALKANES BY RUTHENIUM,
RHODIUM AND PALLADIUM IONS IN THE GAS PHASE:
STRIKING DIFFERENCES IN REACTIVITY
OF FIRST AND SECOND ROW METAL IONS

ACTIVATION OF ALKANES BY RUTHENIUM,
RHODIUM AND PALLADIUM IONS IN THE GAS PHASE:
STRIKING DIFFERENCES IN REACTIVITY
OF FIRST AND SECOND ROW METAL IONS

M.A. Tolbert, M.L. Mandich, L.F. Halle and J.L. Beauchamp

ABSTRACT

The reactions of Ru^+, Rh^+ and Pd^+ with alkanes are studied in the gas phase using an ion beam apparatus. The reactivity of the second row group 8-10 metal ions is shown to be dramatically different than that of their first row congeners. Studies with deuterium labelled alkanes reveal that Ru^+, Rh^+, and Pd^+ all dehydrogenate alkanes by a 1,2-mechamism, in contrast to the 1,4-mechansim of Co^+ and Ni^+ and the combination of 1,2- and 1,4-processes for Fe^+. In most respects, Ru^+ and Rh^+ exhibit similar reactivity quite distinct from that observed for Pd^+. The reactions of Ru^+ and Rh^+ are dominated by the loss of one or more molecules of hydrogen, via mechanisms characterized by C-H bond insertions and β-H transfers. In contrast to the reactions of their first row congeners, neither β-methyl transfers or C-C bond insertions occur competitively at Ru^+ and Rh^+ centers. Furthermore, evidence is presented which indicates that the barriers for reductive elimination of H_2 and HR from Rh-olefin$^+$ complexes are much smaller than the corresponding barriers for the first row group 8-10 metal ions. These low barriers may result in the formation of internally excited products able to undergo a second exothermic elimination reaction. The differences in reactivity of the first and second row group 8 and 9 metal ions are proposed to be due to differences in the sizes and shapes of the orbitals used for bonding. Although the reactivity of Pd^+ appears in some ways to be quite similar to that of Ni^+, the mechanism by which alkanes are activated by Pd^+

may be quite different than for any of the first row metal ions. It is proposed that the uniquely high Lewis acidity of Pd$^+$ results in hydride abstraction as a first step in the mechanism for C-H bond activation, leaving the hydrocarbon fragment with an appreciable amount of carbonium ion character in the reaction intermediate. This mechanism is supported by the fact that Pd$^+$ dehydrogenates n-butane by a 1,2-elimination across the central C-C bond exclusively. Palladium is the only metal ion studied to date which undergoes this selective elimination.

Introduction

The determination of the mechanism by which alkanes are activated by transition metal ions in the gas phase is an intriguing and challenging problem. The reaction mechanisms are necessarily complex, multistep processes. Furthermore, the reactions often result in the formation of many products. Fundamental for understanding the mechanisms of these reactions is a knowledge of the activation parameters for competing processes. What factors control C-C versus C-H bond insertion? What determines the relative rates for β-hydrogen versus β-alkyl transfers?

Clues to the puzzle of hydrocarbon activation by transition metal ions have been obtained from studies using a variety of complementary techniques. The studies to date include the reactions of the entire first row transition metal series and several metal ions in the second row series.[1-6] Ion beam and ion cyclotron resonance (ICR) techniques have been used sucessfully to identify the products of these reactions and to obtain thermochemical information. In addition, recent studies of product translational energy release distributions have probed the potential energy surfaces for elimination of H_2 and small hydrocarbons from ionic iron, cobalt and nickel complexes.[7,8] By the use of these complementary techniques, a more complete picture of hydrocarbon activation processes is emerging.

In this paper, we describe the reactions of three second row metal ions, Ru^+, Rh^+ and Pd^+, with saturated hydrocarbons in the gas phase. We find that the reactivity of these metal ions is dramatically different than that of their first row congeners. From an understanding of these differences, we gain a better understanding of hydrocarbon activation by first row as well as second row transition metal ions.

The first step in a comparison of the differences between the first and second row metal ions has been made in previous studies of the binding energies of H and CH_3 to transition metal ions.[1b,9-11] These results are presented in Table 1 for the first and second row group 8-10 metal ions. Also included in this table are recently determined heterolytic M^+-H^- bond energies.[12,13] These bond dissociation energies are useful to interpret mechanistic differences in comparing the reactivity of first and second row transition metal ions with alkanes.

Experimental

The ion beam apparatus used in the present study has been described previously.[14] Briefly, ion beams of Ru^+, Rh^+, and Pd^+ are produced by vaporization of $Ru(CO)_{12}$, $[Rh(CO)_2Cl]_2$ and $PdCl_2$(anhy) onto a hot rhenium filament, and subsequent surface ionization at 2500 K. In this experimental arrangement, electronically excited ions are less than 1% of the total ion abundance for Ru^+, Rh^+, and Pd^+.[11] The metal ions are collimated, mass and energy selected, and focussed into a collision chamber containing the neutral reactant at ambient temperature. Product ions scattered in the forward direction are

Table 1: Homolytic and Heterolytic Bond Dissociation Energies for Group 8-10 Transition Metal Ions in the Gas Phase.

|	Bond Dissociation Energy (kcal/mol)					
	Fe	Co	Ni	Ru	Rh	Pd
M^+-H	53.[a]	48.[a]	39.[a]	41.[b]	42.[b]	45.[b]
M^+-CH_3	68.[b]	61.[c]	48.[c]	54.[b]	47.[b]	59.[b]
M^+-H^-	208.[d]	218.[d]	224.[d]	208.[d]	214.[d]	231.[d]

[a]Reference 10.

[b]Reference 11.

[c]Reference 32.

[d]Reference 13.

analyzed using a quadrupole mass spectrometer.

The exothermic reactions of Rh-(olefin)$^+$ complexes were studied using the above apparatus equipped with a dual inlet system which allowed independent addition of two reagent gases. Rhodium ethylene and propylene complexes were formed by reaction with ethane and propane as indicated in Equations 1 and 2,

$$Rh^+ + C_2H_6 \longrightarrow Rh(C_2H_4)^+ + H_2 \qquad (1)$$

$$Rh^+ + C_3H_8 \longrightarrow Rh(C_3H_6)^+ + H_2 \qquad (2)$$
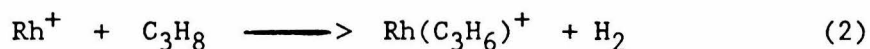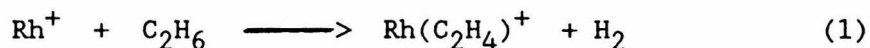
respectively. Loss of H_2 is the only exothermic process observed in these reactions. Further reactions of the olefin complexes were studied by adding an equal pressure of a second reactant gas to the collision chamber, and observing the new products formed. The total pressure of reagent gas was held constant at 4 mtorr. Under these conditions, most of the rhodium ions suffer approximately 2 collisions. If the first collision results in the exothermic formation of Rh(olefin)$^+$, a second collision may result in further reaction of the metal olefin complex. In order to observe only exothermic reactions, the relative kinetic energy used in these experiments was quite low, < 0.25 eV.

Labelled ethane (1,1,1-d_3, 98 % D), propane (2,2-d_2, 98 %D), n-butane (1,1,1,4,4,4-d_6, 98 %D), and 2-methylpropane(2-d_1, 98 %D) were obtained from Merck, Sharp and Dohme.

Results

The second row group 8, 9 and 10 metal ions are all observed to react with alkanes resulting in a wide variety of products.

As an example, consider the reaction of Rh^+ with n-butane. The reaction cross sections as a function of relative kinetic energy are shown in Figure 1. The exothermic products are easily identified since their reaction cross sections decrease with increasing relative kinetic energy as indicated in Figure 1a. The results of reacting Co^+ with n-butane are illustrated in Figure 2 for comparison.[1a] It can be seen that there are significant differences in product distributions and their variation with translational energy in the reactions of Co^+ and Rh^+ with n-butane. Whereas Co^+ reacts to form three exothermic products corresponding to loss of H_2, CH_4, and C_2H_6, only hydrogen loss products are observed as exothermic reactions for Rh^+. The alkane loss channels for Rh^+ appear to have translational energy thresholds, as indicated in Figure 1b.

Product distributions and overall cross sections for the reactions of alkanes with Ru^+, Rh^+, and Pd^+ at a relative kinetic energy of 0.5 ev are given in Table 2. Also included in this table are previous ICR results for the exothermic reactions of Rh^+ with alkanes.[5] It can be seen that, although the results of the ion beam experiment agree fairly well with the ICR data, there are some noteworthy discrepancies in several cases. The ICR experiments utilized rhodium ions that were produced by laser evaporation of a metal target or by electron impact ionization of $(\eta^5\text{-}C_5H_5)Rh(CO)_2$. Electron impact ionization has been shown to produce a distribution of ground and excited state metal ions.[15,16] Recent studies have also shown that metal ions created by laser evaporation are formed with a wide distribution of translational energy and may be electronically excited as well.[17]

Figure 1. Variation in the experimental cross section for the
a) exothermic reactions and b) endothermic reactions of Rh^+
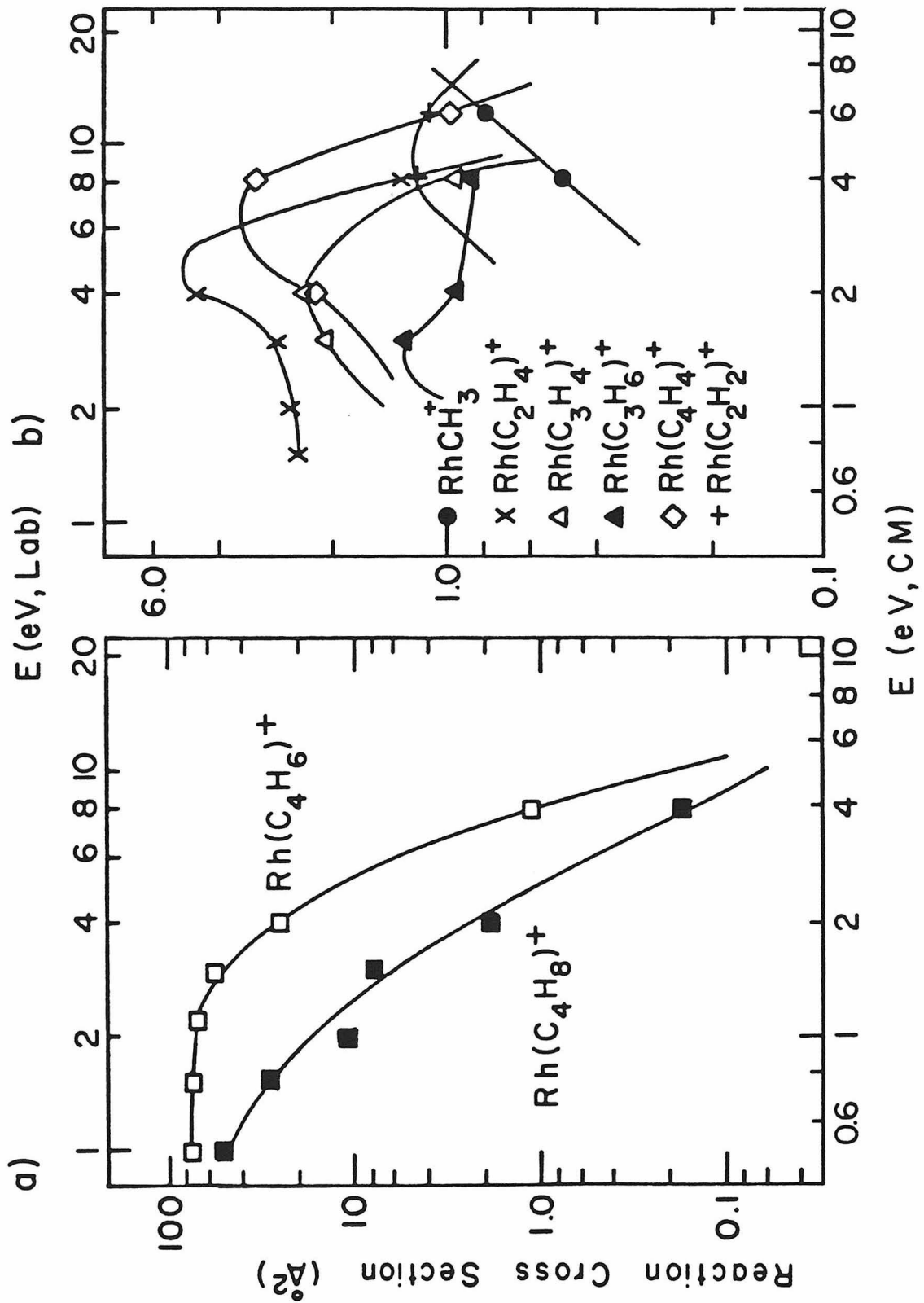with n-butane as a function of relative kinetic energy.

Figure 2. Variation in the experimental cross section for the
a) exothermic reactions and b) endothermic reactions of
Co^+ with n-butane as a function of relative kinetic energy,
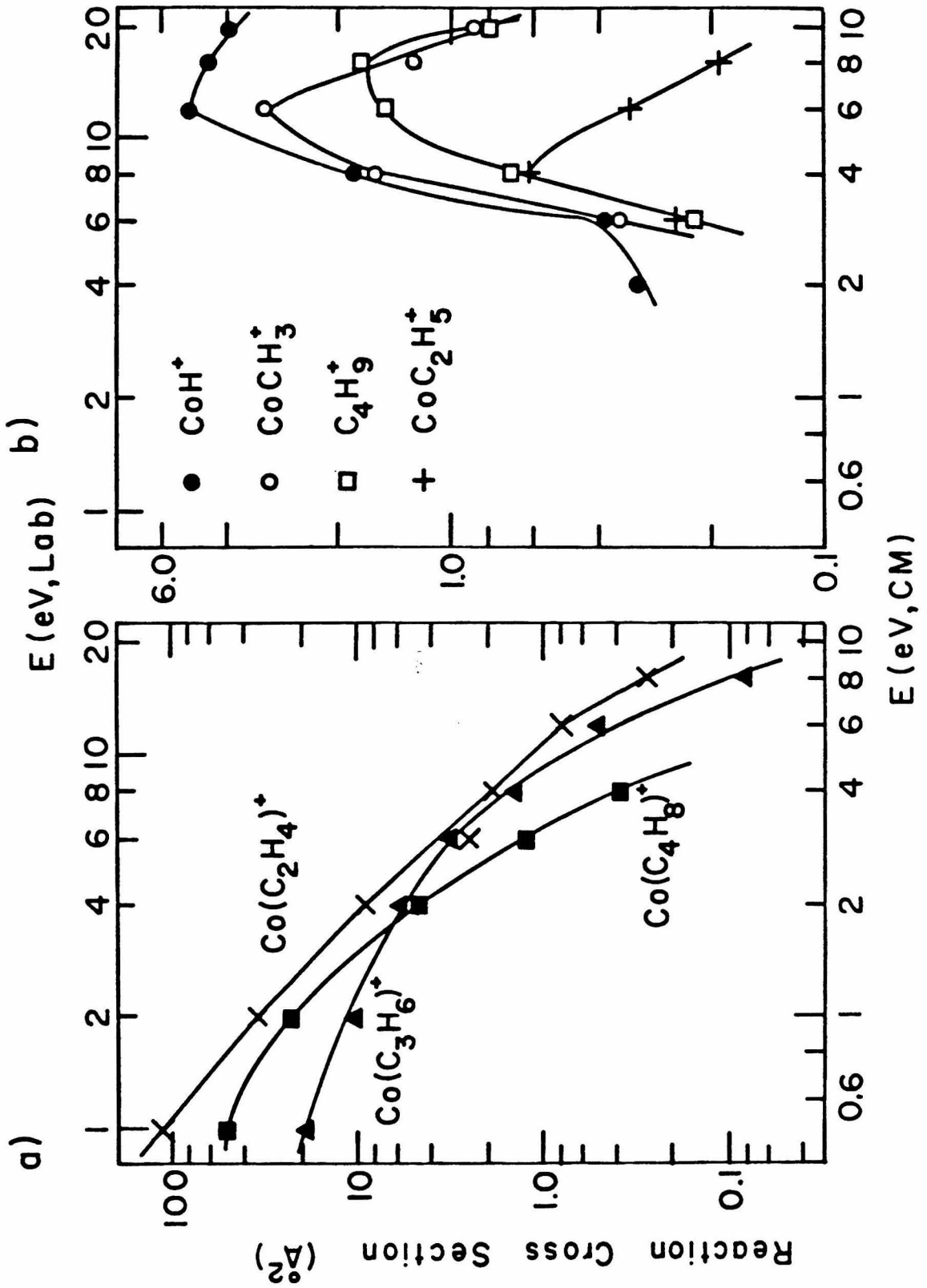Reference 1a.

Table 2: Product Distributions for the reactions of Ru^+, Rh^+, and Pd^+ with Alkanes at a relative kinetic energy of 0.5 ev.[a]

Alkane	Neutral Products	Ru^+	Rh^+			Pd^+
			0.5 ev	2.0 ev	ICR[b]	
CH_4		N.R.	N.R.	N.R.	N.R.	---[c]
C_2H_6	H_2	1.0*	1.0*	1.0*	1.0	N.R.
	Total[d]	10	19	1.0		
C_3H_8	H_2	.90*	.97*	.20*	.94	.54*
	$2H_2$	.10	.03	.67	.06	
	CH_4			.13		.46*
	Total	40	40	8.0		6.3
$n-C_4H_{10}$	H_2	.20*	.27*			.38*
	$2H_2$	.80*	.73*	.88*	1.0	
	CH_4					.21*
	C_2H_6			.12		.41*
	Total	38	48	25		29
$i-C_4H_{10}$	H_2	.73*	.91*	.10*	.43	1.0*
	$2H_2$	.21*	.06	.49	.48	
	CH_4	.02	.01	.08	.09	
	H_2,CH_4	.02	.02	.30		
	C_2H_6	.02		.03		
	Total	95	65	30		110
$neo-C_5H_{12}$	H_2	.22*	.32*	.03*	.15	
	$2H_2$	.05*	.10*	.21*	.29	
	$3H_2$			.05	.02	
	CH_4	.15*	.40*	.14*	.13	1.0*
	CH_4,H_2	.58*	.07*	.34*	.34	
	C_2H_6		.06*	.07*	.05	
	C_2H_6,H_2		.05	.11	.02	
	C_3H_8			.05		
	Total	99	40	29		53

Table 2, continued.

[a]Reaction products which clearly exhibited energy dependent cross sections characteristic of exothermic processes are indicated by an asterisk.

[b]Product distributions for the reactions of Rh^+ reported in earlier ICR study (Reference 5).

[c]Not studied.

[d]Total reaction cross sections, reported in A^2.

From our examination of product distributions as a function of relative kinetic energy, it appears that most of the deviations of our results from earlier ICR measurements can be explained by assuming that the latter results are representative of ion kinetic energies which are much higher than thermal energies. Some reactions observed in the previous ICR study are not observed in the present ion beam experiment at 0.5 ev but are seen at 2.0 ev (Table 2). As an example, the energy dependence of the reactions of Rh^+ with 2-methylpropane are shown in Figure 3. Although the previous study reports three exothermic products (Table 2), our results indicate that only loss of H_2 is exothermic. The other pathways clearly exhibit a translational energy threshold for reaction. The presence of electronically excited ions in the ICR experiment could also contribute to these differences.

Another explanation of the deviation between the ion beam and ICR results may lie in the time scale difference of the two experiments. Inspection of the differences between the two data sets reveals that the major discrepancies involve multiple elimination reactions. Multiple eliminations may be somewhat more prevalent in the ICR due to the longer reaction times (msec), relative to the the reaction times in the present ion beam experiments (usec). However, this is not expected to account for all of the observed differences.

As indicated in Table 2, the main exothermic reactions of Ru^+ and Rh^+ with small alkanes are observed to be single and double dehydrogenations. In contrast, the reaction of Pd^+ with

Figure 3. Variation in the experimental cross section for the reactions
of Rh^+ with 2-methylpropane as a function of relative kinetic
energy.
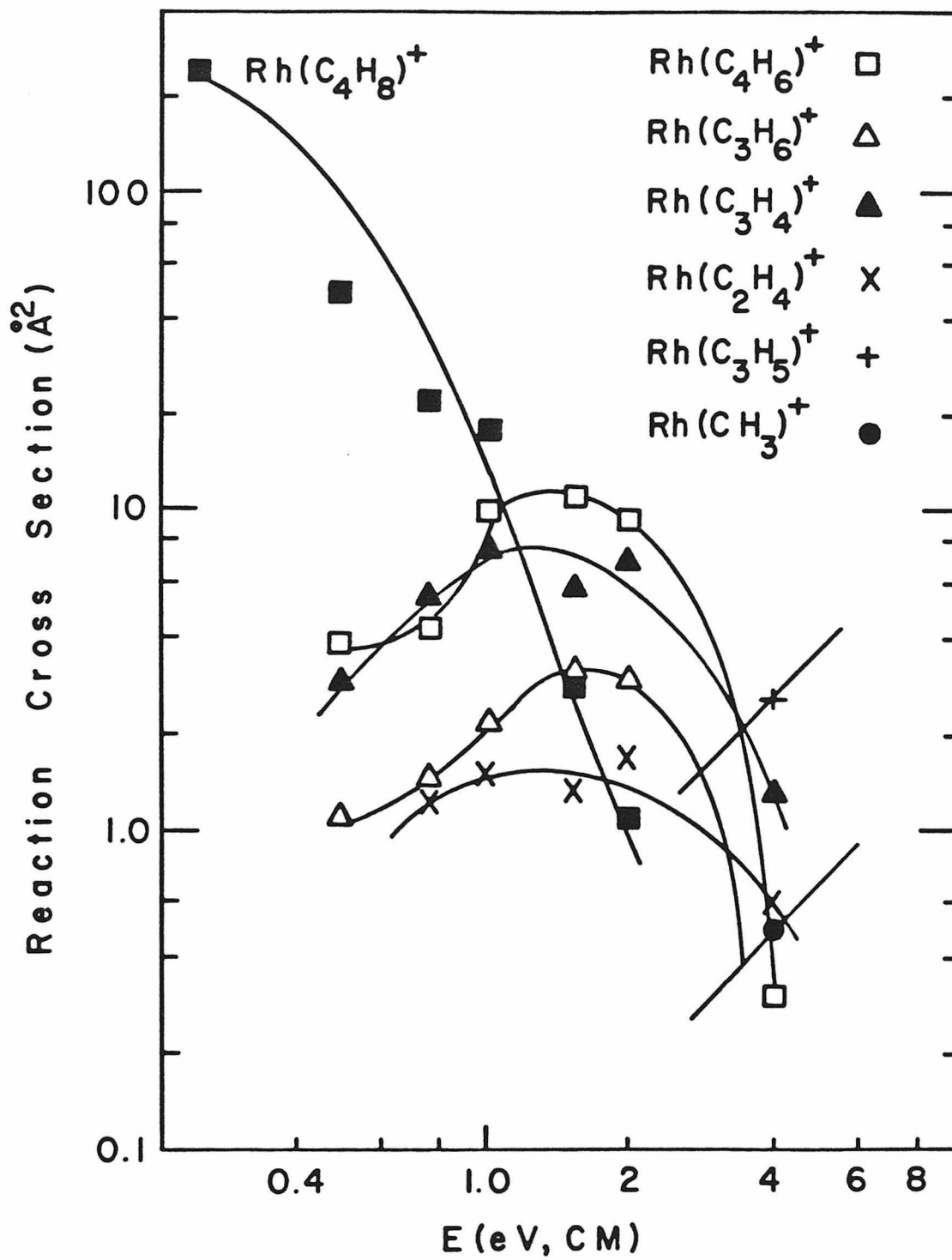
alkanes leads to loss of smaller alkanes in addition to H_2. In order to gain insight into the specific reaction mechanisms, a study of the reactions of Ru^+, Rh^+, and Pd^+ with deuterium labelled alkanes was performed. The results for the exothermic dehydrogenation of labelled alkanes at low kinetic energy are given in Table 3. The alkane loss products formed using labelled alkanes are presented in Table 4.

In addition to reaction products such as those indicated in Tables 1-4, unreacted adduct ions are often observed in the ion beam experiment at low relative kinetic energies. The extent of adduct formation for the first and second row group 8-10 metal ions reacting with alkanes is indicated in Table 5. Although adduct ions are prevalent for Fe^+, Co^+, Ni^+, and Pd^+, no adducts are observed in the reactions of Ru^+ and Rh^+ with alkanes, even at elevated pressures.

In a related experiment aimed at obtaining thermochemical information, the exothermic reactions of Ru^+, Rh^+, and Pd^+ with acetone were studied. The exothermic products formed in these reactions are presented in Table 6. Also included in this table are previous ion beam results for Fe^+, Co^+, and Ni^+.[18] It can be seen that although the product distributions for Pd^+ closely resemble that of the first row ions, two additional reactions, loss of CH_4 and loss of (H_2 + CO),[19] are prevalent for Ru^+ and Rh^+. ICR studies reveal that methane loss was also the dominant process for Rh^+ reacting with acetone (91%).[20]

The fact that all three second row metal ions lose CO in an exothermic process indicates that the sum of the first and second metal-methyl bond energies is greater than 96 kcal/mol.[21] Using

Table 3.   Isotopic Product Distributions for Dehydrogenation of Deuterated Alkanes by Ru^+, Rh^+, and Pd^+.

M^+ Alkane	Neutral Product							
	Single Dehydrogenation			Double Dehydrogenation				
	H_2	HD	D_2	$2H_2$	H_2 +HD	2HD or H_2+D_2	D_2 +HD	$2D_2$
Ru^+								
CH_3CD_3	.15	.73	.12					
$CH_3CD_2CH_3$	.10	.78	.12[a]		.58	.42		
$C(CH_3)_3D$	.20	.80			1.00			
$CD_3CH_2CH_2CD_3$	.20	.46	.34[b]	.09[b]	.30	.38	.17	.06
Rh^+								
CH_3CD_3	.09	.83	.08					
$CH_3CD_2CH_3$	.14	.79	.07		.71[c]	.29[c]		
$C(CH_3)_3D$	.27	.73			1.00			
$CD_3CH_2CH_2CD_3$	.32	.61	.07[a]	.05	.40	.36	.19	
Pd^+								
$CH_3CD_2CH_3$		1.00						
$C(CH_3)_3D$		1.00						
$CD_3CH_2CH_2CD_3$	1.00							

[a]The identity of this product is uncertain due to the identical masses of D_2 and $2H_2$. To make the product distributions best match those in Table 2, all of this mass product was assigned to be loss of D_2.

[b]This product was assigned to be a 50:50 mixture of D_2 and $2H_2$ in order to make the product distributions best match those in Table 2.

[c]Product distribution at a relative kinetic energy of 1.0 ev.

Table 4. Isotopic Product Distributions for Alkane Loss from Deuterated Alkanes by Ru^+, Rh^+, and Pd^+ at a relative kinetic energy of 1.0 ev.

Alkane	Neutral Product	Ru^+	Rh^+	Pd^+
$CH_3CD_2CH_3$	CH_4			1.0^a
$C(CH_3)_3D$	CH_4	1.0	1.0	1.0
	CH_4+H_2	0.5		
	CH_4+HD	0.5	1.0	
$CD_3CH_2CH_2CD_3$	CD_3H			1.0^a
	$C_2H_2D_4$			1.0^a

[a] Product distribution at a relative kinetic energy of 0.5 ev.

Table 5: Adduct formation in the reactions of group 8-10 metal ions with alkanes.[a]

M^+	propane	isobutane	n-butane
Fe[b]	.42	.05	.05
Co[b]	.39	.07	.07
Ni[b]	.25	.09	.06
Ru	0	0	0
Rh	0	0	0
Pd	.35	.23	.57

[a]Fraction of the total product observed, normalized to 1.0, at a relative kinetic energy of 0.5 ev in the center-of-mass frame. The pressure of alkane gas was 1.5 mtorr.

[b]Data from Reference 39.

Table 6: Product Distributions for the Reactions of the Group 8-10 Transition Metal Ions with Acetone at a Relative Kinetic Energy of 0.5 ev.

Neutral Product	Product Distribution					
	Fe^{+a}	Co^{+a}	Ni^{+a}	Ru^+	Rh^+	Pd^+
CO	.07	.10	.06	.15	.03	.07
C_2H_6	.93	.90	.94	.19	.27	.93
CH_4				.58	.60	
H_2+CO				.08	.10	

[a]Reference 18.

previous values for the first metal-methyl bond energies (see Table 1) implies $D(RuCH_3^+-CH_3) > 42$ kcal/mol, $D(RhCH_3^+-CH_3) > 49$ kcal/mol, and $D(PdCH_3^+-CH_3) > 37$ kcal/mol. Observation of exothermic loss of $(H_2 + CO)$ indicates that $D(M-C_2H_4^+) > 38$ kcal/mol for Ru^+ and Rh^+.[22] The lower limits to the bond dissociation energies obtained here will be used to estimate the energies of reaction intermediates discussed later in the paper.

In a somewhat different experiment, sequential reactions of Rh^+ in multiple collisions were studied using different combinations of reactant gases. The goal of these experiments was to determine the reactivity of $Rh-(olefin)^+$ complexes. For example, can $Rh-(olefin)^+$ complexes effect oxidative addition processes similar to those observed for bare rhodium ions? In an attempt to answer this question, the reactions of Rh^+ with a combination of ethane or propane and a reactant gas were studied. The results are indicated in Table 7. It can be seen that, although D_2 and CD_4 do not react with $Rh(C_2H_4)^+$, C_2D_6 reacts to lose H_2, HD and D_2 as exothermic processes. This reaction was also observed with unlabelled ethane in a previous ICR study.[5] The implications of observing this reaction to be exothermic will be discussed later.

In certain cases, the products of the multiple collision reactions could result from two possible reaction sequences. For example, in the reaction of Rh^+ with C_2H_6 and C_2D_6, the product $(C_2H_4)-Rh-(C_2D_4)^+$ could be formed from either $Rh-(C_2H_4)^+$ reacting with C_2D_6 or $Rh-(C_2D_4)^+$ reacting with C_2H_6. In this case, because the primary dehydrogenation products were equally

Table 7: Exothermic reactions of Rh(olefin)$^+$ complexes with small molecules at a relative kinetic energy of ≤ 0.25 ev.

Olefin	Reactant	Hydrogen loss			Ethane loss		
		D_2	HD	H_2	C_2D_5H	$C_2D_4H_2$	$C_2H_4D_2$
Rh-$C_2H_4^+$							
	D_2		N.R.				
	CD_4		N.R.				
	C_2D_6	.41[a]	.46	.13	.50[b]	.37[b]	.13[b]
Rh-$C_3H_6^+$							
	D_2		1.0				
	CH_4		N.R.				
	C_2D_6	.49[c]	.33	.18	.64	.26	.10

[a]The product of this mass, (C_2D_4)-Rh-$(C_2H_4)^+$, could result from the reaction of $RhC_2D_4^+$ with C_2H_6 or from the reaction of $RhC_2H_4^+$ with C_2D_6. Because the primary dehydrogenation peaks are of equal intensity, this product was assigned to be a 50:50 mixture of the two processes.

[b]Three exchange peaks were observed between $RhC_2H_4^+$ (mass=136) and $RhC_2D_4^+$ (mass=140). The double exchange peak (m=138) was assigned to be a 50:50 mixture of exchange from each of the primary dehydrogenation products. The mass 137 peak was assigned to be due primarily (75%) to single exchange from $RhC_2H_4^+$ and only 25% due to triple exchange from $RhC_2D_4^+$. The corresponding assignment was used for the mass 139 peak.

[c]The product of this mass, (C_2D_4)-Rh-$(C_3H_6)^+$, could result from the reaction of either primary olefin. Because the ratio of primary dehdrogenation products favors formation of $RhC_3H_6^+$ by a factor of 3, this secondary reaction product was asigned to be primarily (75%) due to the reaction of $RhC_3H_6^+$ with C_2D_6.

abundant, half of the product in question was estimated to result from each source. There were similar ambiguities in the reactions of Rh$^+$ with C_3H_8 and C_2D_6 simultaneously. The products were assigned based on the relative intensity of the primary olefin products. The secondary reactions presented in Table 5 do not occur for Fe$^+$, Co$^+$ or Ni$^+$.[23] This important difference between the first and second row transition metal ions gives information about the potential energy surfaces which govern the reactions of atomic transition metal ions with saturated hydrocarbons.

Discussion

The reactions of Ru$^+$ and Rh$^+$ with alkanes are fairly similar and are dominated by the loss of one or more molecules of H_2. A comparison of the products formed in the reaction of n-butane with the first and second row group 8-10 metal ions is given in Table 8. It is seen that the reactivity of Ru$^+$ and Rh$^+$ does not resemble that of their first row congeners, Fe$^+$ and Co$^+$. Several questions arise regarding this differential reactivity. First, why does multiple loss of hydrogen occur for Ru$^+$ and Rh$^+$? Second, why are alkane loss channels not prevalent with Ru$^+$ and Rh$^+$? Finally, although all of the metal ions exothermically dehydrogenate alkanes, is the dehydrogenation mechanism the same in all cases? These questions will be addressed below.

In contrast to Ru$^+$ and Rh$^+$, the reactivity of Pd$^+$ appears at first glance to be remarkably similar to the first row metal ions Fe$^+$, Co$^+$, and Ni$^+$ (see Tables 6 and 8). However, the uniquely high Lewis acidity of Pd$^+$ results in distinctive reactivity as

Table 8: Comparison of the Reactions of Group 8-10 Transition Metal Ions with n-Butane at a Relative Kinetic Energy of 0.5 ev.
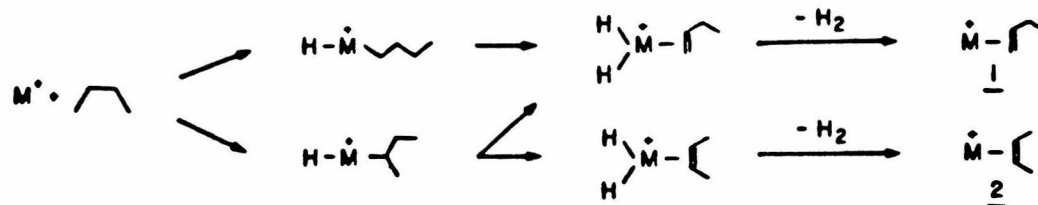
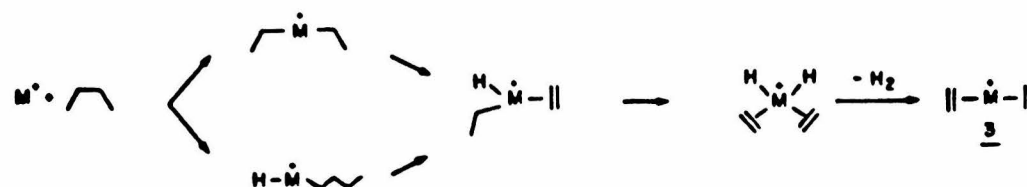| Neutral Product	Product Distribution					
	Fe^{+a}	Co^{+a}	Ni^{+a}	Ru^+	Rh^+	Pd^+
H_2	.20	.29	.48	.20	.27	.38
$2H_2$				.80	.73	
CH_4	.41	.12	.06			.21
C_2H_6	.39	.59	.45			.41

[a]Reference 1c.

discussed below.

Dehydrogenation mechanism for Ru[+] and Rh[+]. Remarkable metal specificity has recently been observed in the dehydrogenation reactions of alkanes by transition metal ions in the gas phase. Studies of product ion structures[2b,3b,7,15,24] in conjunction with experiments involving deuterium labelled n-butane-1,1,1,4,4,4-d_6[1c,4,25] reveal at least three distinct mechanisms. Sc[+] has been shown to undergo a 1,3-dehydrogenation,[4] whereas Co^{+} and Ni^{+} effect 1,4-dehydrogenations forming bis-olefin complexes.[3b,7] Dehydrogenation at Fe^{+} centers appears to occur via a combination of 1,2- and 1,4-mechanisms.[3b,8] These latter two mechanisms are illustrated in Schemes 1 and 2.

Scheme 1

Scheme 2

The product distributions observed for the reactions of Ru^+ and Rh^+ with small labelled alkanes (Table 3) indicates a predominantly 1,2-dehydrogenation mechanism.[26] For example, the main product observed with 2-methylpropane-2d$_1$ is loss of HD. Scrambling leads to the loss of a smaller amount of H_2, a process not observed for the first row metal ions. The presence of scrambled products is consistent with low barriers for β-H transfer for Ru^+ and Rh^+. This will be discussed in more detail later. It is also possible that the scrambled products are actually the result of 1,1-elimination. These two processes cannot be distinguished in this experiment.

The results of the dehydrogenation of n-butane by Ru^+ and Rh^+ are also <u>consistent</u> with a 1,2-mechanism. Arguments presented below against a 1,4-mechanism indirectly support this assignment. The 1,4-mechansim depicted in Scheme 2 involves either initial C-C bond insertion or C-H bond insertion followed by β-ethyl transfer. As will be discussed later, there is evidence that neither exothermic C-C bond insertions or competitive β-alkyl transfers occur at Ru^+ and Rh^+ centers. Furthermore, any elimination mechanims proposed must accomodate the loss of a <u>second</u> H_2 molecule from n-butane, as indicated in Table 2. A 1,2-dehydrogenation mechanism leaves the metal-olefin complex in a geometry favorable for elimination of a second H_2 molecule via allylic hydrogen transfers from <u>1</u> or <u>2</u> as indicated in Scheme 3. However, the product of the 1,4-elimination, a bis-

<u>Scheme 3</u>
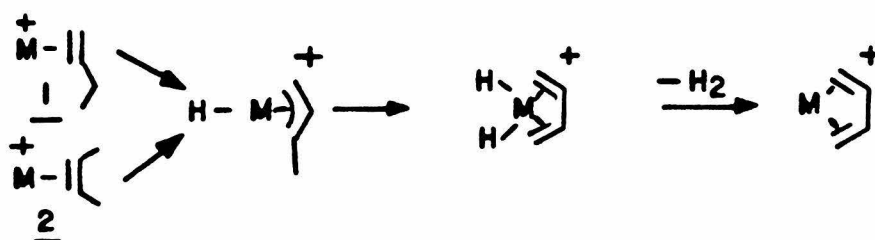
olefin complex $\underline{3}$, may not easily rearrange to eliminate a second molecule of H_2. In ICR experiments, reaction 3 has been

$$Rh(C_2H_4)^+ + C_2H_4 \longrightarrow Rh(C_4H_6)^+ + H_2 \qquad (3)$$
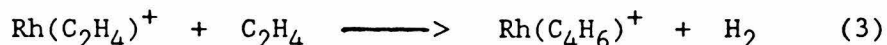
observed to occur very slowly, with a rate of less than 1% of the calculated encounter rate.[27] Because the $Rh(C_2H_4)_2^+$ adduct formed in reaction 3 has <u>at least</u> 12 kcal/mol more internal energy than would $\underline{3}$ formed by reaction with n-butane, it is unlikely that $\underline{3}$ would be able to react to lose H_2 to any significant extent. This evidence against a 1,4-mechanism lends support to the proposed 1,2-dehydrogenation mechanism for Ru^+ and Rh^+.

<u>Observation of multiple hydrogen loss in the reactions of Ru^+ and Rh^+</u>. As indicated in Table 8, Ru^+ and Rh^+ react with n-butane to lose two molecules of H_2, a process that is not observed for the first row transition metal ions as an exothermic reaction. It should be noted that this product does appear with low cross sections at high energy for Co^+ (Figure 2b). The differences in observed reactivity reflect differences in the potential energy surfaces that connect the reactants to the products. Recently, kinetic energy release distributions have been measured for metastable decompositions of Fe^+, Co^+, and Ni^+ adducts with n-butane.[7,8] High translational energy releases were observed for the dehydrogenation reactions, indicating the existence of large activation barriers for the reverse association reactions. The barrier for reductive elimination of alkanes from Co-olefin$^+$ intermediates is not known. However, it

has been suggested that there might be a substantial barrier for this process as well.[7] A simplified potential energy surface indicating these proposed barriers is illustrated in Figure 4, where intermediate $\underline{4}$ can competitively decompose to lose H_2 or C_2H_6. Based on the above observations, reaction 4 should have a

$$M(C_2H_4)^+ + C_2H_6 \longrightarrow M(C_2H_4)_2^+ + H_2 \qquad (4)$$

significant activation barrier for Fe^+, Co^+ and Ni^+. This is supported by the fact that reaction 4 has not been observed for any of the first row group 8-10 metal ions.[23]

The activation parameters which govern the reactions of Rh^+ must be quite different that those observed for Fe^+, Co^+ and Ni^+. As indicated in Table 7, reaction 4 is observed to be an exothermic process for Rh^+. Therefore, this process must occur without a large activation barrier for Rh^+. In fact, there can be essentially no barrier for oxidative addition of R-H at $Rh(C_2H_4)^+$ centers, and a barrier of less than 4 kcal/mol for either β-H transfer from intermediate $\underline{4}$ or reductive-elimination of H_2 from intermediate $\underline{5}$, as indicated in Figure 4. The abundance of scrambled products in reaction 4 using labelled C_2D_6 indicates that the barrier for reversible β-H transfer from $\underline{5}$ is lower than the barrier for H_2 elimination, or that the frequency factor is higher. This is indicated in Figure 4.

Other evidence that the reaction barriers in the potential energy surfaces of the first and second row transition metal ions are vastly different can be obtained from an analysis of the degree to which long-lived adduct ions are formed. As indicated

Figure 4. Qualitative potential energy diagram for the decomposition of $(C_2H_4)MH(C_2H_5)^+$ for M = Rh and Co. The products corresponding to loss of ethane are shown on the left, and those corresponding to loss of H_2 are shown on the right. The bond energies used for calculating the energies of the Co^+ intermediates are given in Reference 7. The bond energies to Rh^+ were estimated to be $D(Rh-C_2H_4)^+ = 43$ kcal/mol, $D(Rh-2C_2H_4)^+ = 86$ kcal/mol, $D(C_2H_4)_2Rh-H_2)^+ = 95$ kcal/mol, and $D(D_2H_4Rh-HR)^+ = 102$ kcal/mol. These bond energies are consistent with the bond energies given in Table 1 and the lower limits discussed in the Results section.
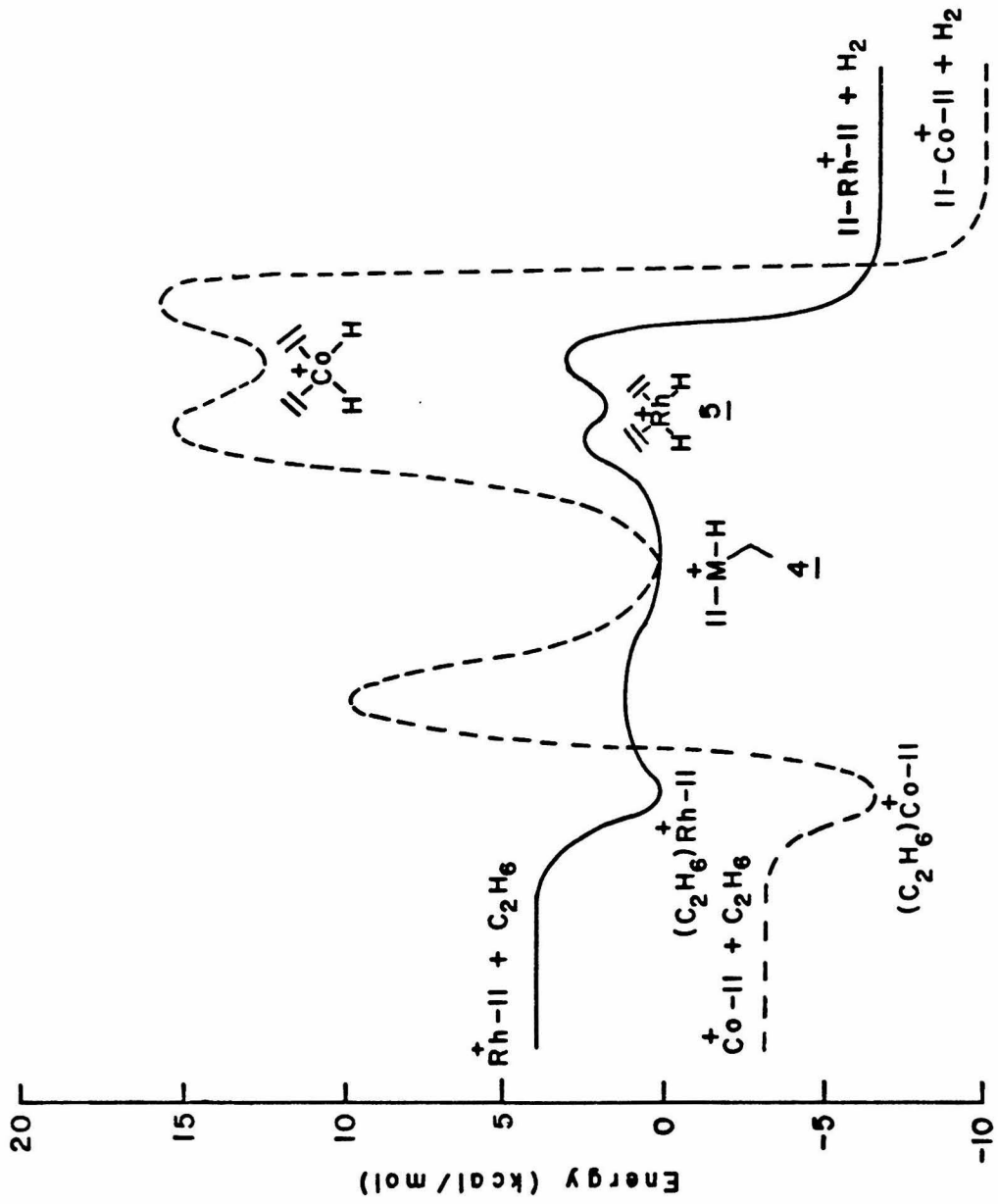
in Table 5, although adduct ions are prevalent for Fe^+, Co^+, Ni^+ and Pd^+, they are not observed for Ru^+ and Rh^+, even at elevated pressures. An example of an adduct formation reaction in the ion beam experiment is indicated in Scheme 4 for the case of a metal

Scheme 4
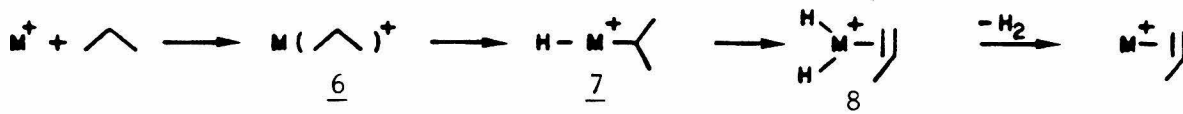
ion reacting with propane. The adduct ion detected can have any of a number of different structures. One possibe structure is the initially formed collision complex, 6, held together by ion-induced dipole interactions. The adduct ion could also be an inserted species such as 7, or a rearranged complex as indicated by 8. Since only the mass of the adduct ion is detected in this experiment, differentiation of these structures is not possible.

The overall rate of adduct decomposition depends on the rates for the various reaction steps in Scheme 4. The relative activation parameters for C-H bond insertion, β-hydrogen transfer and H_2 elimination determine which adduct structure is dominant. At low pressures, if the overall decomposition rate is slow enough ($< 4 \times 10^4$ sec^{-1}), then the internally excited adducts will be detected directly. At high pressures, if the adduct decomposition rate is slow enough ($< 10^6$ sec^{-1}), the adducts may live long enough to suffer a second stabilizing collision. In this case, adducts sufficiently cooled will be detected. For

overall reaction rates $> 10^7$ sec^{-1}, it is unlikely that any adduct would be detected, even at elevated pressures. The fact that no adducts are observed for Ru$^+$ and Rh$^+$ reactions thus indicates faster reaction rates than observed for their first row congeners. This is consistent with the very small β-H transfer and reductive elimination barriers proposed above for Ru$^+$ and Rh$^+$.

The implications of low H$_2$ elimination barriers for the potential energy surfaces of Ru$^+$ and Rh$^+$ reactions can be seen in the dehydrogenation reaction of n-butane. As discussed above, Ru$^+$ and Rh$^+$ appear to dehydrogenate n-butane by a 1,2-elimination mechanism. As discussed in Reference 7, if no energy redistribution occurs after the transition state for dehydrogenation ("late barrier"), then the entire reverse activation barrier will appear as product translation. The remainder of the available energy will be partitioned statistically between the reaction coordinate and all other internal degrees of freedom.

In accord with the low barrier for reductive elimination of H$_2$ from $\underline{5}$ (Figure 4), the elimination of H$_2$ to form $\underline{1}$ or $\underline{2}$ (Scheme 1) is expected to proceed without a large barrier. Therefore, it is expected that the dehydrogenation products be formed with relatively low translational energy, and thus relatively high internal energy. The high internal excitation of Rh(C$_4$H$_8$)$^+$ may result in the occurrence of a subsequent reaction, i.e., loss of a second molecule of H$_2$.

Absence of alkane loss products for Ru^+ and Rh^+. As
indicated in Figure 3, the only clearly exothermic product
observed in the reaction of Rh^+ with 2-methylpropane is H_2 loss.
Although loss of CH_4 is the thermochemically preferred product,[28]
it is not observed at low energy and becomes prominent only at
relative kinetic energies in the range 1-2 ev. Two mechanisms
have been proposed previously for the loss of CH_4 from 2-
methylpropane in the reaction with Fe^+, Co^+, and Ni^+.[1b] One
involves insertion of the metal ion into a C-C bond, followed by
β-H transfer and subsequent reductive elimination of CH_4.
Alternatively, insertion into a C-H bond can be followed by β-
methyl transfer and elimination of CH_4. The lack of alkane loss
processes for Ru^+ and Rh^+ indicates that neither of the above
processes occurs for these metal ions.

This difference in reactivity between the first and second
row metal ions may be attributed to differences in any of three
steps: 1) initial insertion into a C-C versus C-H bond 2) β-H
transfer versus β-alkyl transfer and 3) reductive elimination of
HR versus reversible β-H transfers. As discussed previously, the
barrier for reductive elimination of HR from $Rh(olefin)^+$
complexes is very small. Therefore, it is unlikely that the lack
of alkane loss observed for Ru^+ and Rh^+ is a result of non-
competitive HR elimination. Furthermore, β-hydrogen transfers
are thought to be facile for Rh^+ (Figure 4). Therefore, an
activation barrier or an extremely low frequency factor for
carbon-carbon bond insertion by Ru^+ and Rh^+ is postulated.
Hydrogen loss products are observed in abundance for Ru^+ and Rh^+
reacting with alkanes. The first step in these processes is most

certainly exothermic C-H bond insertion. Therefore, the activation barrier for β-methyl transfer must be much higher than for β-hydrogen transfer, or the frequency factor much lower. This renders β-methyl transfer unable to compete with β-hydrogen transfer and results in the observation of only H_2 loss products.

An important exception is the loss of CH_4 observed in the reaction of 2,2-dimethylpropane with Ru^+ and Rh^+. In fact, loss of CH_4 is the major exothermic reaction observed at low energy for Rh^+. This is consistent with the above ideas in that, after C-H insertion, no β-H's are available, which then permits competitive transfers of less favorable groups such as CH_3. Furthermore, once β-methyl transfer occurs to form a hydridoalkyl-rhodium complex, there is essentially no barrier for elimination of RH. Thus the Rh(olefin)$^+$ complex is formed with very high internal excitation which allows the products to react further. This is consistent with the prevalent loss of (CH_4+H_2) in the reactions of Ru^+ and Rh^+ with 2,2-dimethylpropane at low energies, and with 2-methylpropane at higher energies. In these reactions, it is also possible that the H_2 molecule is lost first, followed by elimination of methane from the highly excited metal-olefin complex. Studies with deuterium labelled 2-methylpropane-2-d$_1$ (Table 4) indicate that the methane lost in the reactions with Ru^+ and Rh^+ is purely CH_4. Furthermore, although a 50:50 mixture of (CH_4+H_2) and (CH_4+HD) loss is observed in the reaction with Ru^+, only the latter product is observed for Rh^+. From these data alone, it is not possible to explain this difference in the reactivity between Ru^+ and Rh^+ or

to predict which molecule is lost first in this multiple loss process. Collisional stabilization studies or metastable decompositions could give information about the sequence in which the products are formed.

The reactions of Ru^+ and Rh^+ with acetone are also consistent with the idea that C-H bond insertions are favored over C-C insertions. After initial C-H bond insertion, the lack of β-H's results in the transfer of a β-methyl group and elimination of CH_4. Although this is by far the dominant process for Ru^+ and Rh^+, it is not observed in the ion beam experiment with Fe^+, Co^+, or Ni^+ (Table 6).

Comparison of first and second row transition metal ion reactivity. The difference in reactivity between Ru^+ and Rh^+ and their first row congeners suggests differences in the potential energy surfaces which are summarized below. First, whereas Fe^+, Co^+ and Ni^+ complexes have large activation barriers for reductive elimination of H_2 and possibly HR, the corresponding eliminations at Ru^+ and Rh^+ centers appear to have little or no barriers. Second, there may be differences in the activation parameters for carbon-carbon bond insertion by transition metal ions of the first and second row. Although C-C bond activation has been proposed for reactions occurring at Fe^+, Co^+ and Ni^+ centers,[1c,3b,25] in most cases the results may also be explained by C-H bond insertion followed by β-alkyl shifts. Unfortunately, labelling studies do not differentiate these two mechanisms. In contrast, results for the second row metal ions clearly indicate that Ru^+ and Rh^+ do not exothermically cleave C-C bonds.

Finally, there may be differences in the relative activation parameters for β-H and β-alkyl transfers for the first and second row metal ions. Although there are few unequivocal observations of β-methyl transfers for gas phase transition metal ions, there is evidence for competitive β-methyl transfers at Fe^+ centers.[1c] Migratory insertions of ethylene into the $M-CH_3^+$ bond of Co^+,[29] Sc^+,[4] and Ti^+ [30] complexes also indicate that β-methyl transfers can occur for the first row transition metal ions. Similar β-methyl transfers do not occur in competition with β-hydrogen transfers for Ru^+ and Rh^+.

It is possible that the observed differences in the activation parameters for the processes discussed above may be related to bonding differences for the first row versus second row transition metal ions. Clues into these differences can be obtained from an examination of the bond strengths and bonding orbitals used for the transition metal ion reactions.

Ab-initio calculations on the ground states of the diatomic metal hydrides FeH^+, CoH^+, and NiH^+ indicate that the bonding in these molecules involves a metal orbital which is 85-90% s-like in character.[31] This is in agreement with the experimentally observed trend that the M^+-H bond dissociation energies for the first row transition metals increase with decreasing promotion energy from the ground state to a state with an electronic configuration which is s^1d^n, indicating a bond that involves a metal 4s orbital.[32] Because the first bond utilizes what is primarily an 4s orbital, formation of a second bond to Fe^+, Co^+, and Ni^+ must involve primarily a metal 3d orbital. The second bond will thus be inherently weaker than the first due to the

smaller size and poorer overlap of the 3d orbital relative to the 4s orbital. For example, the strength of the second bond in dimethylcobalt ion, $D(CoCH_3^+-CH_3)$ = 45 kcal/mol,[7b] is considerably less than the strength of the first bond, $D(Co^+-CH_3)$ = 61 kcal/mol. This is the case even though formation of the first bond requires promotion of Co^+ to an s^1d^n configuration, as discussed above for CoH^+.

The description of the bonding to the second row metal ions, however, is quite different. When bonding a hydrogen atom to the ground states of Ru^+, Rh^+, and Pd^+, which are all derived from d^n configurations, the metal orbital involved is predominantly d-like in character.[11] This is due to the more similar size of the 5s and 4d orbitals in the second row transition series. Thus, the second bond to Ru^+-H and $Rh-H^+$ might be expected to have the same inherent bond energy as the first bond. Furthermore, because less exchange energy is lost in forming the second bond to a d-orbital, the second bond might actually be stronger than the first.[33] However, as indicated in Table 1, the first bond energy tends to be somewhat greater for the first row metal ions than for the second row.[34] Therefore, the sum of the first and second bond energies may be comparable for the metal ions of both rows. It is thus unlikely that the observed differences in reactivity are a direct result of the strengths of the bonds in the transition metal reaction intermediates. Note, however, that the orbitals used in forming these bonds are quite different for the metal ions of the two rows, and this may be responsible for the differential reactivity.

The s-d hybrid orbitals used in the first row bonding are much more diffuse than the pure d orbitals used for the second row bonds.[35] The second row 4d orbitals are also much smaller than the first row 4s orbitals.[35] This difference is reflected in the shorter bond lengths for RuH^+ and RhH^+ relative to FeH^+ and CoH^+.[35] When inserting into a very directional C-C bond, more favorable overlap may be possible using relatively large, diffuse s-d hybrid orbitals than when using two tight d orbitals. It has been recently pointed out that metal d-orbital character is essential for facile β-H transfers involving a four center transition state.[36] However, due to the directionality of a methyl orbital, less bonding is expected in the transition state for β-methyl transfer than for β-H transfer. This may be more of a problem for the second row transition metal ions where tight metal d orbitals are involved. Perhaps more diffuse s-d hybrid orbitals provide better overlap in the transition state for β-methyl transfer. It is thus possible that the d^n configurations of the second row transition metal ions favor insertion into less directional bonds, i.e., the C-H bonds of alkanes, and also favor transfer of a spherically symmetric hydrogen atom.

The orbitals used for bonding may also be useful in understanding the relatively low barriers for reductive elimination of H_2 in the reactions of the second row versus first row transition metal ions. Recent calculations indicate that the bond angle of MH_2^+ can be much smaller for bonds that have a significant amount of d-orbital character. For example, the hydrogen bonds to Mo^+ in MoH_2^+ are 80% d in character with a bond angle of 64°.[37] In contrast, the hydrogen bonds to Sc^+ in ScH_2^+

are only 50% d with a bond angle of 106°.[38] If this trend is true in general, then smaller bond angles for the second row metal ions may result in lower activation barriers for reductive elimination of H_2 relative to the first row.
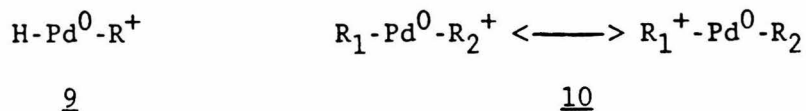
Reaction mechanism for alkane activation by Pd^+. The product distributions for the reactions of Pd^+ with alkanes are seemingly quite similar to those observed for Fe^+, Co^+, and Ni^+ as indicated in Tables 6 and 8. In fact, the alkane loss products resulting from the reactions of Pd^+ with deuterium labelled alkanes (Table 4) are almost identical to those observed for Fe^+, Co^+, and Ni^+.[1c] However, closer inspection of the hydrogen loss products reveals some substantial differences in reactivity. For example, reaction of Pd^+ with n-butane-1,1,1,4,4,4-d_6 yields exclusive elimination of H_2, in contrast to the scrambled products observed for Fe^+ and Co^+, and loss of D_2 for Ni^+.[1c,2b,3b] Both Co^+ and Ni^+ dehydrogenate n-butane exclusively via a 1,4-mechanism, with scrambling occurring in the Co^+ case.[7] In contrast, dehydrogenation by Pd^+, appears to occur by a quite distinct 1,2-mechanism across the central C-C bond exclusively.

Another difference in the reactivity of Pd^+ can be found from an examination of the overall reaction cross sections. Palladium ions react with branched alkanes to a much larger extent that with linear alkanes. Although this trend also occurs for Ru^+ and Rh^+, it is much less pronounced. The opposite trend occurs for Fe^+, Co^+, and Ni^+.[39]

An examination of the bonding to Pd^+ gives insight into its

unusual reactivity. The configuration giving rise to the ^2D ground state of Pd^+ is $4d^9$,[40] which has only one unpaired electron available for formation of a covalent bond. In this respect, Pd^+ is quite similar to its first row congener Ni^+ ($3d^9$). The high reactivity of Ni^+ is thought to be a result of the low promotion energy (only 23 kcal/mol) required to excite Ni^+ to a bonding s^1d^8 configuration which is able to make up to three covalent bonds. In contrast, the promotion energy required to excite Pd^+ to a bonding s^1d^8 configuration is much larger, 83 kcal/mol. From this point of view, Pd^+ is more similar to Mn^+ (s^1d^5). Mn^+ forms a strong first bond but apparently has such a weak second bond due to the half-filled d shell and high promotion energy that Mn^+ does not undergo exothermic reactions with alkanes.[32] The issue then, is how Pd^+ is able to activate alkanes while Mn^+ is not.

Possible mechanisms for the activation of alkanes by Pd^+ involve using different oxidation states of palladium. For example, Pd^+ may insert into alkane C-H or C-C bonds by H^- or R^- abstraction, leading to Pd(0) complexes as shown in structures 9 and 10, respectively. In these structures, the

$$H\text{-}Pd^0\text{-}R^+ \qquad\qquad R_1\text{-}Pd^0\text{-}R_2^+ <\longrightarrow> R_1^+\text{-}Pd^0\text{-}R_2$$

$$\underline{9} \qquad\qquad\qquad\qquad\qquad \underline{10}$$

alkyl cation remains bound to the metal center by acid-base interactions.

The configuration giving rise to the ^1S ground state of Pd(0) is $4d^{10}$, which is unable to make any covalent bonds. However, the promotion energy to the $5s^1 4d^9$ configuration

favorable for bonding is only 18.7 kcal/mol.[40] The bonding in intermediates such as 9 would then involve a covalent bond to H using the singly occupied 5s orbital, and a donor-acceptor bond to R^+ using a filled 4d orbital as illustrated schematically by 11 and 12.

11   12

The hydride affinities for a number of transition metal ions have been recently measured and are illustrated in Figure 5.[12,13,41] It is seen that the hydride affinity of Pd^+ is comparable to that of tertiary alkyl cations. Thus formation of intermediates such as 9 are energetically reasonable for tertiary C-H bond insertion and are possible for secondary C-H insertion if the strength of the donor-acceptor bond is greater than 16 kcal/mol. The hydride affinity of Mn^+ is much lower,[42] making hydride abstraction energetically unreasonable as a first step in C-H bond activation by Mn^+.

As indicated in Figure 5, primary C-H insertion by Pd^+ requires a donor-acceptor bond energy in excess of 35 kcal/mol. It is possible that this energy requirement renders primary hydride abstraction unreasonable. In this case, another mechanism must be invoked to explain the reaction of Pd^+ with 2,2-dimethylpropane to lose CH_4. Insertion into a C-C bond in this case would form an intermediate such as 10 where the charge is delocalized as shown by the two canonical forms, perhaps

Figure 5. Hydride affinities for gas phase metal ions and alkyl cations.

rendering C-C insertions by Pd^+ a favorable reaction pathway. Unfortunately, this cannot be quantified due to lack of thermochemical data. These ideas correctly predict that ethane should be unreactive toward Pd^+. No reaction is observed because after initial C-C insertion to form $\underline{10}$, only thermodynamically unfavorable products could be formed, namely, CH_4 and $PdCH_2^+$ via α-hydrogen abstraction.[43]

The hydride abstraction model presented above is supported by the reaction of Pd^+ with deuterium labelled n-butane-$1,1,1,4,4,4-d_6$. The only dehydrogenation product observed in this reaction is loss of H_2. A 1,2-mechanism across the central C-C bond would be expected for a reaction which proceeds via a carbonium ion intermediate. For example, the gas phase ionic dehydration of 2-butanol via a carbonium ion intermediate occurs to produce predominantly 2-butene as opposed to 1-butene.[44] Dehydration of 2-butanol on Al_2O_3 surfaces also produces mainly 2-butene.[45] This supports our belief that we are indeed observing hydride abstraction as a first step in the reactions of Pd^+ with saturated alkanes. It should be noted that in condensed phase studies at Pd(II) centers, carbonium ion intermediates have been previously proposed.[46] For example, oligomerization and isomerization of olefins by $Pd(CH_3CN)_4^{2+}$ have been proposed to proceed via carbonium ion intermediates.

Conclusion

The reactivities of Ru^+, Rh^+ and Pd^+ are shown to be remarkably different from their first row congeners. Whereas Co^+ and Ni^+ dehydrogenate alkanes by a 1,4-elimination mechanism, the

corresponding second row metal ions appear to effect 1,2-dehydrogenations. The reactions of Ru^+ and Rh^+ are characterized by C-H insertions and facile β-H transfers. Unlike their first row congeners, β-methyl transfers and C-C insertions do not occur for Ru^+ and Rh^+. Furthermore, the barriers for reductive elimination of RH and H_2 from Rh-olefin$^+$ complexes are quite small, in contrast to those proposed previously for Co^+. This may result in high internal excitation of the primary dehydrogenation products for Ru^+ and Rh^+ reactions. In this case, the products themselves may undergo an exothermic elimination of a second molecule of H_2, a process not observed for the first row group 8-10 metal ions. These differences in reactivity are proposed to be due to differences in the sizes and shapes of the bonding orbitals for the first and second row metal ions.

The mechanism by which alkanes are activated by Pd^+ is quite distinct from any other metal ion studied to date. It is proposed that the uniquely high Lewis acidity of Pd^+ results in a hydride abstraction mechanism for C-H bond activation.

References

1. (a) Armentrout, P. B.; Beauchamp, J. L. J. Am. Chem. Soc. 1981, 103,784. (b) Halle, L. F.; Armentrout, P. B.; Beauchamp, J. L. Organometallics 1982, 1, 963. (c) Houriet, R.; Halle, L. F.; Beauchamp, J. L. Organometallics 1983, 2, 1818.

2. (a) Allison, J.; Freas, R. B.; Ridge, D. P. J. Am. Chem. Soc. 1979,101,1332. (b) Larson, B. S.; Ridge, D. P. J. Am. Chem. Soc. 1984, 106, 1912.

3. (a) Byrd, G. D.; Burnier, R. C.; Freiser, B. S. J. Am. Chem. Soc. 1982, 104, 3565. (b) Jacobson, D. B.; Freiser, B.S. J. Am. Chem. Soc. 1983, 105, 5197.

4. Tolbert, M. A.; Beauchamp, J. L. J. Am. Chem. Soc. 1984, 106, 8117.

5. Byrd, G. D.; Freiser, B. S. J. Am. Chem. Soc. 1982, 104, 5944.

6. Carlin, T. J.; Jackson, T. C., Freiser, B. S., to be submitted.

7. (a) Hanratty, M. A.; Beauchamp, J. L.; Illies, A. J.; Bowers, M. T. J. Am. Chem. Soc. 1985, 107, 1788. (b) Hanratty, M. A.; Beauchamp, J. L.; Illies, A. J.; Bowers, M. T., submitted to J. Am. Chem. Soc.

8. Jacobson, D. B.; Beauchamp, J. L.; Bowers, M. T., unpublished results.

9. (a) Aristov, N.; Armentrout, P. B., submitted. (b) Elkind, J. L.; Ervin, K. N.; Aristov, N.; Armentrout, P. B., submitted.

10. Elkind, J. L.; Armentrout, P. B., submitted.

11. Mandich, M. L.; Halle, L. F.; Beauchamp, J. L. J. Am. Chem. Soc. 1984, 106, 4403.

12. Sallans, L.; Lane, K, R.; Squires, R. R.; Freiser, B. S., J. Am. Chem. Soc. 1985, 107, 4379.

13. Tolbert, M. A.; Beauchamp, J. L, to be submitted.

14. (a) Armentrout, P. B.; Beauchamp, J. L. Chem. Phys. 1980, 50, 21. (b) Armentrout, P. B.; Beauchamp, J. L. J. Chem. Phys. 1981, 74, 2819.

15. Freas, R. B.; Ridge, D. P. J. Am. Chem. Soc. 1980, 102, 7129.

16. Halle, L. F.; Armentrout, P. B.; Beauchamp, J. L. J. Am. Chem. Soc. 1981, 103, 962.

17. Kang, H.; Beauchamp, J. L., submitted to J. Phys. Chem.

18. Halle, L. F.; Crowe, W. E.; Armentrout, P. B.; Beauchamp, J. L. Organometallics 1984, 3, 1694.

19. Loss of (H_2 + CO) cannot be distinguished from loss of H_2CO in this experiment. Formation of the former product is the favored process by 0.5 kcal/mol (Reference 21).

20. Bryd, G. D., PhD thesis, Purdue University, 1982, p. 134.

21. Auxiliary heats of formation are taken from Cox, J. D.; Pilcher, G. Thermochemistry of Organic and Organometallic Compounds. Academic Press: New York, 1970. $\delta H_f(CH_3) = 35.1$ kcal/mol from McMillen, D. F.; Golden, D. M. Ann. Rev. Phys. Chem. 1982, 33, 493

22. Another possible structure for this product is $CH_2RhCH_2^+$. If this were the product formed, then the reaction exothermicity implies $D(Rh^+-2CH_2) > 210$ kcal/mol. The $RhCH_2^+$ bond strength has been determined previously to be 94 ± 5 kcal/mol (Jacobson, D. B.; Freiser, B. S. J. Am. Chem. Soc., in press). It therefore seems unlikely that the biscarbene ion is being formed in the reaction with acetone.

23. Jacobson, D. B.; Freiser, B. S. J. Am. Chem. Soc., in press.

24. Jacobson, D. B.; Freiser, B. S. J. Am. Chem. Soc. 1983, 105, 736.

25. Halle, L. F.; Houriet, R.; Kappes, M. M.; Stalesy, R. H.; Beauchamp, J. L. J. Am. Chem. Soc. 1982, 104, 6293.

26. The term 1,2-elimination implies that the hydrogen atoms are eliminated from adjacent carbon atoms. This term does not specify which carbon atoms are involved in the elimination.

27. This reaction is reported in Jacobson, D. B.; Freiser, B. S. J. Am. Chem. Soc., in press. The rate of this reaction was obtained from Jacobson, D. B., private communication.

28. If the bond strengths of propylene and isobutene to Rh^+ are assumed to be equal, then loss of methane is thermochemically favored over H_2 loss by 9 kcal/mol; see Reference 21.

29. Jacobson, D. B.; Freiser, B. S. J. Am. Chem. Soc., in press.

30. Uppal, J. S.; Johnson, D. E.; Staley, R. H. J. Am Chem. Soc. 1981, 103, 508.

31. Schilling, J. B.; Goddard, W. A. III., submitted to <u>J. Am. Chem. Soc.</u>

32. Armentrout, P. B.; Halle, L. F.; Beauchamp, J. L. <u>J. Am. Chem. Soc.</u> 1981, <u>103</u>, 6501.

33. Formation of the first d-type bond in Ru^+ and Rh^+ requires uncoupling of the high spin metal configuration, which somewhat weakens the resulting bond. The second bond does not suffer this same energetic loss and is therefore expected, on this basis, to be somewhat stronger than the first. See Reference 11 for further discussion.

34. The inherent bond energies of H and CH_3 to the first row transition metal ions were shown to be 60 and 70 kcal/mol, respectively, Reference 32. Although no such inherent bond energies have been determined for the second row metal ions, the values presented in Table 1 are typically lower than for the first row.

35. Schilling, J. B., Goddard, W. A. III.; Beauchamp, J. L., to be submitted to J. Am. Chem. Soc.

36. Steigerwald, M. L.; Goddard, W. A. III <u>J. Am. Chem. Soc.</u> 106, 308.

37. Calculations indicate that the lowest energy configuration for this molecule is not an η_2 complex, but rather consists of two sigma M-H bonds (Schilling, J. B. S.; Goddard, W. A. III.; Beauchamp, J. L., work in progress).

38. Alvarado-Swaisgood, A. E.; Harrison, J. F., submitted.

39. Halle, L. F. Armentrout, P. B.; Beauchamp, J. L., unpublished results.

40. Moore, C. E. <u>Atomic Energy Levels.</u> National Bureau of Standards: Washington, D. C., 1949.

41. The hydride affinities for the cationic alkyl species in Figure 5 are from: Schultz, J. C.; Houle, F. A.; Beauchamp, J. L. <u>J. Am. Chem. Soc.</u> 1984, <u>106</u>, 7336.

42. The homolytic Mn-H bond dissociation energy is not well known. The experimental values are contradictory and range from 56 to < 32 kcal/mol. This problem is discussed in: Squires, R. R. <u>J. Am. Chem. Soc.</u> 1985, <u>107</u>, 4385. A value of D(Mn-H)=32 kcal/mol was used for Figure 5. The Mn^+ hydride affinity is equal to D(Mn-H) + IP(Mn) - EA(H), where IP(Mn) = 7.43 ev (Reference 40), and EA(H) = 17.4 kcal/mol.

43. Typical M-CH$_2^+$ bond strengths are 70-90 kcal/mol (Reference 32). Using this range, Pd$^+$ + C$_2$H$_6$ ---> PdCH$_2^+$ + CH$_4$ is expected to be endothermic by 4-24 kcal/mol. Activation barriers for α-H transfer may make this an even less favorable process.

44. Beauchamp, J. L.; Caserio, M. C. <u>J. Am. Chem. Soc.</u> **1972**, <u>94</u>, 2638.

45. Pines, H.; Haag, W. O. <u>J. Am. Chem. Soc.</u> **1961**, <u>83</u>, 2047.

46. Sen, A.; Lai, T. W. <u>J. Am. Chem. Soc.</u> **1981**, <u>103</u>, 4627.

CHAPTER III

HOMOLYTIC AND HETEROLYTIC BOND DISSOCIATION ENERGIES
OF THE SECOND ROW GROUP 8, 9 AND 10
DIATOMIC TRANSITION METAL HYDRIDES:
CORRELATION WITH ELECTRONIC STRUCTURE

Homolytic and Heterolytic Bond Dissociation Energies of the

Second Row Group 8, 9, and 10 Diatomic Transition Metal

Hydrides: Correlation with Electronic Structure

.

M. A. Tolbert and J. L. Beauchamp

ABSTRACT

The heterolytic and homolytic bond dissociation energies of the first and second row group 8-10 metal hydrides are determined using an ion beam apparatus. These bond energies are obtained by monitoring the hydride transfer reactions of the corresponding metal ions with a series of hydride donating reagents. The homolytic bond energies for RuH, RhH and PdH are found to be comparable, 56 ± 5, 59 ± 5 and 56 ± 6 kcal mol^{-1}, respectively. In contrast, the corresponding bond energies for FeH, CoH and NiH are quite varied, 43 ± 6, 54 ± 10 and 65 ± 6 kcal mol^{-1}, respectively. With the exception of PdH, the strengths of the metal hydride bonds correlate well with the atomic promotion energy to a state derived from an $s^1 d^n$ configuration. This suggests a bond to hydrogen which utilizes what is predominantly a metal s orbital. The bonding in PdH is quite distinct from the other metal hydrides, as evidenced by a lack of correlation of this bond energy with atomic promotion energy. This may be a result of increased d electron participation in the bonding of PdH due to the stable d^{10} configuration of ground state Pd atoms. The metal hydride bond dissociation energies determined in this study are compared to available theoretical calculations.

Introduction

Activation of the C-H bonds of saturated hydrocarbons by transition metals requires the formation of strong M-H and M-alkyl bonds. Knowledge of these bond strengths is essential for understanding all catalytic processes where C-H bonds are formed or broken. The prominence of the second row group 8-10 metals in homogeneous and heterogeneous catalysis makes knowlege of the bond strengths to these metals especially important.[1-4] Understanding the bonding in the corresponding diatomic metal hydrides may help to access the importance of reaction steps which involve the metal hydrogen bond. Metal hydrogen bonds are the simplest model for sigma bonding to a metal center, and as such are amenable to examination with high quality ab initio calculations. In spite of their importance, only limited results are available which relate to the experimental determination of these bond energies.

A typical value for the M-H bond energy in organometallic complexes is approximately 60 kcal mol^{-1}.[5-7] Measurements of diatomic metal hydrogen bond energies show a large variation of the bond energy as a function of metal atom. Diatomic metal hydrides have been studied previously for the entire first row transition metal series,[8-14] as well as for several metals of the second and third row series.[10b,13,15,16] Theoretical descriptions of the bonding in metal hydrides has been predominantly limited to those metal atoms in the first transition series.[17-19] In many cases, there is a large deviation in the experimental and

theoretical bond energies, as well as between various experimen-
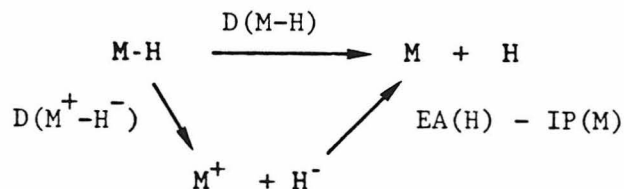tal bond energies.

In this paper, we report experimental values for the
diatomic hydrides RuH, RhH, and PdH. For RuH and RhH, these
values represent the first reported experimental measurements.
For PdH, the only previous experimental determination of the bond
energy was obtained using spectroscopic techniques. Metal
hydride bond energies determined from extrapolations of
spectroscopic data are thought to be somewhat unreliable.[8,20] We
also report bond energies for FeH, CoH, and NiH for comparison
with previous work.

Homolytic metal-hydrogen bond dissociation energies, D(M-H),
may be obtained from the heterolytic values, $D(M^+-H^-)$, in
conjunction with the ionization potential of the metal atom and
the electron affinity of hydrogen,[21] as indicated by Equation 1,

$$D(M-H) = D(M^+-H^-) - IP(M) + EA(H) \qquad (1)$$

derived from Scheme 1. The heterolytic M^+-H^- bond dissociation

Scheme 1

$$
\begin{array}{ccc}
 & D(M-H) & \\
M-H & \longrightarrow & M + H \\
D(M^+-H^-) \searrow & & \nearrow EA(H) - IP(M) \\
 & M^+ + H^- & \\
\end{array}
$$

energies are obtained in this study by observing the exothermic
and endothermic hydride abstraction reactions of metal ions, as
indicated by reaction 2. The observance of reaction 2 as an

$$M^+ + AH \longrightarrow MH + A^+ \qquad (2)$$

exothermic process indicates $D(M^+-H^-) > D(A^+-H^-)$. Failure to observe reaction 2 as an exothermic process is consistent with the reaction being endothermic. In the absence of competing reactions or an activation barrier, it is generally believed that a reaction which is not observed at thermal energies is endothermic.[22,23]

It should be noted that the heterolytic as well as homolytic metal hydrogen bond dissociation energies are of great interest. The chemistry which occurs at a metal ion center may be governed by the strength of the heterolytic M^+-H^- bond. For example, the present work was motivated in part by the observation of exothermic hydride abstraction as a first step in the reactions of Pd^+ with alkanes.[24]

The bond energies for the group 8-10 metal ions determined in this way are interpreted in terms of the electronic structures of the diatomic metal hydrides and the electronic configurations of the isolated products of homolytic and heterolytic dissociation.

Experimental

The ion beam apparatus used in the present study has been described previously.[25] Briefly, ion beams of Ru^+, Rh^+ and Pd^+ are produced by vaporization of $Ru_3(CO)_{12}$, $[Rh(CO)_2Cl]_2$ and $PdCl_2(anhy)$ onto a hot rhenium filament, and subsequent surface ionization at 2500 K. In this experimental arrangement, electronically excited ions are less that 1.5% of the total ion abundance for Ru^+, Rh^+, and Pd^+ as indicated in Table 1.[26] Ion

TABLE 1. Lower Electronic States of Ru^+, Rh^+, Pd^+, Fe^+, Co^+ and Ni^+ and their Relative Ion Populations at 2500 K.

	State	Configuration	Energy[a]	Relative Population
Ru+	^4F	$4d^7$	0.00	.986
	^4P	$4d^7$	0.88	.006
	^6D	$4d^6 5s^1$	1.09	.006
	^2G	$4d^7$	1.25	.002
Rh^+	^3F	$4d^8$	0.00	.995
	^1D	$4d^8$	0.81	.004
	^3P	$4d^8$	1.18	.001
	^1G	$4d^8$	1.64	.000
Pd^+	^2D	$4d^9$	0.00	1.000
	^4F	$4d^8 5s$	3.19	.000
	^2F	$4d^8 5s$	3.94	.000
Fe^+	^6D	$3d^6 4s^1$	0.00	.765
	^4F	$3d^7$	0.25	.230
	^4D	$3d^6 4s^1$	0.98	.005
	^4P	$3d^7$	1.64	.000
Co^+	^3F	$3d^8$	0.00	.812
	^5F	$3d^7 4s^1$	0.43	.185
	^3F	$3d^7 4s^1$	1.21	.003
Ni^+	^2D	$3d^9$	0.00	.981
	^4F	$3d^8 4s^1$	1.09	.018
	^2F	$3d^8 4s^1$	1.68	.001

[a]The state energies cited are a weighted average over the J states from Reference 26.

beams of Fe^+, Co^+, and Ni^+ were obtained using $FeCl_3$ (anhy), $CoCl_2 \cdot 6H_2O$, and $NiCl_2.6H_2O$. The excited state population of these ions at 2500 K, which are appreciable in the cases of Fe^+ and Co^+, are also included in Table 1. The metal ions are collimated, mass and energy selected, and focussed into a collision chamber containing the neutral reactant at ambient temperature. Product ions scattered in the forward direction are analyzed using a quadrupole mass spectrometer. It should be emphasized that only the ions are detected in this experiment. Thus, reaction 2 is observed by monitoring the fragment A^+, and inferring the product MH.

Results and Discussion

Analysis of the bracketing technique. The reactions of metal ions with a series of hydride donating reagents have been examined in order to bracket the heterolytic M^+-H^- bond dissociation energies. Similar bracketing techniques have been used sucessfully in a number of instances. For example, the bond energy for MnH^+ was determined by measuring the proton transfer reactions from MnH^+ to bases of varying strengths using ion cyclotron resonance (ICR) techniques.[22] In a similar ICR experiment, the proton affinities of alkylbenzene radicals were bracketed by determining the rates of reaction of alkylbenzene ions with a series of reference bases.[23] The bond energy D(FeH-H) was determined in an ion beam experiment by bracketing the hydride affinity of FeH^+ with a series of hydride donors.[27] These techniques work well because at thermal energies an endothermicity of just 3 kcal mol^{-1} can result in a decrease in

the reaction rate of over two orders of magnitude. For example,
in the proton transfer reactions of MnH^+, the rate constant
varies from below 10^{-11} to 1.5×10^{-9} cm^3 molecule^{-1} sec^{-1} over a
range of 5 kcal mol^{-1} as the reaction changes from endothermic to
exothermic.[22]

Several factors must be considered in using the bracketing
technique to determine heterolytic M^+-H^- bond dissociation
energies. This technique will not work if the reaction studied
proceeds via an activation barrier. A simplified potential
energy surface which we postulate for a hydride transfer reaction
is shown in Figure 1. The initial interaction of the metal ion
with the hydride donor leads to the formation of a chemically
activated adduct represented as $M^+\cdots HA$. An _intrinsic_ barrier
separates this species from an adduct of the products, indicated
by $MH\cdots A^+$. The two adducts are _local minima_ on the potential
energy surface. If the maximum in the intrinsic barrier exceeds
the energy of the reactants, then there will be an overall
barrier to reaction, even for an exothermic process. The overall
barriers, which may be substantial for nearly thermoneutral
reactants, are generally reduced as the reaction exothermicity
increases. This effect is illustrated by the two curves in
Figure 1. Even in the absence of an overall barrier, reactions
where intrinsic barriers are present may be slow due to phase
space constraints. These effects have been considered in detail
for processes such as anionic nucleophilic displacement
reactions[28,29] and proton transfer processes.[30] Unfortunately,
there are no potential energy surfaces which have been well

Figure 1. Simplified double-minimum potential energy surface for
hydride transfer reactions.
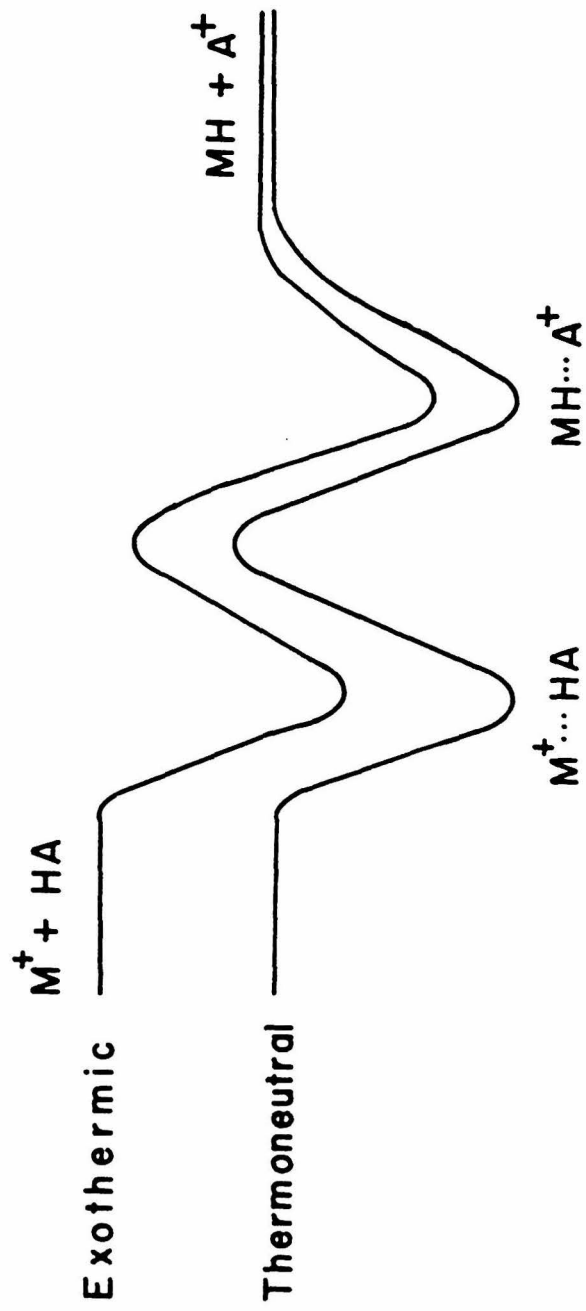
characterized for hydride transfer between organic molecules and transition metal ion centers. If substantial intrinsic barriers are present and lead to small overall barriers for exothermic reactions, then the bracketing technique used in the present work may yield erroneously <u>low</u> M-H bond dissociation energies.

A further complication may arise if multiple reaction pathways exist. In this case, it is possible that hydride transfer may not compete effectively with other reactions, and thus may not be observed. This could lead to reaction cross sections for hydride transfer which increase with increasing ion energy, even though the reaction is exothermic and the overall cross section decreases. The presence of multiple reaction pathways that render hydride transfer unable to compete effectively would result in erroneously <u>low</u> M-H bond energy determinations.

The presence of electronically excited ions in the present experiment could lead to erroneously <u>high</u> M-H bond energy determinations. Electronically excited ions may undergo exothermic hydride abstraction reactions that are not possible for ground state ions. This problem will be discussed in detail below.

<u>Reactions of hydride donors with transition metal ions.</u> The reactions of Fe^+, Co^+, Ni^+, Ru^+, Rh^+ and Pd^+ with a series of hydride donating reagents at a relative kinetic energy of 0.5 eV are indicated in Table 2. It can be seen that many of these systems are quite complicated and often result in the formation of a large number of products. Since endothermic reactions have cross sections that increase with increasing kinetic energy, we

TABLE 2. Product Distributions for the Reactions of the Group 8-10 Metal Ions with Hydride Donating Reagents at a Relative Kinetic Energy of 0.5 eV.[a]

		Fe$^+$	Co$^+$	Ni$^+$	Ru$^+$	Rh$^+$	Pd$^+$
CH_3CHO	H_2		----	----		.26[b]	----
	CH_4		1.0	1.0		.74[b]	.74
	MH		----	----		----	.26
	σTOT[c]		45.	38.		26.[b]	17.
C_2H_5CHO	H_2	.43[d]	.27	.43	.19	.09	----
	CH_4	----	----	----	----	.03	----
	$C_2H_6(CH_2O)$	.57[d]	.73	.47	.81	.87	.27
	MH	----	----	.10	----	.01	.73
	σTOT	61.[d]	148.	156.	79.	46.	90.
CH_3NH_2	H_2	1.0[d]	.74	.40	1.0	1.0	
	MH	----	.26	.60	----	----	
	σTOT	8.[d]	85.	62.	56.	22.	
$(CH_3)_2NH$	H_2	----			.72	.70	
	$2H_2$	----			----	.21	
	CH_4	.62			----	----	
	$CH_4 + H_2$	----			.13	.03	
	MH	.38			.15	.06	
	σTOT	270.			230.	248.	

TABLE 2. (cont'd).

		Fe^+	Co^+	Ni^+	Ru^+	Rh^+	Pd^+
$(CH_3)_3N$	H_2	----			.48	.59	
	$CH_4 + H_2$	----			.18	.12	
	M	.30			----	----	
	MH	.70			.34	.29	
	σTOT	284.			282.	82.	
$SiH(CH_3)_3$	H_2	.40[e]	.12[e]	.04		----	
	CH_4	.60[e]	.33[e]	.34		1.0	
	MH	----	.55[e]	.62		----	
	σTOT	23.[e]	190.[e]	261.		268.	
$(CH_3)_2O$	H_2			----		.38	NR[f]
	CH_4			1.0		----	NR
	$CH_4 + H_2$ or H_2O			----		.62	NR
	σTOT			18.		55.	
$(C_2H_5)_2O$	H_2	----	.11	.01[g]	.23	.16	----
	C_2H_4	.64	.39	.13[g]	----	----	----
	C_2H_6	.20	.08	.01[g]	.09	.08	----
	C_2H_6O	.16	.11	.04[g]	.42	.37	----
	$CH_4 + H_2$ or H_2O	----	----	----	.25	.22	----
	MH	----	.31	.81[g]	.01	.17	1.0
	σTOT	157.	262.	136[g]	208.	83.	220.
C_2H_5OH	H_2						1.0
	σTOT						97.

TABLE 2. (cont'd).

---

[a]Blanks indicate the reaction was not studied.

[b]Relative kinetic energy 0.7 eV

[c]Total reaction cross section in $\overset{\circ}{A}{}^2$. Cross sections reported are ± 50% and are used only as a guide for relative reaction rates.

[d]Relative kinetic energy 0.25 eV.

[e]Kang, H.; Jacobson, D.B.; Beauchamp, J.L.; Bowers, M.T., submitted.

[f]No reaction was observed.

[g]Relative kinetic energy 0.6 eV.

examined the effect of metal ion translational energy on the processes indicated in Table 2. An example of the reactivity observed is given in Figure 2 for the case of Ru^+ and Rh^+ reacting with diethyl ether. It can be seen that, although the same five products are formed in each case, their variation with relative kinetic energy is quite different. In particular, whereas hydride transfer clearly exhibits the behavior expected for an exothermic process in the case of Rh^+, the same reaction with Ru^+ exhibits a translational energy threshold expected for an endothermic reaction. The fact that this reaction is observed for Rh^+ supports our belief that the reaction involving Ru^+ is indeed endothermic. These differences in reactivity reflect differences in the heterolytic M^+-H^- bond energies.

The thermochemistry for the hydride transfer reactions reported in Table 2 has been determined from the cross-section behavior of the reactions as a function of relative kinetic energy. The results are summarized in Figure 3, along with recent results for Mo^+.[31] In this figure, the metal ions abstract H^- in exothermic processes from those reagents whose heterolytic bond energies are less than that of the metal ion.[32] Either an endothermic H^- abstraction or no H^- abstraction was observed for those reagents with a higher heterolytic bond energy than that of the metal ion. In the reaction of Ni^+ with C_2H_5CHO, the hydride abstraction product was observed with a fairly low cross section which was relatively independent of ion kinetic energy. By comparison with processes which are known to be exothermic or endothermic, we have inferred this behavior to be

Figure 2. Variation in the experimental cross section for the reactions of Ru^+ and Rh^+ with diethylether as a function of relative kinetic energy in the center of mass frame.
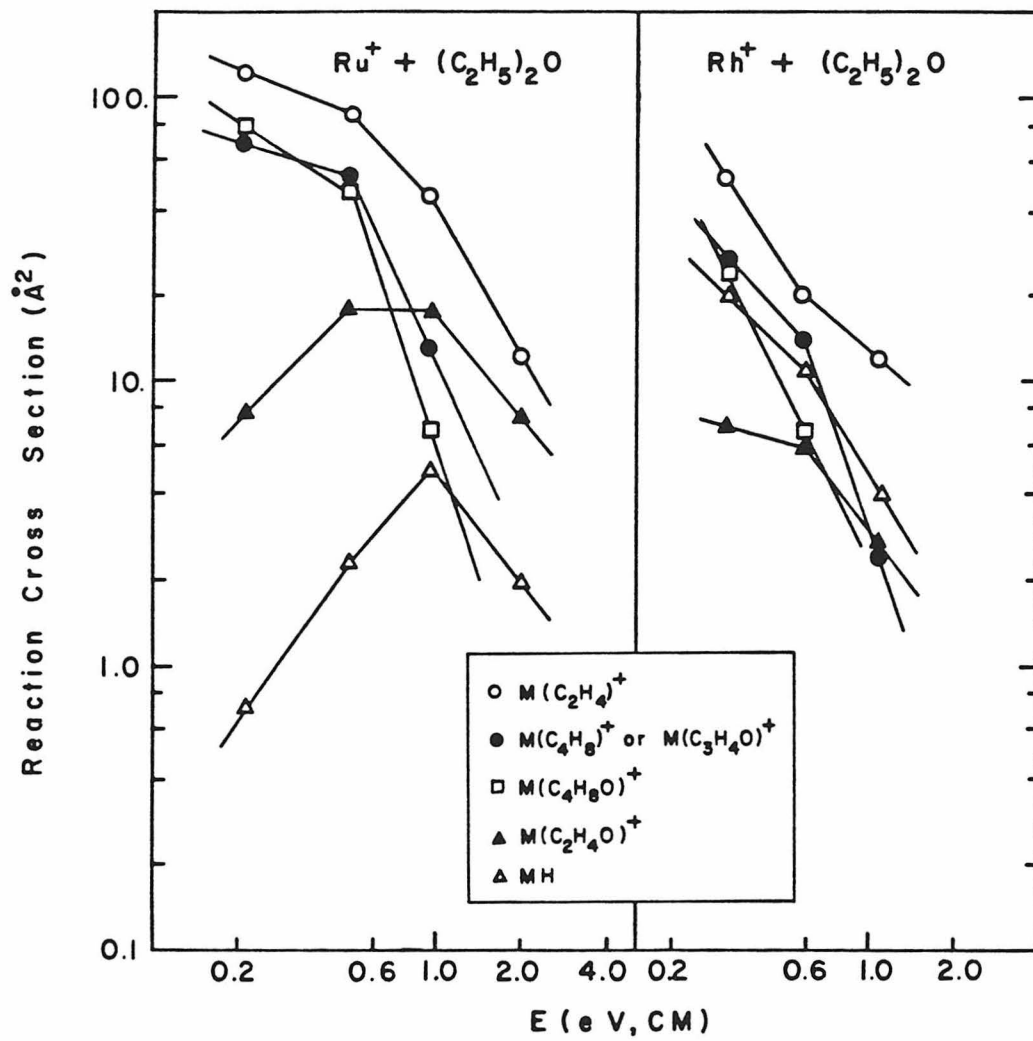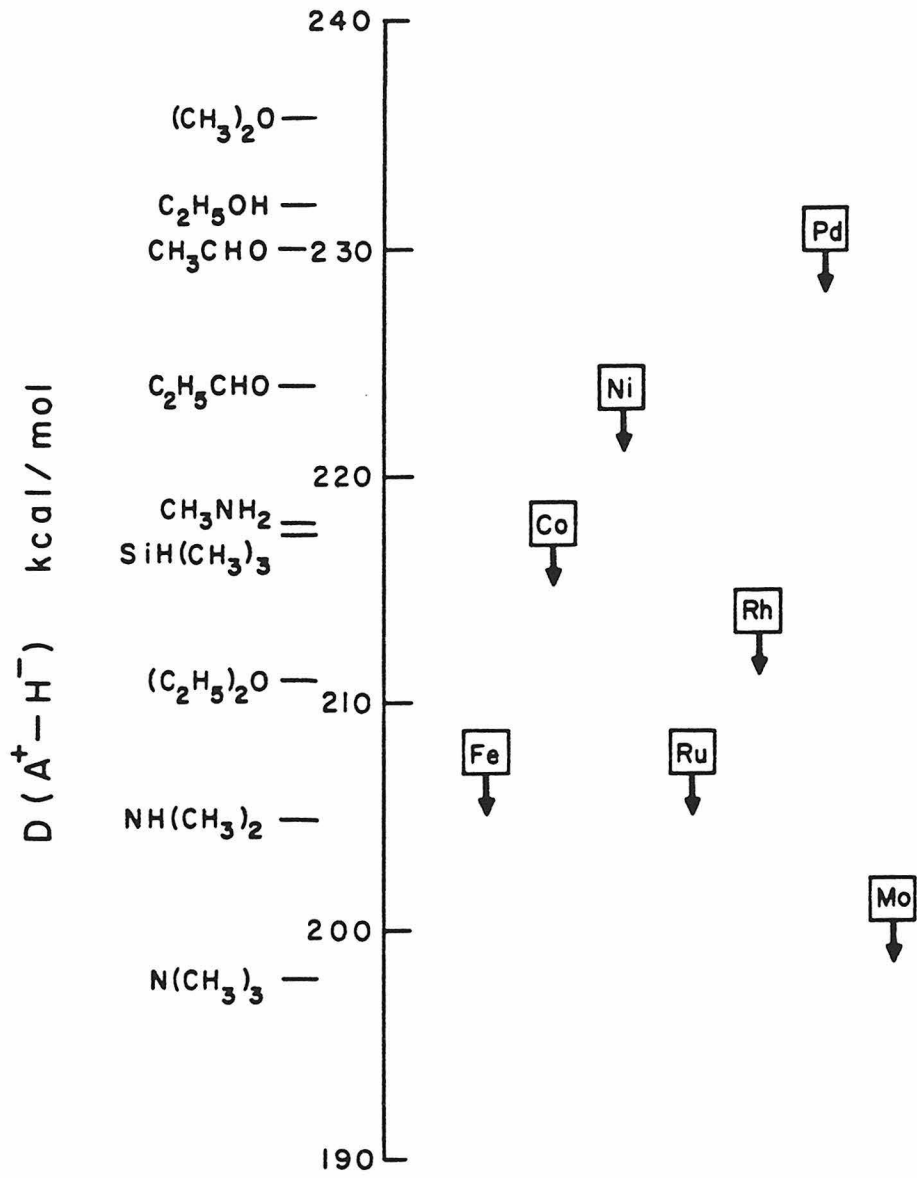
Figure 3. Heterolytic bond dissociation energies $D(A^+-H^-)$ for Fe, Co, Ni, Ru, Rh, Pd and Mo and for various hydride donating reagents.

indicative of a thermoneutral process. Thus, the heterolytic bond energy for Ni^+-H^- was chosen to be equal to that of C_2H_5CHO.

The above results are in agreement with the previous reactions that have been studied using ICR techniques. ICR studies of the reaction of Co^+ with ammines and ethers indicated that the reaction with CH_3NH_2 produced CoH as the major product.[33] This study also observed CoH as a significant product in the reaction of Co^+ with ethyl ether. In other ICR work, Fe^+ was <u>not</u> observed to abstract H^- from ethyl ether.[34] All of the above data are in agreement with our ion beam results for hydride abstraction by Fe^+ and Co^+.

A summary of the heterolytic bond dissociation energies obtained in this study is presented in Table 3. The homolytic bond dissociation energies calculated using Equation 1 are also included in this table. The bond dissociation energies obtained in this study may be used in conjunction with previously determined M^+-H bond energies[35-38] to obtain the ionization potentials of MH, using Equation 3. Similarly, for those metal

$$D(M^+-H) = D(M-H) + IP(M) - IP(MH) \qquad (3)$$

hydrides for which the electron affinities are known,[39,40] our values can be used to obtain values for $D(M^--H)$ using Equation 4.

$$D(M^--H) = D(M-H) + EA(MH) - EA(M) \qquad (4)$$

The relationships between these quantities is illustrated in Figure 4. The values obtained from Equations 3 and 4 are indicated in Table 4.

TABLE 3. Metal-Hydrogen Bond Dissociation Energies.[a]

		This Study			Previous Studies		
M	Ground State MH[b]	$D(M^+-H^-)$	$D(M-H)$	Sallans[c]	Spec.[d]	$D(M-H)$ Other	Theory
Fe	$^4\Delta$	208±6	43±6	30±3	39(46)[e]	<43[f]	37[g]48[h]34[i]36[j]
Co	$^3\Phi$	218±10	54±10	42±3		45±3[f]>39[k]	48[g]
Ni	$^2\Delta$	224±6	65±6		60(71)[l]	59±2[f]	55[g]62[h]64[m]45[n]
Ru	$^4\Phi$	208±5	56±5				36[i]
Rh	$^3\Phi$	214±5	59±5				
Pd	$^2\Sigma$	231±6	56±6		<76[o]		32[n]30[p]46[q]
Mo	$^6\Sigma$	201±5	53±5	46±3			

[a] All energies in kcal/mol.

[b] See discussion in text.

[c] Reference 13.

[d] Values determined spectroscopically. The numbers in parentheses are the actual values obtained from a Birge-Sponer extrapolation. The preceding values are the ones recommended by the respective authors.

[e] Reference 20.

[f] Reference 10.

[g] Reference 18. The value for the ground $^4\Delta$ state of FeH was obtained by adding the calculated value for the excited $^6\Delta$ state to the experimentally determined excitation energy to the $^6\Delta$ state (Reference 39).

[h] Reference 19. The value for the ground $^4\Delta$ state of FeH was calculated as in g.

[i] Reference 44. The value for RuH is for the $^4\Delta$ state, not the ground $^4\Phi$ state.

[j] Schilling, J.B., unpublished results.

[k] Reference 11.

[l] Reference 8.

TABLE 3. (cont'd).

[m]Goddard, W.A.III; Walsh, S.P.; Rappe, A.K.; Upton, T.H. $\underline{J}$. $\underline{Vac}$. $\underline{Sci}$. $\underline{Technol}$. 1977, $\underline{14}$, 416.

[n]Reference 54.

[o]Reference 16.

[p]Reference 50.

[q]Reference 51.

Figure 4. Simplified potential energy surfaces for the binding of hydrogen to M^-, M and M^+.
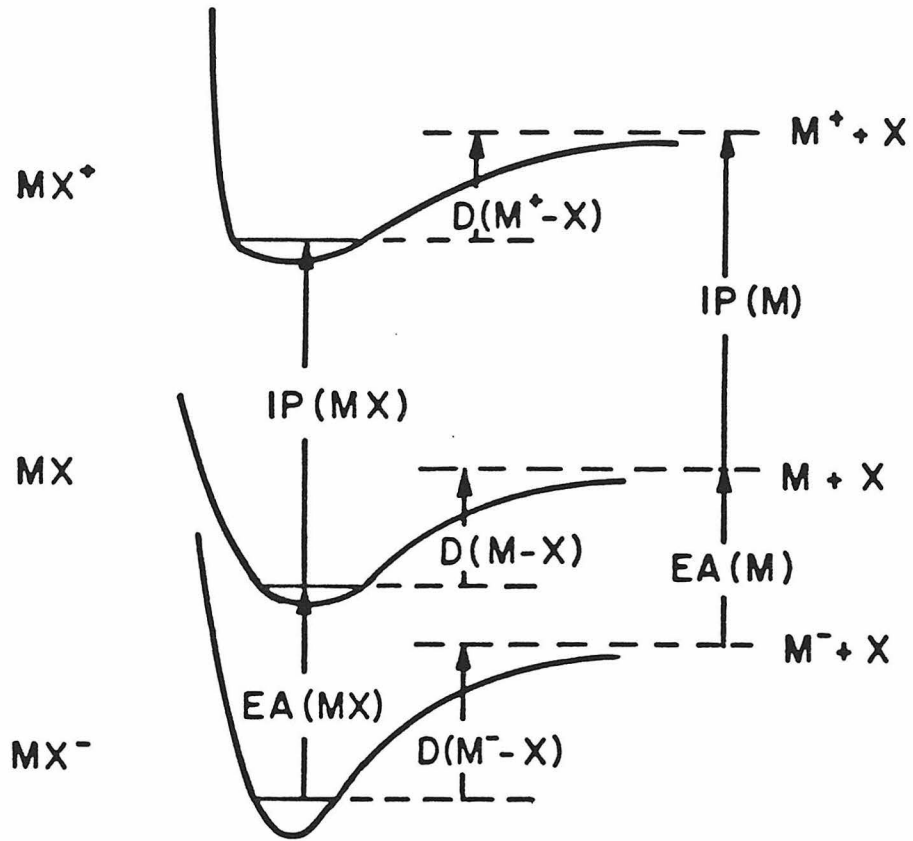
TABLE 4. Thermochemical Values Derived from MH Bond
Dissociation Energies Using Figure 4.

M	D(M-H)	D(M^+-H)	IP(M)	IP(MH)[a]	EA(M)[b]	EA(MH)	D(M^--H)
	kcal/mol		eV		kcal/mol		
Fe	43.	53.[d]	7.9	7.47	3.78	21.54[e]	60.8
Co	54.	47.5[d]	7.86	8.14	15.3	15.54[b]	54.2
Ni	65.	38.[d]	7.63	8.80	26.7	11.16[b]	49.5
Ru	56.	41.[f]	7.36	8.01	24.2		
Rh	59.	42.[f]	7.46	8.20	26.2		
Pd	56.	45.[f]	8.33	8.81	12.9		
Mo	53.	41.[d]	7.18	7.70	17.2		

[a]Derived from MH bond energies using Equation 3.

[b]Reference 39.

[c]Derived from MH bond energies using Equation 4.

[d]Reference 38.

[e]Reference 40.

[f]Reference 37.

Effects of electronic excitation on hydride abstraction

reactions. As mentioned earlier, erroneous results may occur if electronically excited ions are present. As indicated in Table 1, the abundance of M^+ formed in an excited state is less than 0.5 % of the total ion abundance for Rh^+, Pd^+, and Mo^+,[31] and less than 2% for Ru^+ and Ni^+. Even these small amounts of electronic energy excitation can lead to complications. For example, approximately 2% of the nickel ions are formed in an excited state with 25 kcal mol^{-1} excess electronic energy. The cross-section behavior for the hydride abstraction reaction of Ni^+ with methyl ether as a function of relative kinetic energy is shown in Figure 5. The cross section clearly demonstrates bimodal behavior, where the ground state reaction is endothermic and the excited state reaction is exothermic. The collision cross section for the reaction of Ni^+ with dimethyl ether is estimated to be at least 78 A^2 at a relative kinetic energy of 0.25 eV.[41] The apparent cross section observed for the hydride transfer reaction at 0.25 eV is 1 A^2. Because excited state Ni^+ comprises only 2% of the total ion beam, the excited state exothermic cross section is approximately 50 A^2. This can be contrasted to the ground state endothermic reaction which exhibits a maximum cross section of only 7 A^2 at a relative kinetic energy of 3.6 eV. Because their excited state populations are so low, any exothermic excited state reactions of Ru^+, Rh^+, Pd^+ and Mo^+ would show extremely low apparent cross sections at low energy, similar to those observed for Ni^+. Thus, the truly exothermic ground state reactions of these metal ions

Figure 5. Variation in the experimental cross section for the reaction of Ni^+ with dimethylether as a function of relative kinetic energy in the center of mass frame.

$Ni^+ + (CH_3)_2O \longrightarrow NiH + CH_3OCH_2^+$
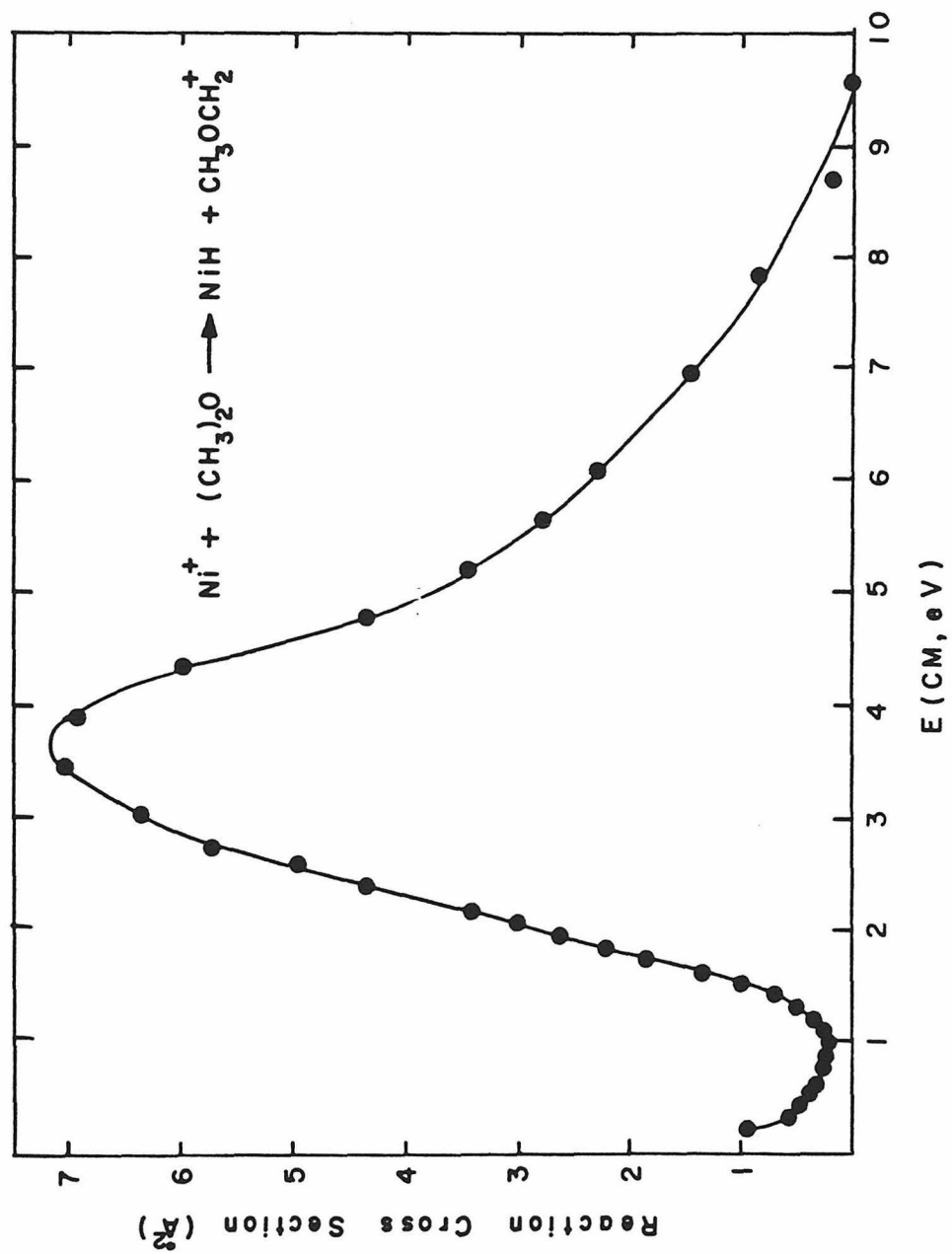
can be identified with little ambiguity due to their much larger cross sections.

In contrast, the reactions of Fe^+ and Co^+ suffer severe complications due to the abundance of electronically excited state ions present in the ion beam. The excited state populations for Fe^+ and Co^+ in our experiment are estimated to be 24% and 19%, respectively. Because of the extensive formation of electronically excited ions, it is extremely difficult to separate out the ground and excited state reactions for Fe^+ and Co^+. Previous studies of the endothermic reactions of these metal ions with H_2 to form MH^+ have indicated that, although the ground state of Co^+ is the reactive species, only the excited state of Fe^+ is reactive.[42] This, however, may not be the case for the exothermic hydride transfer reactions of the present study. The hydride transfer reactions for all of the metal ions except Fe^+ are spin allowed processes. The fact that the reactions with Fe^+ are not spin allowed may discriminate against ground state hydride transfer reactions for Fe^+.

With one exception, the hydride abstraction reactions observed with Fe^+ and Co^+ occur with very large cross sections. For example, the cross-section behavior for the exothermic reactions of Co^+ with $SiH(CH_3)_3$ are illustrated in Figure 6. It can be seen that hydride abstraction is a dominant process at low relative kinetic energies. The abundance of this product suggests that it is not formed solely from an electronically excited state of Co^+. Similarly, the reactions of Fe^+ with $NH(CH_3)_2$ and $N(CH_3)_3$ result in hydride transfer with cross sections too large to be assigned entirely to an excited state

Figure 6. Variation in the experimental cross section for the reaction of Co$^+$ with SiH(CH$_3$)$_3$ as a function of relative kinetic energy in the center of mass frame.
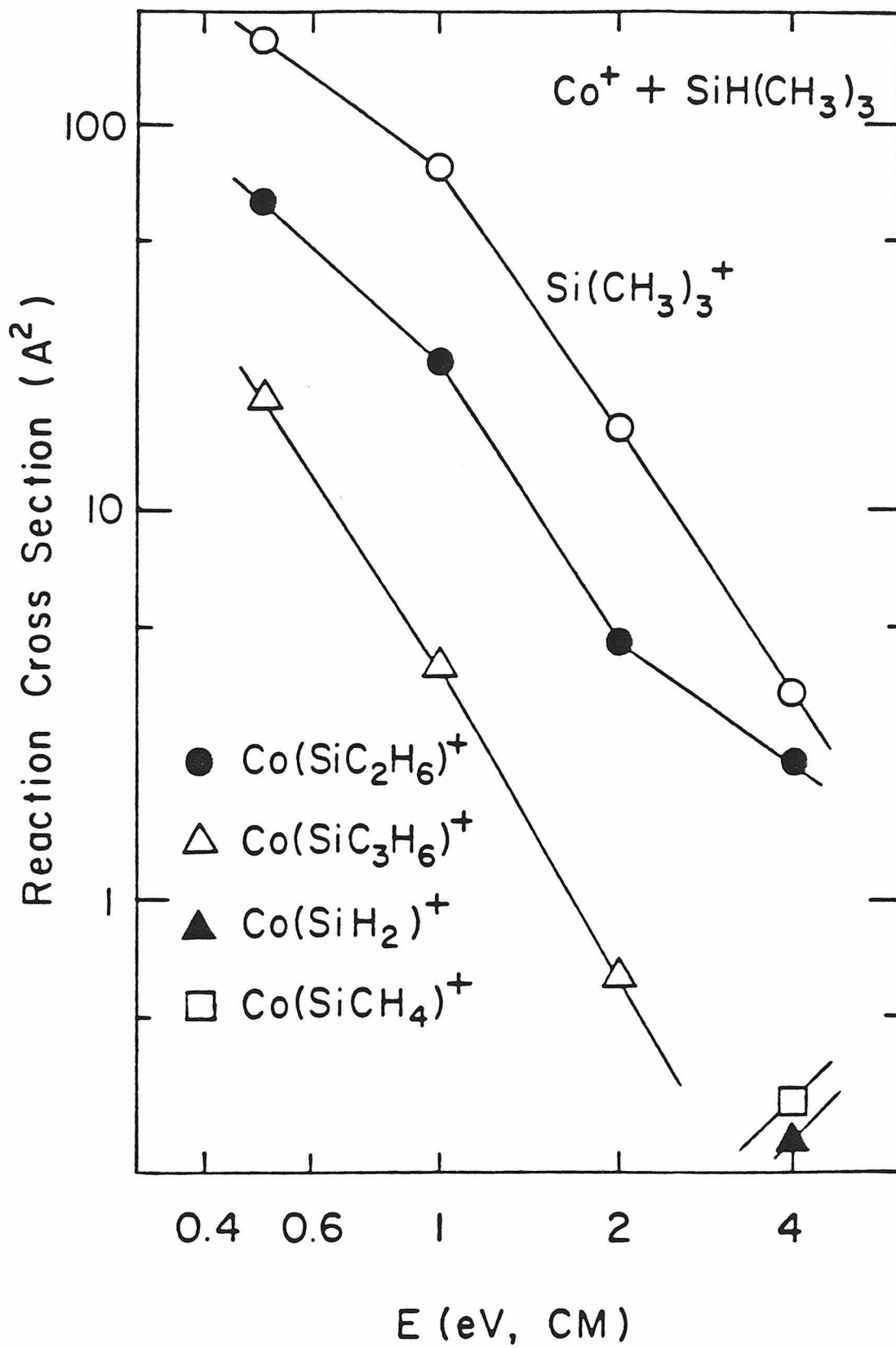
reaction. The hydride abstraction reaction of Co^+ with CH_3NH_2 has a much lower cross section, and it is possible that this process is due to an excited state of Co^+. The heterolytic Co^+-H^- bond energy is thus chosen to be equal to the heterolytic bond energy of CH_3NH_2, as indicated in Figure 3.

Previous ion beam experiments have determined bond energies very accurately from measurements of the thresholds for endothermic reactions.[43] However, for the hydride abstraction reactions studied here, this procedure is very difficult. For the case of Fe^+, Co^+ and Ni^+, excited state species complicate the threshold region, as illustrated in Figure 5. In addition, many exothermic processes are competing with endothermic hydride abstraction. This can greatly complicate the cross-section behavior, especially in the threshold region. The exothermicity or endothermicity of the hydride abstraction reactions is thus considered a better diagnostic probe of the thermochemistry for these reactions.

<u>Comparison with previous results.</u> The homolytic bond energies determined in the present study may be compared to available previous data, as indicated in Table 3. It can be seen that our numbers are systematically higher than those of Sallans et al.[13] by 7-13 kcal mol^{-1} for the three hydrides FeH, CoH, and MoH, that were studied using both methods. The numbers from Sallans et al. were obtained using a bracketing technique where the anionic M^- were allowed to react with a variety of acids (proton donors) to form metal hydrides. In the absence of excited state ions, which are not a problem in the case of the

negative ions, bracketing experiments necessarily give <u>lower</u>
<u>limits</u> to the bond energies. If the bond energies determined in
the present study are too high, a factor that could account for
this is the possibility of forming electronically excited
positive ions. As discussed previously, this is not a serious
problem for Ni, Ru, Rh, Pd or Mo.

It should be noted that the bond dissociation energies for
the first row metal hydrides obtained in this study compare
favorably with other experimental and theoretical values
available, with the exception of CoH. Our value for the bond
energy of CoH is substantially higher than any other previous
determination, especially the value of 39 kcal mol^{-1} reported in
an earlier study from our laboratory.[11] This value was obtained
by measuring the competitive decay of HCoR$^+$ to form either CoH$^+$ +
R or CoH + R$^+$. Preferential formation of the former product
resulted in the inference IP(CoH) < IP(R). This method
necessarily gives a lower limit for the ionization potential of
CoH because CoH$^+$ can also be formed by a direct stripping
reaction. This leads to a bond dissociation energy which is
actually a lower limit.

For the second row metal hydrides, there are few previous
experimental or theoretical values. No theoretical bond energies
are availabe for RhH and only an excited state value has been
determined for RuH.[44] Furthermore, the theoretical values
obtained for PdH are substantially lower than those measured in
this work. This is discussed in greater detail below.

<u>Analysis of bonding in transition metal hydrides.</u> The
second row group 8-10 metal hydrogen bond energies are all quite

similar, 56-59 kcal mol^{-1}, in contrast to the range of bond
dissociation energies observed for the first row metal hydrides
(43 - 65 kcal mol^{-1}). These values may be compared to the
binding of hydrogen to organometallic complexes. The data
available for group 8-10 metal hydrogen bonds in complexes are
presented in Table 5. It can be seen that most of these values
for M-H bonds are around 60 kcal mol^{-1}. This is in excellent
agreement with the values for the diatomic metal hydrides of the
second row. Note, however, that the bond energies to hydrogen in
the complexes are much greater than in the corresponding diatomics
for Fe and to a lesser extent for Co. Why is this the case?
This difference may be better understood by a close inspection of
the bonding of the diatomic hydrides.

Previous studies of bonding in the first row ionic hydrides
(M^{+}-H) have shown that the bond energies increase with decreasing
promotion energy from the ground state to a state derived from an
s^1d^n configuration.[38] This suggests a bond which involves a
metal s-orbital. In order to see if this trend is also true for
the neutral metal hydrides, the promotion energy needed to excite
the neutral metals to an s^1d^n configuration is needed. In
calculating this promotion energy, it is necessary to include any
exchange energy that is lost in forming the bond. When an s
electron is used for bonding, some s-d exchange energy may be
lost, depending on the electronic configuration of the metal
atom. This is because the bonding s electron is now only coupled
high spin to the remaining d electrons 50% of the time. This
effect can be roughly accounted for by averaging the energy to

TABLE 5. Metal–Hydrogen Bond Dissociation Energies in
Organometallic Complexes.

Complex	$\bar{D}(M{-}H)^a$, kcal/mol
$Fe(CO)_4H_2$	<65
$HCo(CO)_4$	57
$HCo(CN)_5^{3-}$	58
$H_3Ru(COCH_3)(CO)_9$	65
$Cp(PMe_3)RuH$	46[b]
$H_2RhCl(PAr_3)_3$	58[c]
$H_2RhCl(PAr_3)_2THTP^d$	58[c]
$Mo(Cp)_2H_2$	60

[a] From Reference 5, unless otherwise noted.

[b] Paciello, R.; Bercaw, J.E., work in progress.

[c] Drago, R.D.; Miller, J.G.; Hoselton, M.A.; Farris, R.D.;
Desmond, M.J. J. Am. Chem. Soc. 1983, 105, 444.

[d] THTP = tetrahydrothiophene.

promote to high and low spin coupled states, as indicated by Equation 5. The promotion energy defined in this way for the

$$P.E. = [E(s^1d^n \text{ high spin}) + E(s^1d^n \text{ low spin})] / 2 \qquad (5)$$

metals studied here are presented in Table 6.[45]

A plot of the bond energies determined in this study as a function of the promotion energy as defined above is indicated in Figure 7. With the notable exception of PdH, the first and second row metal hydrides fit the correlation reasonably well. This again suggests that a metal s orbital is being used for bonding in these metal hydrides. The "inherent" metal hydrogen bond energy determined by the intercept is 67 kcal mol^{-1}. It should be noted that previous determinations of bond energies fit marginally well onto the above graph. For example, Cu, Ag and Au all have promotion energies as defined by Equation 5 to be zero, due to their s^1d^{10} ground states. Their metal hydrogen bond energies are 67,[12] 54,[10b] and 74 kcal mol^{-1},[10b] respectively. Thus, although Cu and Au appear to fit the above correlation well, the value for Ag seems quite low.

The bond energies for the early transition metal hydrides do not fit the correlation depicted in Figure 7. This may be due to two possibilities. First, there are large deviations in the experimental values for the early transition metal hydrides. For example, the bond energy for CrH is given as 41 $\pm$ 3[13] or 67 $\pm$ 12 kcal mol^{-1}.[8] Furthermore, for ScH, VH, and MnH, there is only one experimental determination of the bond energy, and none for TiH.[46] If the determined bond energies are accurate, another explanation for the poor fit with the early metals may be that

TABLE 6. Promotion Energies to $s^1 d^n$ Configurations for Transition Metal Atoms.

| M | GROUND STATE | | | EXCITED STATE | | | |
	Config.	Des.	E^a kcal/mol	Config.	Des.	E^a kcal/mol	P.E.[b] kcal/mol
Fe	$d^6 s^2$	^5D	0.0	$d^7 s^1$	^5F	20.1	27.
				$d^7 s^1$	^3F	34.4	
Co	$d^7 s^2$	^4F	0.0	$d^8 s^1$	^4F	9.7	15.
				$d^8 s^1$	^2F	20.3	
Ni	$d^9 s^1$	^3D	0.0	$d^9 s^1$	^1D	7.6	4.
Ru	$d^7 s^1$	^5F	0.0	$d^7 s^1$	^3F	18.	9.
Rh	$d^8 s^1$	^4F	0.0	$d^8 s^1$	^2F	14.5	7.
Pd	d^{10}	^1S	0.0	$d^9 s^1$	^3D	21.9	28.
				$d^9 s^1$	^1D	33.4	
Mo	$d^5 s^1$	^7S	0.0	$d^5 s^1$	^5S	30.9	15.5

[a]Energies are weighted average of J states, Reference 26.

[b]Promotion energy calculated using Equation 5.

Figure 7. Variation in the monolytic metal-hydrogen bond energy as a function of metal atom promotion energy to an $s^1 d^n$ configuration.
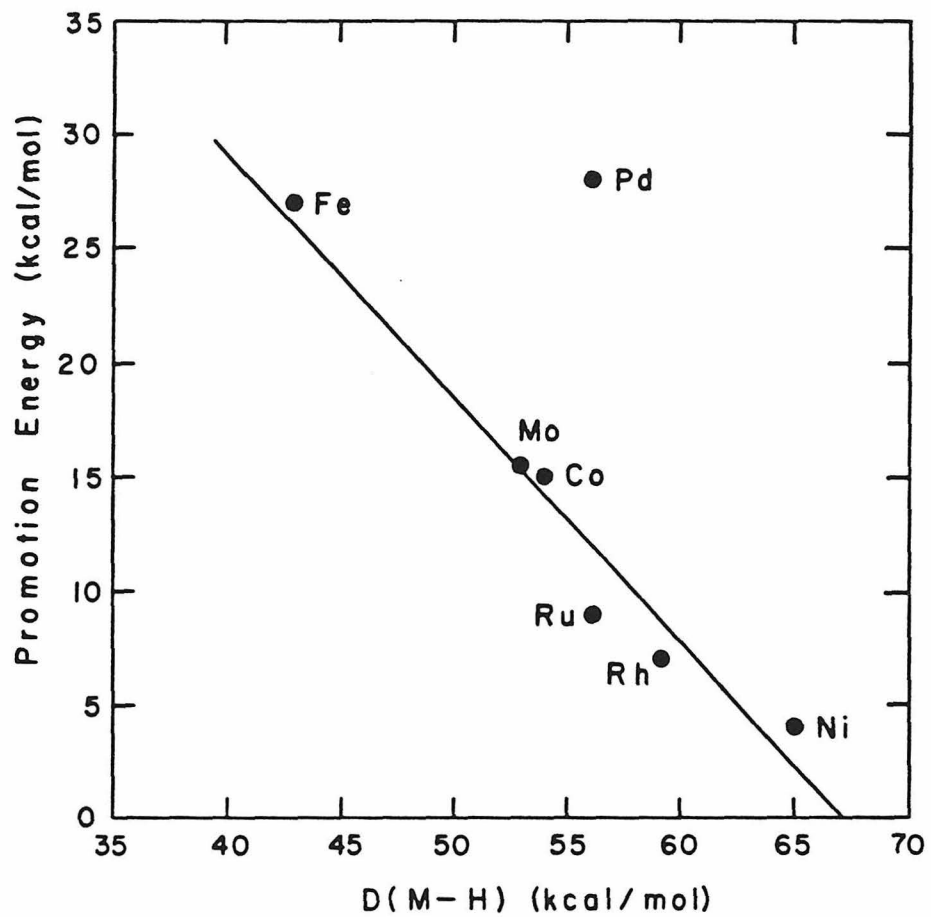
the bonding is quite different for these hydrides. For example, it has been found from ESR experiments that the chromium hydride bond has a significant amount of ionic character and is best described as $Cr^{+}-H^{-}$.[47] A correlation with promotion energy to an s^1d^n configuration would thus not be expected.

Note that the promotion energy for Fe is much larger than for Ru. This may be responsible for the difference between the diatomic and organometallic M-H bond dissociation energies for Fe. Addition of ligands may help to overcome the promotion energy and leave the iron orbitals better prepared for bonding. The same considerations also apply to CoH, but to a lesser extent due to the lower promotion energy. Thus the organometallic FeH and CoH bond energies are approximately the same strength as the RuH and RhH diatomic and organometallic bond energies.

A correlation between the metal hydride bond energies and the electron affinity of the metal atoms has recently been reported by Squires.[46] We also observe this correlation, as shown in Figure 8a, again with the exception of PdH. Although the slopes of the two correlation lines are similar, the intercepts are different in the two cases.

For all of the metals studied here except Pd, binding an electron leads to a metal anion whose ground state is derived from an s^2d^n configuration.[39] The ground states of Fe and Co are derived from s^2d^6 and s^2d^7 configurations, respectively. Thus in order to form FeH and CoH, one of two things must occur. Promotion to an s^1d^{n+1} configuration allows a bond to be made to the s orbital leading to a $d^{n+1}\sigma^2$ molecular configuration.

Figure 8. Variation in the a) homolytic M-H bond dissociation energy
and b) metal atom promotion energy as a function of metal
atom electron affinity.
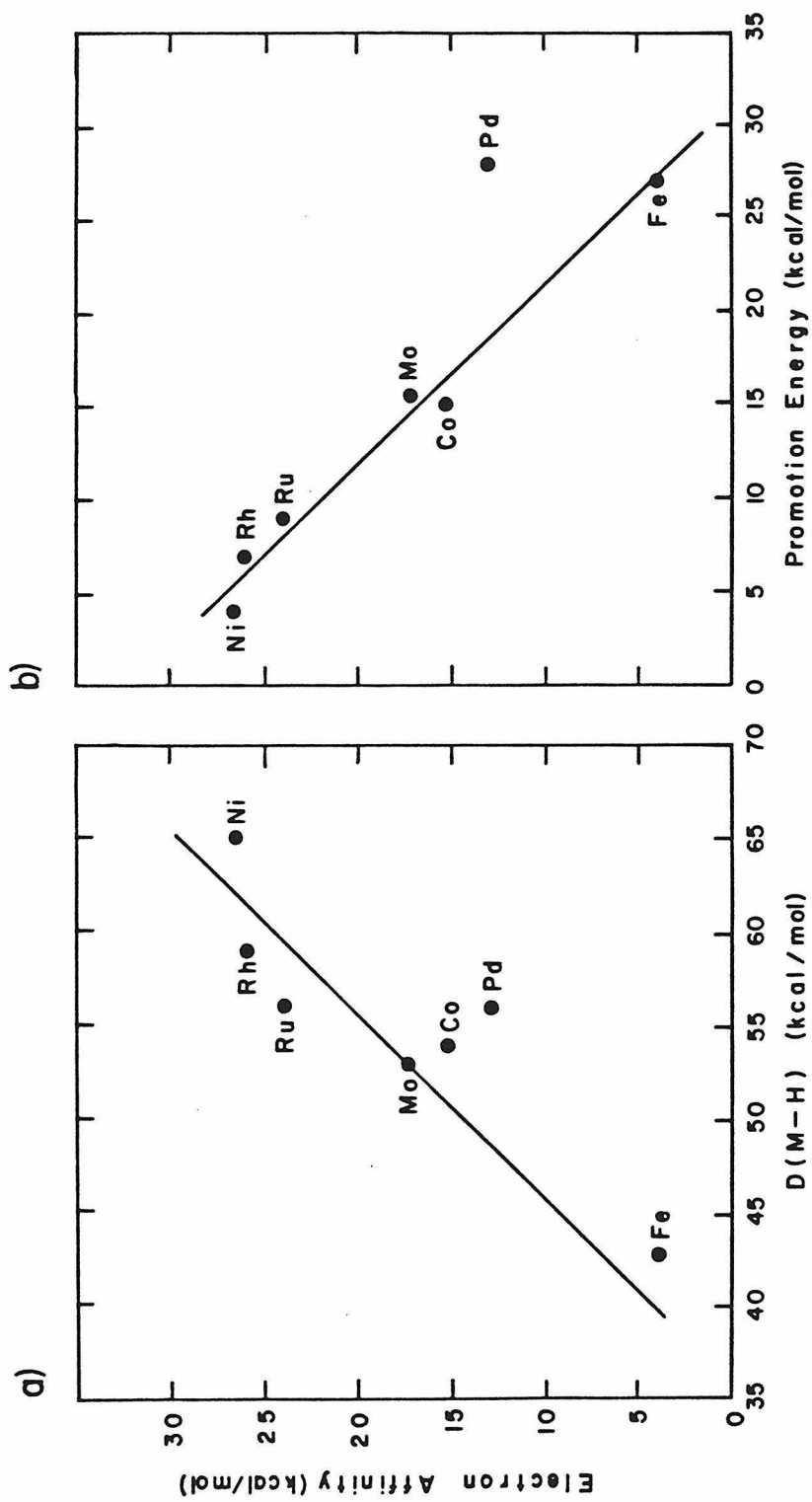
Alternatively, using an s^2d^n configuration, sp hybrid orbitals can be used to form $\sigma^{*1}d^n\sigma^2$ molecular configurations. As discussed by Mead et al.,[39] the former case occurs for Fe, Co and Ni, resulting in $^4\Delta$, $^3\Phi$ and $^2\Delta$ ground states, respectively. It is likely that the metal hydrides of Ru, Rh, and Mo also have $d^n\sigma^2$ ground state configurations due to their atomic s^1d^n ground states. This would lead to $^4\Phi$, $^3\Phi$, and $^6\Sigma$ ground states for RuH, RhH and MoH, respectively. Calculations indicate that the ground state for RuH is indeed the $^4\Phi$ state.[44] It should be noted that the s^2d^n configuration which would lead to sp hybrid bonding is significantly higher in energy for Mo, Ru and Rh,[26] making this possibility less likely. The correlation between the diatomic configuration $d^n\sigma^2$, and the negative metal ion configurations d^ns^2 has previously been noted.[46] This correlation between electron and hydrogen atom binding lends additional support to the belief that a metal s orbital is being used in the formation of the MH bond. Furthermore, calculations for FeH, CoH and NiH also find bonds which are predominantly s-like in character, using a metal s^1d^n configuration.[17]

It is important to note that the above correlation with electron affinity does not imply that the M-H bond is best described as M^--H^+. In fact, if any ionic character is present in the bonds, a much more likely structure would be M^+-H^-, due to the low metal ionization potentials relative to that of hydrogen. For example, a correlation between the MH bond energy and the electron affinity for the alkali metals has previouly been noted.[46-48] In this case, the bonding should certainly not be described as M^--H^+. The correlation with electron affinity in

our study probably reflects the similar metal atom promotions that must occur in order to bind either an electron or a hydrogen atom. In both cases, the metal atom is promoted to an s^1d^n configuration where the s electron is coupled equally high and low spin to the remaining d electrons. It is thus not surprising that there is a linear correlation between the electron affinity and the promotion energy, as indicated in Figure 8b.

As mentioned earlier, the ionization potentials of MH have been determined using Equation 3 and are presented in Table 4. It can be seen that for Co, Ni, Ru, Rh, Pd and Mo, IP(MH) > IP(M). It should be noted that attempts to form ionic metal hydrides using surface ionization have failed, perhaps due to the higher ionization potential of the metal hydrides relative to the metal atoms. As indicated in Table 6, the ground states of Ru, Rh, and Mo are derived from s^1d^n configurations. As discussed previously, the bond to H involves the metal s orbital, as indicated by structure 1. As seen in Table 1, the ionic ground
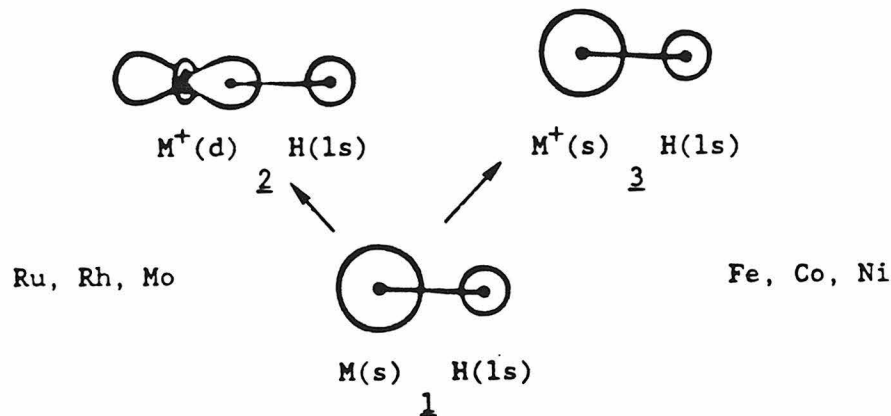
state for Ru^+, Rh^+ and Mo^+ are all derived from d^n configurations, and the bonding orbitals are thought to be primarily d in character for M^+-H,[37] as indicated by structure 2.

Note that in both cases, M and MH, an s electron is ionized. However, ionization of MH for Ru, Rh, and Mo involves ionizing an s electron that is used for bonding. This results in an ionization potential of MH which exceeds that of M for these metals.

The case for Fe, Co, and Ni is somewhat different. The bonding in MH still involves a metal s orbital as indicated by $\underline{1}$. However, for these metals, the ionic hydrides also form bonds using primarily s-like orbitals,[35,49] as indicated by structure $\underline{3}$. Therefore, ionization of MH for Fe, Co and Ni involves a d electron which is not used in bonding. As discussed previously, neutral iron and cobalt both posess ground states derived from $s^2 d^n$ configurations. Promotion to an $s^1 d^{n+1}$ configuration must occur in order to bind hydrogen to these atoms. On the other hand, the $s^1 d^n$ ionic configurations used for bonding in $\underline{3}$ do not represent the ground state configurations for Co^+ and Ni^+ (ground d^n configurations).[26] Thus for Fe, Co and Ni, the differences in atomic and metal hydride ionization potentials reflect differences in the atomic and ionic promotion energies to a bonding $s^1 d^n$ configuration. For cobalt, the two promotion energies are roughly equal, and the ionization potentials are similar as well. For nickel, a much larger promotion energy for the ion results in a larger MH ionization potential. Finally, for iron, a much larger atomic promotion energy results in a larger atomic ionization potential.

As noted previously, palladium does not fit well onto the correlations described above. This suggests that the bonding in PdH is significantly different than for the other metals

discussed thus far. There is a large discrepancy in the experimental and theoretical estimates for the PdH bond energy. As indicated in Table 3, two experimental values have been determined; 56 $\pm$ 6 (this work) and < 76 kcal mol^{-1}.[16] The theoretical values determined are much lower, ranging from 30 kcal mol^{-1},[50] to 46 kcal mol^{-1}.[51]

The ^{1}S ground state of Pd is derived from a $4d^{10}$ configuration[26], which is unable to form covalent bonds with hydrogen. The ^{3}D state derived from a $5s^1 4d^9$ configuration is 0.95 eV higher in energy. If the ^{3}D state were used to form a purely s bond to H, the correlations in Figures 7 and 8a would predict D(Pd-H)=42 and 48 kcal mol^{-1}, respectively. These values, especially the former, are much lower than the observed value. This indicates that the bonding in PdH is probably more complicated.

The ground state of PdH has been determined spectroscopically to be a $^2\Sigma$ state.[16] Low temperature ESR studies of PdH in rare gas matrices have indicated that the bonding in PdH is almost purely ionic Pd$^+$-H$^-$, with the singly occupied orbital being predominantly a Pd 4d orbital.[52] The spectroscopically determined bond length for PdH is quite small, 1.534 A. An estimate for the strength of a purely electrostatic bond can be calculated from Equation 6, where q_1 and q_2 are the

$$D_e(M^+-H^-) = (q_1 q_2 / R_o) - IP(M) + EA(H) - E_R \qquad (6)$$

ionic charges, R_o is the equilibrium separation, and E_r is the Pauli repulsion energy of the electron clouds on the two centers.

Ignoring repulsions, an ionic bond energy of 42 kcal mol^{-1} is calculated for PdH at a bond length of 1.534 A using Equation 6. Of course, the actual ionic contribution will be less due to electronic repulsions. Possible justification for a fairly large ionic contribution to the PdH bond lies in the fact that the orbitals for Pd$^+$ are actually quite small. The ground state configuration of Pd$^+$ is 4d^9, and the size of these d orbitals is approximately 0.8 A.[53] This is about half the size of the occupied 4s orbitals of the early first row transition metal ions. The Pd$^+$ 4d orbitals are also smaller than the 3d orbitals for the early metal ions of the first row.[53] Smaller orbitals for Pd$^+$ may result in less Pauli repulsion energy and perhaps make a partially ionic bond possible.

Theoretical calculations all indicate participation of 4d electrons in the bonding of H to Pd. However, the results differ as to the exact nature of this bond. One group finds an ionic chemical bond where the metal atom is mainly involved in sigma donation.[50] Other calculations indicate only a partially ionic bond where the electronic charge on hydrogen is -0.3 electrons.[54] The above calculations find the bond energies D(Pd-H)=30 and 35 kcal mol^{-1}, respectively. It should be noted that in the latter study, the bond energy of NiH was reported to be 45 kcal mol^{-1}, which is substantially lower than the generally accepted value of 60-65 kcal mol^{-1} (Table 3). Other theoretical results get a somewhat higher bond energy of 46 kcal mol^{-1} for PdH.[51] However, these calculations also find the order of the two lowest electronic states inverted by 1.20 eV. Thus the calculations have been unable to reproduce the high experimental value

obtained for the PdH bond energy. It appears that the reason PdH does not fit the correlations well is due to two factors: participation of d electrons in the bonding, and at least partial ionic bond character. It should be noted that the PdH bond dissociation energy determined here is in excellent agreement with the _average_ bond energy calculated recently for PdH_2, 53 kcal mol^{-1}.[55] However, this agreement is likely to be fortuitious. Promotion to an s^1d^9 state leaves the metal well suited to form two covalent sigma bonds, where the first bond would be expected to be weaker than the second.

Implications for transition metal ion reactivity. As mentioned in the Introduction, the present study was in part motivated by the observation of quite distinct reactivity for Pd^+ with alkanes relative to that for Ru^+ and Rh^+. The uniquely high hydride affinity of Pd^+ was proposed to be responsible for the reactivity observed.[24] It was suggested that Pd^+ activates the C-H bonds of alkanes by a heterolytic process whereby H^- is transferred to Pd^+ as a firt step. Because the hydride affinities of the other metal ions presented in this study are so much lower, they are not likely to undergo similar heterolytic C-H bond activation. Rather, it is likely that alkane activation for these metal ions proceeds via 3-center homolytic bond insertions.

Conclusion

The homolytic metal hydrogen bond dissociation energies for RuH, RhH and PdH are all comparable, in the range 56-59 kcal

mol^{-1}. In contrast, the corresponding bond energies for FeH, CoH and NiH are more varied; 43, 54 and 65 kcal mol^{-1}, respectively. With the exception of PdH, these observed bond energies can be understood in terms of the promotion energy of the metal atom to a state derived from an s^1d^n configuration. The bonds of these metal hydrides utilize what is predominantly a metal s orbital. This is supported by a correlation with the electron affinities of the metal atoms. The bonding in PdH is quite distinct from the other metal hydrides. This is indicated by the lack of correlation of the metal-hydrogen bond strength with metal atom promotion energy or electron affinity. This is probably due to participation of metal d electrons in the bonding, as well as partial ionic bond character for PdH.

References

1. Hlatky, G. G.; Crabtree, R. H. Coord. Chem. Rev. 1985, 65, 1, and references therein.

2. Tolman, C. A. in Transition Metal Hydrides, Meutterties, E. L., ed.. Marcel Dekker: New York, 1971.

3. Dombek, B. D. Organometallics 1985, 4, 1707.

4. Hiraki, K.; Ochi, N.; Sasada, Y.; Hayashida, H. Fuchita, Y.; Yamanaka, S. J. Chem. Soc. Dalton Trans. 1985, 5, 873.

5. Pearson, R. G. Chem. Rev. 1985, 85, 41.

6. Halpern, J. Inorg. Chim. Acta 1985, 100, 41.

7. Simoes, J. A. M.; Beauchamp, J. L. Chem Rev., in press.

8. Gaydon, A. G. Dissociation Energies and Spectra of Diatomic Molecules. Chapman and Hall: London, 1968.

9. Huber, K. P.; Herzberg, G. Molecular Spectra and Molecular Structure IV. Constants of Diatomic Molecules. Van Nostrand-Reinhold Co.: New York, 1979.

10. a) Kant, A.; Moon, K. A. High Temp. Sci. 1981, 14, 23.

    b) Kant, A.; Moon, K. A. High Temp. Sci. 1979, 11, 55.

11. Armentrout, P. B.; Beauchamp, J. L. J. Am. Chem. Soc. 1981 103, 784.

12. Burnier, R. C.; Byrd, G. D.; Freiser, B. S. Anal. Chem. 1980, 52, 1641.

13. Sallans, L.; Lane, K. R.; Squires, R. R.; Freiser, B. S. J. Am. Chem. Soc. 1985, 107, 4379.

14. Connor, J. A. Top. Curr. Chem. 1977, 71, 101.

15. Cheetham, C. J.; Barrow, R. F. Adv. in High Temp. Chem. 1967, 1, 7.

16. Malmberg, C.; Scullman, R.; Nylen, P. Ark. Fys. 1969, 39, 495.

17. Scott, P. R.; Richards, W. G. Mol. Spectroscopy. Chem. Soc. Spec. Per. Reports. 1976, 4, 70.

18. Das, G. J. Chem. Phys. 1981, 74, 5766.

19. Walch, S. P.; Bauschlicher, C. W. J. Chem. Phys. 1983, 78, 4597.

20. Dendramis, A.; Van Zee, R. J.; Weltner, Jr. W. Astrophys. J. 1979, 231, 632.

21. EA(H) = 17.4 kcal/mol from Wagman, D. D.; Evans, W. H.; Parker, V. B.; Harlow, I.; Bailey, S. M.; Schumm, R. H. Natl. Bur. Stand. Tech. Note 270-3, 1968.

22. Stevens, A. E.; Beauchamp, J. L. Chem. Phys. Lett. 1981, 78, 291.

23. Meot-Ner, M. J. Am. Chem. Soc. 1982, 104, 5.

24. Tolbert, M. A.; Mandich, M. L.; Halle, L. F.; Beauchamp, J. L., submitted to J. Am. Chem. Soc.

25. a) Armentrout, P. B.; Beauchamp, J. L. Chem. Phys. 1980, 50, 21.

    b) Armentrout, P. B.; Beauchamp, J. L. J. Chem. Phys. 1981, 74, 2819.

26. Moore, C. E. Atomic Energy Levels. National Bureau of Standards: Washington DC, 1949.

27. Halle, L. F.; Klein, F. S.; Beauchamp, J. L. J. Am. Chem. Soc. 1984, 106, 2543.

28. Pellerite, M. J.; Brauman, J. I. J. Am. Chem. Soc. 1983, 105, 2672.

29. Pellerite, M. J.; Brauman, J. I. J. Am. Chem. Soc. 1980, 102, 5993.

30. Moylan, C. R.; Brauman, J. I. Ann. Rev. Phys. Chem. 1983, 34, 187.

31. Schilling, J. B.; Beauchamp, J. L., work in progress.

32. Unless otherwise noted, the heterolytic bond dissociation energies for the hydride donors were taken from Lossing, F. P.; Holmes, J. L. J. Am. Chem. Soc. 1984, 106, 6917. $D(N(CH_3)_2NCH_2^+-H^-)$ from Lossing, F. P.; Lam, Y. T.; Maccoll, A. Can J. Chem. 1981, 59, 2228. $D((CH_3)_3Si^+-H^-)$ from Corderman, R. R.; Beauchamp, J. L., unpublished results. Other values for $D(A^+-H^-)$ calculated from heats of formation of A^+. $\Delta H_f(CH_3OCH_2^+)=157$ kcal/mol and $\Delta H_f(C_2H_5OCHCH_3^+)=116$ kcal/mol from Lossing, F. P. J. Am. Chem. Soc. 1977, 99, 7526. $\Delta H_f(C_2H_4OH^+)$ from Rafaey, K. M. A.; Chupka, W. A. J. Chem. Phys. 1968, 48, 5205. Auxiliary heats of formation of the neutral molecules AH from Cox, J. D.; Pilcher, G. Thermochemistry of Organic and Organometallic Compounds. Academic Press: New York, 1970.

33. Radecki, B. D.; Allison, J. J. Am. Chem. Soc. 1984, 106, 946.

34. Burnier, R. C.; Byrd, G. D.; Freiser, B. S. J. Am. Chem. Soc. 1981, 103, 4360.

35. Armentrout, P. B.; Halle, L. F.; Beauchamp, J. L. J. Am. Chem. Soc. 1981, 103, 6501.

36. Halle, L. F.; Armentrout, P. B.; Beauchamp, J. L. Organometallics 1982, 1, 963.

37. Mandich, M. L.; Halle, L. F.; Beauchamp, J. L. J. Am. Chem. Soc. 1984, 106, 4403.

38. Elkind, J. L.; Armentrout, P. B., submitted.

39. Mead, R. D., Stevens, A. E.; Lineberger, W. C. in Gas Phase Ion Chemistry, Vol. III, Bowers, M. T., ed.. Academic Press: New York, 1984.

40. Stevens, A. E.; Feigerle, C. S.; Lineberger, W. C. J. Chem. Phys. 1983, 78, 5420.

41. This estimate for the collision cross section is based on the interaction of an ion with a polarizable neutral: Gioumousis, G.; Stevenson, D. P. J. Chem. Phys. 1958, 29, 294. This value is actually a lower limit to the collision cross section because it does not take into account ion-dipole interactions which are important for the reaction with dimethylether.

42. Armentrout, P. B., private communication.

43. Elkind, J. L.; Armentrout, P. B. J. Phys. Chem. 1984, 88, 5454.

44. Krauss, M.; Stevens, W. J. J. Chem. Phys. 1985, 82, 5584.

45. A more detailed calculation of the promotion energy including exchange terms is given in Reference 37.

46. Squires, R. R. J. Am. Chem. Soc. 1985, 107, 4385.

47. Van Zee, R. J.; DeVore, T. C.; Weltner, W. Jr. J. Chem. Phys. 1979, 71, 2051.

48. Yang, S. C. J. Chem. Phys. 1983, 78, 4541.

49. Schilling, J. B.; Goddard, W. A. III.; Beauchamp, J. L., J. Am. Chem. , accepted.

50. Pacchioni, G.; Koutecky, J.; Fantucci, P. Chem. Phys. Lett. 1982. 92, 486.

51. Basch, H.; Cohen, D.; Topiol, S. Isr. J. Chem. 1980, 19, 233.

52. Knight, L. B.; Weltner, W. Jr. J. Mol. Spectrosc. 1971, 40, 317.

53. Schilling, J. B.; Goddard, W. A. III.; Beauchamp, J. L., to be submitted.

54. Bagus, P. S.; Bjorkman, C. Phys. Rev. A. 1981, 23, 461.

55. Low, J.; Goddard, W. A. III. J. Am. Chem. Soc. 1984, 106, 8321.

CHAPTER IV

ACTIVATION OF ALKANES BY Ti^+ AND V^+ IN THE GAS PHASE:
MECHANISTIC STUDY USING DEUTERIUM LABELLED ALKANES

Activation of Alkanes by Ti$^+$ and V$^+$ in the Gas Phase:

Mechanistic Study Using Deuterium Labelled Alkanes

M. A. Tolbert and J. L. Beauchamp

ABSTRACT

The reactions of Ti$^+$ and V$^+$ with alkanes and deuterium labelled alkanes are studied using an ion beam apparatus. The dominant reactions observed for both of these metal ions are single and double dehydrogenations. Alkane loss reactions are also observed for Ti$^+$, but may be due to electronically excited states. The dehydrogenation mechanisms are investigated using partially deuterated alkanes. The results are consistent with 1,2-eliminations for both V$^+$ and Ti$^+$, where deuterium scrambling may occur in the latter case. It is proposed that some 1,3-elimination of hydrogen also occurs in the reaction of Ti$^+$ with n-butane. Although the dehydrogenation reactions of V$^+$ and Ti$^+$ appear to be similar to those of Ru$^+$ and Rh$^+$, there are some important differences in the reactivity of V$^+$. Extensive adduct formation and large deuterium isotope effects are consistent with reaction intermediates which are relatively long-lived for V$^+$ in comparison to Ti$^+$, Ru$^+$ and Rh$^+$. The cause of this behavior is suggested to arise from the inability of V$^+$ to form two strong sigma bonds due to the $3d^4$ electronic configuration of the ground state ion. This renders C-H bond insertion energetically much less favorable for V$^+$ than for the other metal ions and limits the excitation energy of reaction intermediates.

Introduction

Recent studies have indicated that a wide variety of transition metal ions are capable of activating the bonds of totally saturated hydrocarbons.[1-6] These studies have revealed that, although groups of transition metal ions exhibit similar reactivity (i.e., Ru^+, Rh^+; Fe^+, Co^+, Ni^+), there are also intriguing differences in reactivity from one metal ion to another. For example, the metal ion mediated dehydrogenation of n-butane has been shown to proceed via at least three distinct mechanisms, illustrated in Scheme 1. It has been proposed that

Scheme 1
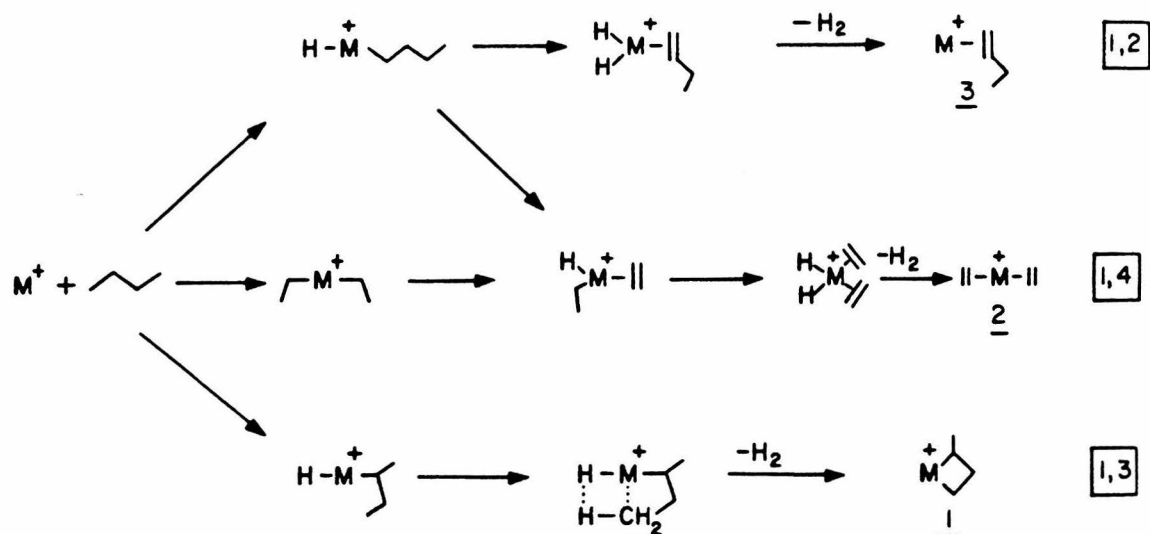
Sc^+ effects a predominantly 1,3-elimination,[5] resulting in the formation of a metallocyclobutane complex, **1**. Dehydrogenation at Ni^+ centers has been shown to occur by a 1,4-elimination mechanism,[3] resulting in the formation of a metal-bisolefin

complex, 2. Pd[+] appears to effect a selective 1,2-elimination across the central C-C bond exclusively,[4] forming a monoolefin complex, 3. Although these studies have led to a greater understanding of C-H bond activation processes, it is still not possible to predict, _a priori_, the mechanisms by which the bonds of alkanes are cleaved by transition metal ions.

In the present study, we report the reactions of Ti^{+} and V[+] with alkanes, with the specific objective of examining the dehydrogenation reactions that occur at these metal ion centers. The bond strengths of H and CH_3 to these metal ions have been reported previously[7,8] and are summarized in Table 1. Some of the chemistry of Ti^{+} and V[+] with hydrocarbons has been reported previously,[8-12] but these studies have not utilized deuterium labelled alkanes. Earlier studies in our laboratory have benefited greatly from the use of labelled hydrocarbons.[1c,3,4,5] In this study, partially deuterated alkanes are used to help elucidate the reaction mechanisms for alkane activation by Ti^{+} and V[+]. Deuterium isotope effects are explored by studying the reactions with partially and totally deuterated alkanes. The reactivity of Ti^{+} and V[+] is compared to that of other transition metal ions, both early, (Sc[+]),[5] and late (Fe^{+}, Co^{+}, Ni^{+}, Ru[+], Rh[+] and Pd[+]).[1,4] The differences in reactivity and isotope effects are discussed in terms of the electronic configurations of the metal ions.

Experimental

The ion beam apparatus used in the present study has been described previously.[13] Briefly, ion beams of Ti^{+} and V[+] are

TABLE 1. Bond Dissociation Energies.[a]

| M^+ | $D(M^+-H)$ | | $D(M^+-CH_3)$ |
	Exp	Theory[b]	Exp
Ti^+	55.[c]	55.	56.5[c]
V^+	48.[d]	44.5	50[d]

[a]All values in kcal/mol.

[b]Reference 33.

[c]Reference 7.

[d]Reference 8.

produced by vaporization of $TiCl_4$ and $VOCl_3$ onto a hot rhenium filament, and subsequent surface ionization at 2500 K. The excited state distributions of Ti^+ and V^+ at 2500 K are indicated in Table 2.[14] It can be seen that a substantial portion of the ions are formed in electronically excited states for Ti^+ and V^+, 37% and 23%, respectively. Furthermore, because the transitions between the low-lying states are all parity forbidden, it is expected that the excited state lifetimes will be quite long.[15] The metal ions are collimated, mass- and energy-selected, and focussed into a collision chamber containing the neutral reactant at ambient temperature. Product ions scattered in the forward direction are analyzed using a quadrupole mass spectrometer. The flight time of the metal ions through the apparatus is approximately 10-30 usec, which may be shorter than the excited state lifetimes of the metal ions. Thus, the reactions observed could be a combination of ground and excited state reactions.

Deuterium labelled CH_3CD_3(98 %D), propane-2,2-d_2(98 %D), propane-d_8 (98.5% D), n-butane-1,1,1,4,4,4-d_6(98 %D), n-butane-d_{10} (98.5 %D), and 2-methylpropane-2-d_1(98 %D) were obtained from Merck, Sharp and Dohme.

Results

Both Ti^+ and V^+ react with alkanes to form a variety of products. Although the major products of these reactions are quite similar, there are substantial differences in the minor products. For example, the cross-section behavior for the reactions of Ti^+ and V^+ with n-butane is illustrated in Figures 1

TABLE 2. Lower Electronic States of Ti^+ and V^+ and Their Relative Ion Populations at 2500 K.

	State	Configuration	Energy[a]	Relative Population
Ti^+	^4F	$3d^2 4s^1$	0.00	.61
	^4F	$3d^3$	0.11	.37
	^2F	$3d^2 4s^1$	0.56	.02
	^2D	$3d^2 4s^1$	1.05	<.01
V^+	^5D	$3d^4$	0,00	.77
	^5F	$3d^3 4s^1$	0.34	.23
	^3F	$3d^3 4s^1$	1.08	<.01

[a]State energies in eV are a weighted average over the J states from Reference 14.

and 2, respectively. The exothermic reactions are easily identi-
fied since their cross sections decrease with increasing relative
kinetic energy. It can be seen that the two most prominent
exothermic processes for Ti^+ and V^+ reacting with n-butane are
the same, namely, loss of one and two molecules of H_2. However,
the reaction of Ti^+ with n-butane also results in a variety of
minor exothermic products not observed for V^+. This trend is
true in general for the reactions of Ti^+ and V^+ with alkanes.

Product distributions and overall cross sections for the
reactions of Ti^+ and V^+ with alkanes at a relative kinetic energy
of 0.5 eV are given in Table 3. Also included in this table are
previous results from ion cyclotron resonance (ICR) experi-
ments.[9,10] The major products in most cases are similar, using
the two methods. However, our study finds a number of minor
products not reported previously for Ti^+. There are two possible
explanations for the differences. First, it is possible that
these products were overlooked in the earlier study because they
comprise such a small fraction of the product distribution. No
products were reported in the earlier study that had an abundance
of less than 4% of the total product. A second possibility is
that the minor processes we observe are due to electronically
excited state ions. This may certainly be the case. However, it
is expected that excited state ions would be as abundant, or even
more so in the ICR studies because the ions are created by elec-
tron impact ionization of volatile organometallic precursors at
70 eV. Ions created in this way have previously been shown to be
formed with a high degree of electronic as well as translational
excitation.[16-18] The possiblility that different electronically

Figure 1. Variation in the experimental cross section for the reaction of Ti^+ with n-butane as a function of relative kinetic energy in the center of mass frame.
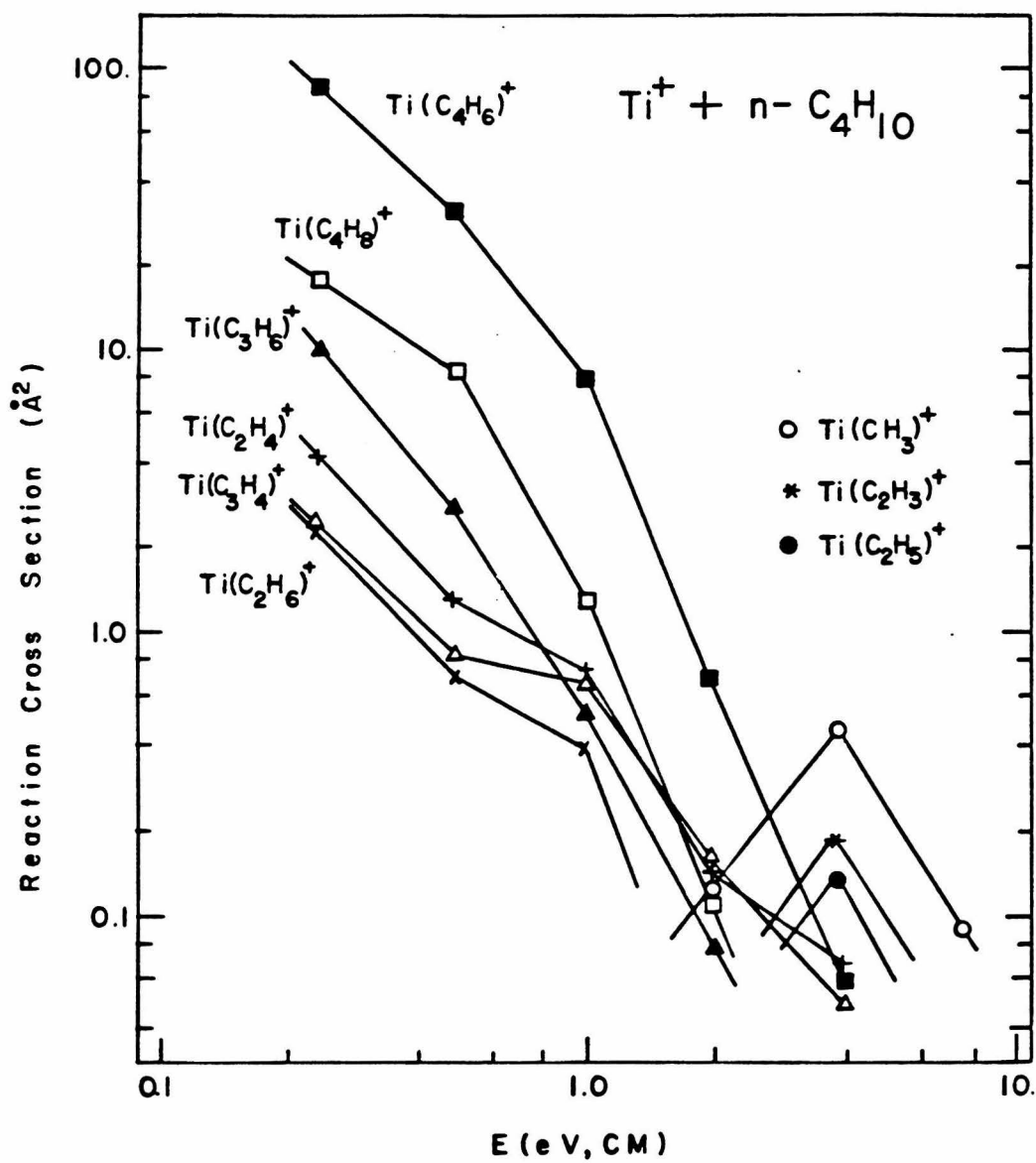
Figure 2. Variation in the experimental cross section for the reaction
of V^+ with n-butane as a function of relative kinetic energy
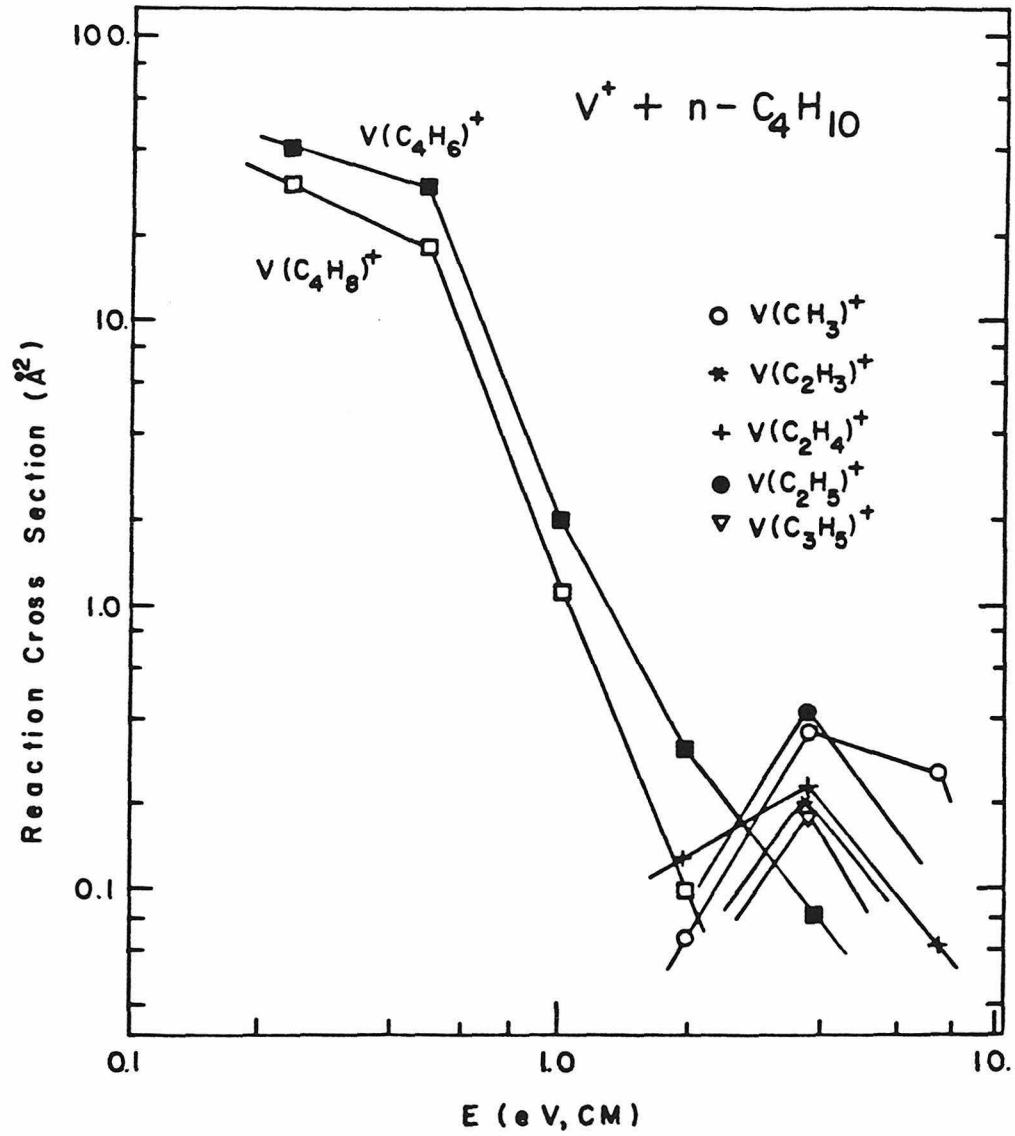in the center of mass frame.

TABLE 3. Product Distributions for the Reactions of Ti^+ and V^+ with Alkanes at a Relative Kinetic Energy of 0.5 eV.[a]

Alkane	Neutral Products	Ti^+ Ion Beam	Ti^+ ICR[b]	V^+ Ion Beam	V^+ ICR[c]	σMax[d]
C_2H_6	H_2	.96	1.0	1.0	no reaction	
	$2H_2$*	.04				
	σTOT[e]	5.2		0.9		50.
C_3H_8	H_2	.94	1.0	1.0	1.0	
	$2H_2$*	.03				
	CH_4	.03				
	σTOT	55.		13.		60.
$n-C_4H_{10}$	H_2	.17		.39		
	$2H_2$	.66	1.0	.61		
	CH_4	.09		tr		
	CH_4+H_2	.03				
	C_2H_4	.02				
	C_2H_6	.03		tr		
	σTOT	45.		48.		68.
iso-C_4H_{10}	H_2	.90	.84	1.0		
	$2H_2$	.06	.16			
	CH_4	.02				
	CH_4+H_2	.01				
	C_2H_4	.01				
	σTOT	154.		65.		68.

TABLE 3. (cont'd).

| Alkane | Neutral Products | Ti^+ | | V^+ | | d |
		Ion Beam	ICR[b]	Ion Beam	ICR[c]	σMax
2,2-dimethyl-propane	H_2	.54	.22			
	$2H_2$	.05	.16			
	CH_4	.15		.76		
	CH_4+H_2	.26	.62	.24		
	σTOT	73.		3.0		75.
2,2,3,3-tetra-methyl-butane	$2H_2$	.70		.67		
	CH_4+H_2	.11				
	$C_2H_6+H_2$	.09				
	C_3H_8	.05				
	$C_3H_8+H_2$	.01				
	C_4H_{10}	.03		.33		
	$C_4H_{10}+H_2$	.01				
	σTOT	141.		30.		94.

[a]Reaction products which exhibit reaction thresholds characteristic of endothermic processes are indicated by an asterisk.

[b]Reference 9.

[c]Reference 10.

[d]Maximum cross section predicted from the encounter rate based on an ion interacting with a polarizable neutral: Gioumousis, G.; Stevenson, D.P. J. Chem. Phys. 1958, 29, 294. Polarizabilities from Chan, S.C.; Rabinovitch, B.S.; Bryant, J.T.; Spicer, L.D.; Fujimoto, Y.N.; Pavlou, S.P. J. Phys. Chem. 1970, 24, 3160. Cross sections in A^2.

[e]Total reaction cross section are ±50%, in $\overset{\circ}{A}^2$.

excited states are accessed by the two methods of ion formation could account for some of the observed differences.

As mentioned above, the minor products in the reactions of Ti^+ and V^+ might very well be due to electronically excited states. This would result in the observed cross sections being combinations of exothermic excited state reactions and endothermic ground state reactions. This type of cross-section behavior was recently reported for the reaction of V^+ with ethane.[8] The authors concluded that the exothermic reaction was due entirely to excited state V^+. Our results for the reaction of V^+ with C_2H_6 are in agreement with these previous results. We observe other reactions for V^+ which may be due solely to excited state reactions. For example, the reaction of V^+ with 2,2-dimethylpropane forms two products, but the total reaction cross section is extremely low, only 3 A^2 at a relative kinetic energy of 0.5 ev (Table 3). It is very likely that both of these products are due entirely to excited state reactions, and that the ground state of V^+ does not undergo any exothermic reactions with 2,2-dimethylpropane.

In addition to the reaction products indicated in Table 3, adducts of the reactant metal ions with the parent hydrocarbon are often observed in the ion beam experiment at low relative kinetic energies. As mentioned previously, the flight time through the collision chamber and detector is approximately 10-30 usec. Thus, adducts with lifetimes in this range will be detected directly in the present experiment. At pressures of 1.5 mtorr, the time between collisions is also approximately 10 usec. Thus,

adducts which live 10 usec have the possiblilty of suffering a second collision. This could lead to stabilization of the adduct ion which might then live long enough to be detected. The extent of adduct formation for Ti^+ and V^+ reacting with alkanes is indicated in Table 4, along with previous results for other metal ions. It can be seen that, although similar products are formed in the reactions of Ti^+ and V^+, the extent of adduct formation is dramatically different for the two metal ions. Whereas adducts of Ti^+ are only a very small fraction of the total product, V^+ reactions are characterized by extensive adduct formation. In fact, adducts make up over 97% of the total products for the reactions of V^+ with 2,2-dimethylpropane. This indicates that the lifetimes of the adducts of V^+ are much longer-lived than the corresponding adducts of the other metal ions, with the exception of Pd^+.

In order to gain insight into the specific reaction mechanisms, the reactions of Ti^+ and V^+ with deuterium labelled alkanes were studied. The results for the exothermic dehydrogenations of labelled alkanes at a relative kinetic energy of 0.5 eV are given in Table 5. The results for the alkane loss reactions are presented in Table 6.

As indicated in Table 3, a minor product observed in the reaction of Ti^+ with n-butane is $Ti(C_2H_6)^+$. With the use of labelled n-butane-1,1,1,4,4,4-d_6, it is seen that this product corresponds to $Ti(C_2D_6)^+$. This suggests a dimethyl species similar to that proposed previously for Sc^+.[5] If formation of this product is due to ground state Ti^+, then exothermic observation of this reaction indicates that the sum of the first

TABLE 4. Adduct Formation in the Reactions of Transition Metal Ions with Alkanes.[a]

	Sc^{+}[b]	Ti^{+}	V^{+}	Fe^{+}[c]	Co^{+}[c]	Ni^{+}[c]	Ru^{+}[c]	Rh^{+}[c]	Pd^{+}[c]
C_2H_6	0	.01	.25	d	d	d	0	0	d
C_3H_8	0	.01	.32	.42	.39	.25	0	0	.35
$n\text{-}C_4H_{10}$	0	.01	.28	.05	.07	.06	0	0	.57
iso-C_4H_{10}	0	.01	.27	.05	.07	.09	0	0	.23
2,2-dimethyl-propane	.10	.18	.97	.04	.02	.10	0	0	.31

[a]Fraction of the total product observed, normalized to 1.0, at a relative kinetic energy of 0.5 eV in the center of mass frame. The pressure of alkane gas was 1.5 m torr.

[b]Tolbert, M.A.; Beauchamp, J.L., unpublished results.

[c]Reference 4.

[d]Not studied.

[e]Halle, L.F.; Armentrout, P.B.; Tolbert, M.A., unpublished results.

TABLE 5. Isotopic Product Distributions for Dehydrogenation of Deuterated Alkanes by Ti^+ and V^+ at a Relative Kinetic Energy of 0.5 eV.

		SINGLE DEHYDROGENATION			DOUBLE DEHYDROGENATION		2HD or	
M^+	Alkane	H_2	HD	D_2	$2H_2$	H_2+HD	$H_2+ D_2$	D_2+H_2
Ti^+	CH_3CD_3	.05	.91	.04				
	$CH_3CD_2CH_3$	.07	.93					
	$(CH_3)_3CD$	.12	.88		.66	.64		
	$CD_3CH_2CH_2CD_3$	.10	.90		.07[a]	.25	.55	.13
V^+	CH_3CD_3		1.0[b]					
	$CH_3CD_2CH_3$		1.0					
	$(CH_3)_3CD$		1.0					
	$CD_3CH_2CH_2CD_3$	.71	.29			.15	.67	.18

[a] The identity of this product is uncertain due to the identical masses of D_2 and $2H_2$. To make the product distributions best match those in Table 3, all of this mass product was assigned to be $2H_2$.

[b] Reference 8.

TABLE 6. Isotopic Product Distributions for Hydrocarbon Loss from
Deuterated Alkanes by Ti$^+$ at a Relative Kinetic Energy
of 0.5 eV.

Alkane	CH_4	CH_3D	CH_2D_2	CHD_3	CD_4	$C_2H_2D_4$	$C_2H_3D_3$	C_2H_4	C_2HD_3
$CH_3CD_2CH_3$	.68	.32	----	----	----				
$(CH_3)_3CD$	.81	.19	----	----	----			----	1.0
$CD_3CH_2CH_2CD_3$	----	.06	.09	.53	.32	.59	.41	1.0	----

and second metal-methyl bond energies is greater than 112 kcal/mol.[19] Using the previous value for the first titanium methyl bond (Table 1) implies $D(TiCH_3^+-CH_3) \geq 56$ kcal/mol.

In the reaction of V^+ with n-butane-1,1,1,4,4,4-d_6, it was observed that the product distribution was different than for unlabelled n-butane. To investigate this further, the reactions of Ti^+ and V^+ with totally deuterated alkanes, i.e., with n-butane-d_{10} and propane-d_8, were studied. The product distributions for the dehydrogenation reactions of Ti^+ and V^+ with n-butane as a function of deuteration are illustrated in Figure 3. It can be seen that for both metal ions, as the extent of deuteration increases, the extent of double dehydrogenation decreases relative to single dehydrogenation and adduct formation. This effect is remarkably pronounced, however, in the reaction with V^+, where for labelled n-butane, the dominant process is no longer loss of $2H_2$, but rather formation of the adduct ion. A large isotope effect is also observed in the reactions of V^+ with propanes. Although adduct formation is 32 % of the total product for propane (Table 3), it is 70 % of the total product for propane-d_8.

Discussion

The reactions of Ti^+ and V^+ with hydrocarbons are dominated by the loss of one or more molecules of hydrogen. In addition, smaller amounts of alkane loss products are observed for Ti^+. A comparison of the reactions of transition metal ions with n-butane is given in Table 7. It can be seen that the major

Figure 3. Product distribution for the dehydrogenation of n-butane by Ti^+ and V^+ as a function of the extent of deuteration. The single and double dehydrogenation processes are referred to as H_2 and $2H_2$, respectively, regardless of the deuterium label.
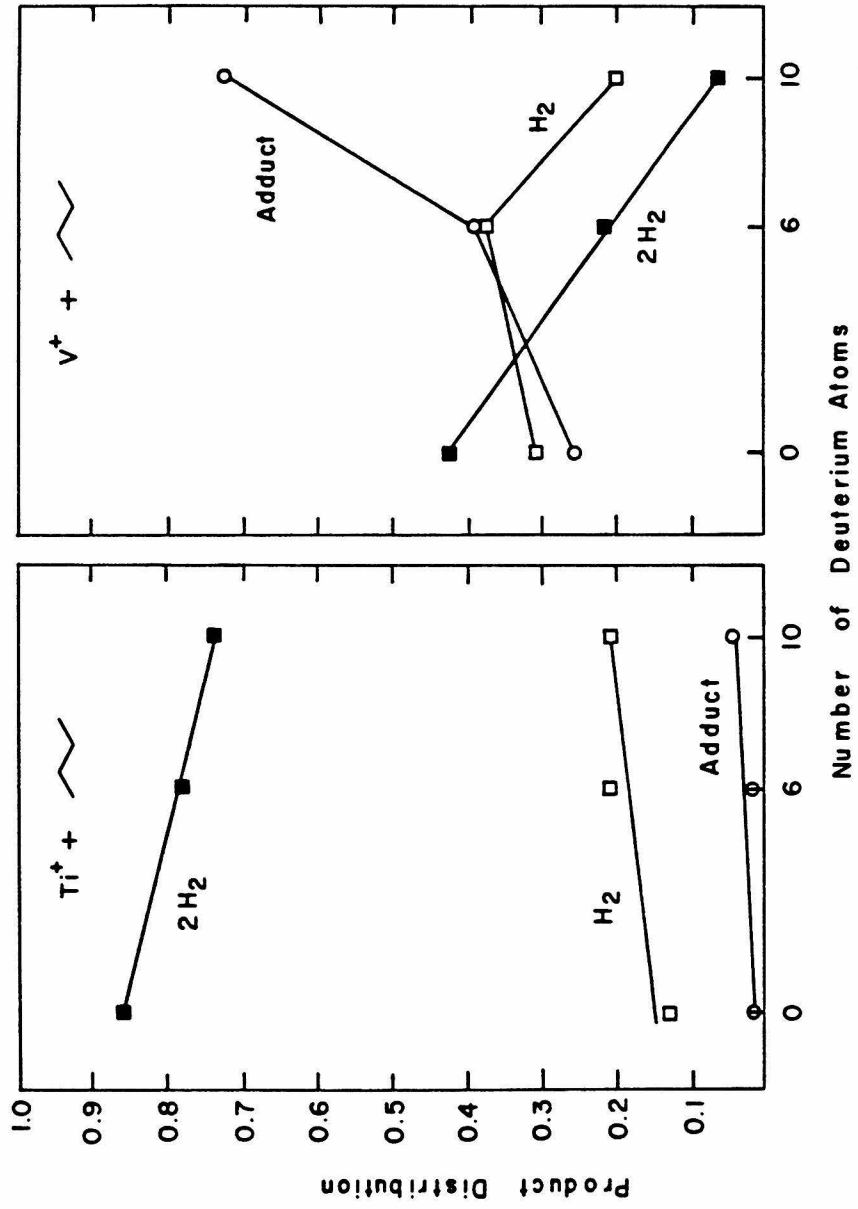
TABLE 7. Comparison of the Reactions of Transition Metal Ions with n-Butane at a Relative Kinetic Energy of 0.5 eV.

NEUTRAL PRODUCT	Sc^+ [a]	Ti^+	V^+	Fe^+ [b]	Co^+ [c]	Ni^+ [d]	Ru^+ [e]	Rh^+ [e]	Pd^+ [e]
H_2	.37	.17	.39	.20	.29	.48	.20	.27	.38
$2H_2$	.22	.66	.61	---	---	---	.80	.73	---
CH_4	.01	.09	---	.41	.12	.06	---	---	.21
CH_4+H_2	.02	.03	---	---	---	---	---	---	---
C_2H_4	.36	.02	---	---	---	---	---	---	---
C_2H_6	.02	.03	---	.39	.59	.45	---	---	.41
σTotal	103.	45.	48.	98.	170.	88.	38.	48.	29.

[a] Reference 5.

[b] Reference 1 and Halle, L.F. and Beauchamp, J.L., unpublished results.

[c] Reference 1b.

[d] Reference 3.

[e] Reference 4.

reactions of Ti^+ and V^+ are <u>not</u> analogous to those of the remaining first row transition metal ions. Instead, there is a similarity, perhaps superficial, to the reactivity of the second row ions Ru^+ and Rh^+. Although the reactivity appears to be quite similar, there are substantial differences as well. For example, adduct ions are very abundant in the reactions of V^+ but are not observed at all for Ru^+ and Rh^+ (Table 4). Furthermore, although no alkane loss products are observed in the reactions of V^+, these reactions are observed in certain circumstances for Ru^+ and Rh^+. Other clues that provide an understanding of the reactivity of V^+ and Ti^+ may be obtained from an examination of the dehydrogenation mechanisms and deuterium isotope effects that occur in the reactions of these metal ions. In addition, the similarities and differences in reactivity among the various metal ions can be explained in part in terms of the electronic configuration of the metal ions and the corresponding bonding configurations.

Dehydrogenation mechanisms for Ti^+ and V^+. Remarkable metal ion specificity has been observed in the dehydrogenation reactions of alkanes at transition metal ion centers. These reactions have been studied using a variety of techniques. These include deuterium labelling studies,[1c,3-5] product structural determinations using collision-induced dissociation,[20-22] and kinetic energy release distribution (KERD) measurements.[23-25] The results have indicated that dehydrogenation of small alkanes by Fe^+, Co^+, Ni^+, Ru^+, Rh^+, and Pd^+ proceed via a 1,2-process where hydrogens from adjacent carbons are eliminated. In contrast, hydrogen elimination at Sc^+ centers has been proposed to

occur via a 1,3-process wherein a metallocyclobutane complex is formed and H_2 is eliminated via a 4-center transition state.[5]

The reactions of V^+ with small alkanes are consistent with a predominantly 1,2-elimination. For example, as indicated in Table 5, HD loss is the only process observed in the reactions with deuterated alkanes smaller than n-butane. The reactions of Ti^+ are somewhat more complicated. The major dehydrogenation products for Ti^+ are also consistent with a 1,2-elimination mechanism. However, as indicated in Table 5, small amounts of H_2 elimination occur from CH_3CD_3, propane-2,2-d_2 and 2-methylpropane-2-d_1. These could be a result of scrambling or could be due in the case of the propanes to a 1,3-elimination mechanism similar to that inferred for Sc^+. These two different processes cannot be distinguished in this experiment. KERD measurements could perhaps distinguish between the 1,2- and 1,3-elimination mechanisms.

As mentioned previously, a great deal of interest and attention has recently been paid to the dehydrogenation mechanisms of n-butane by transition metal ions (Scheme 1). A summary of the products observed using labelled n-butane-1,1,1,4,4,4-d_6 and the proposed dehydrogenation mechanism for the various metal ions studied to date is presented in Table 8. Note that each metal ion, including Ti^+ and V^+, reacts in a quite distinct manner.

The reaction with Ti^+ results in a large amount of HD loss, second only to that observed for Sc^+. It is thus possible that a combination of a 1,2- and 1,3-dehydrogenation mechanism is

TABLE 8. Comparison of Dehydrogenation Products and Proposed Mechanisms for Transition Metal Ions Reacting with n-Butane-1,1,1,4,4,4-d_6.

	Sc+[a]	Ti+	V+	Fe+[b]	Co+[c]	Ni+[c]	Ru+[d]	Rh+[d]	Pd+[d]
H_2	---	.10	.71	.59	.18	---	.20	.32	1.0
HD	1.0	.90	.29	.18	.31	---	.46	.61	---
D_2	---	---	---	.23	.51	1.0	.34	.07	---
Proposed Mechanism	1,3	1,2 1,3	1,2	1,4 1.2	1,4	1,4	1,2	1,2	1,2

[a]Reference 5.

[b]References 1 and 25.

[c]References 1,2, 23 and 24.

[d]Reference 4.

operative in the reactions of Ti$^+$ with n-butane. It is possible
that Ti$^+$ preferentially inserts into the tertiary or secondary C-
H bonds of alkanes. This would prevent abundant 1,3-eliminations
of H$_2$ from propane and 2-methylpropane because only β-hydrogens
are available after initial C-H bond insertion. However, in the
case of n-butane, secondary C-H bond insertion can be followed by
either β-H or γ-H transfer. If γ-H transfer occurs, a
metallocyclobutane complex is formed which probably cannot
undergo subsequent hydrogen elimination. If, instead, β-H transfer
occurs, the metal-olefin product formed, <u>3</u>, may undergo
subsequent hydrogen elimination via allylic hydrogen transfers as
indicated in Scheme 2. This is consistent with the experimental

Scheme 2

observations that the major single dehydrogenation product is HD,
whereas the major double dehydrogenation product is 2HD (H$_2$ +
D$_2$). Note that double dehydrogenation is the dominant process at
low energies (Figure 1), which suggests that β-H transfers are
more facile than γ-H transfers. This also explains the prominant
loss of H$_2$ from 2,2-dimethylpropane. In this reaction, after C-H
bond insertion, no β-hydrogens are available for transfer. This
allows the transfer of less competitive groups, such as γ-
hydrogens or methyl groups. The occurrence of 1,3-eliminations
for Ti$^+$ is also supported by the fact that other reactions of Ti$^+$

with n-butane are similar to Sc$^+$. For example, formation of M(C$_2$H$_6$)$^+$ observed here for Ti$^+$ is the major product in the reaction of Sc$^+$ with n-butane, and is not observed at all for the other first row transition metal ions.

The reaction of V$^+$ with labelled n-butane-1,1,1,4,4,4-d$_6$ results in the prominent elimination of H$_2$. The product distribution observed for V$^+$ is similar to that of Pd$^+$, where only H$_2$ loss is observed. The mechanism proposed for dehydrogenation by Pd$^+$ involves hydride abstraction as the first step, leaving a carbonium ion to interact with the metal center.[4] The product distribution observed for V$^+$ is consistent with a 1,2-mechanism, where the secondary C-H bonds are preferentially attacked. Note that this mechanism is probably not initiated by hydride abstraction due to the much lower hydride affinity of V$^+$, 176 kcal/mol,[26] relative to Pd$^+$, 231 kcal/mol.[27] It should also be noted that an isotope effect could account for the preferential loss of H$_2$ from n-butane-1,1,1,4,4,4-d$_6$ by V$^+$.

The dehydrogenation mechanisms for V$^+$ and Ti$^+$ thus appear to be somewhat similar to those proposed for Ru$^+$ and Rh$^+$. The products observed are consistent with a predominantly 1,2-elimination mechanism for small alkanes. The reaction of Ti$^+$ with n-butane, however, appears to result in some 1,3-elimination not observed in the reactions of Ru$^+$ or Rh$^+$. The scrambling observed in the reactions of Ti$^+$ may be explained by either a 1,3-elimination, or reversible β-H transfers, or both. A difference in the reactivity of V$^+$ as compared to Ti$^+$, Ru$^+$, and Rh$^+$ is that no deuterium scrambling occurs in the V$^+$ reactions.

This indicates that reductive elimination of H_2 competes effectively with olefin insertion into the M-H bond at V^+ centers. Note that this is not the case for Ti^+, where scrambled products are observed in the dehydrogenation reactions. Other previous results have indicated that olefins can easily insert into the Ti^+-CH_3 bond.[28] This is in agreement with our findings of scrambled products for Ti^+. Olefin insertion processes are also thought to be facile at Ru^+ and Rh^+ centers.[4,29]

Comparison of alkane loss reactions for transition metal ions. As evident from Table 7, the major reactions of Ti^+ and V^+ are quite similar to those observed with Ru^+ and Rh^+. The major reactions involve the loss of one or two molecules of H_2. Alkane loss reactions occur with fairly low cross section for Ti^+ and may be due to electronically excited Ti^+. These products are not observed as exothermic processes for V^+ at all. As discussed in previous work, C-C bond insertions do not occur competitively with C-H insertions at Ru^+ and Rh^+ centers.[4] Similarly, β-alkyl transfers do not occur competitively with β-H transfers for these metal ions.[4] From the observed reactivities, it appears that these same considerations may also apply to Ti^+ and V^+. However, there are some important differences in the reactions of V^+.

A major difference in the reactivity of V^+ relative to Ti^+, Ru^+ and Rh^+ can be seen in the reaction with 2,2-dimethylpropane. After C-H bond insertion at these metal ion centers, no β-hydrogens are available, which makes possible the transfer of less favorable groups, such as a β-methyl group. Thus, Ti^+, Ru^+ and Rh^+ react with 2,2-dimethylpropane to lose CH_4 with quite large cross sections. This suggests that β-alkyl transfers are not

energetically unfeasible for these metal ions, even though they
are unable to compete with β-hydrogen transfer. The case for V^+,
however, is quite different. As discussed previously, ground
state V^+ does not react with 2,2-dimethylpropane at all. The
only major product observed in this reaction is the formation of
the adduct ion. Thus, if primary C-H bond insertion occurs, it
is not followed by β-methyl transfer and alkane elimination.
This may indicate that β-methyl transfer is not merely
noncompetitive, but rather energetically unfeasible. Another
explanation for the lack of reactivity is that primary C-H bond
insertions do not occur for V^+. This possibility is discussed
below.

Observation of adduct ions. The reaction of V^+ with
alkanes leads to extensive formation of adduct ions (Table 4).
As mentioned previously, this indicates that the adduct lifetimes
are at least 10 usec. In contrast, no adducts are observed for
Ru^+ and Rh^+, even at elevated pressures. Adducts are formed to
only a very small degree in the reactions of Ti^+. An example of
an adduct formation reaction in the ion beam experiment is
indicated in Scheme 3 for the case of a metal ion reacting with

Scheme 3
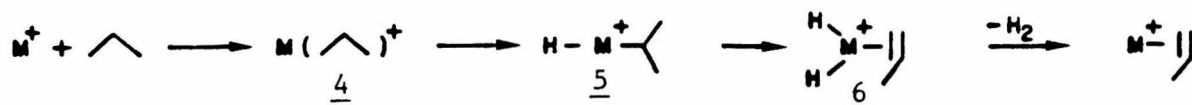
propane. The adduct ion detected can have any of a number of

different structures. One possible structure is the initially formed collision complex, 4, held together by ion-induced dipole interactions or weak acid base interactions. The adduct ions could also be an inserted species such as 5, or a rearranged complex as indicated by 6. Since only the mass of the adduct ion is detected in this experiment, differentiation of these structures is not possible.

The overall unimolecular rate of adduct dissociation depends on the rates for the various reaction steps in Scheme 3. The relative activation parameters for C-H bond insertion, β-hydrogen transfer and H_2 elimination determine which adduct structure is dominant. At low pressures, (< 1 mtorr), if the unimolecular decomposition rate is slow enough (< 10^5 sec^{-1}), then the internally excited adducts will be detected directly. At high pressures, (20 mtorr), if the adduct decomposition rate is slow enough (< 10^6 sec^{-1}), the adducts may live long enough to suffer a second stabilizing collision. In this case, adducts sufficiently cooled will be detected. For overall unimolecular dissociation rates > 10^7 sec^{-1}, it is unlikely that any adduct ions would be detected, even at elevated pressures. The fact that adducts are so prevalent in the reactions of V^+ thus suggests that at least one of the processes depicted in Scheme 3 is quite slow. Weisshaar et al.[30] have recently studied the reactions of Ti^+ with small alkanes in a high pressure flow tube. They found that adducts of Ti^+ with propane are not formed even when entrained in 1 torr of helium as a stabilizing gas. Only dehydrogenation was observed in the high pressure reaction of Ti^+ with propane. This supports our belief that the reaction rates

for Ti$^+$ are much greater than for V$^+$. This is also evident from the lower reaction cross sections observed for V$^+$ than for Ti$^+$, especially for the reaction with propane (Table 3). The slower rates for V$^+$ (i.e., longer adduct lifetimes) are due to relatively high activation barriers or low frequency factors compared to those operative for Ti$^+$, Ru$^+$ and Rh$^+$. Although the reactions of V$^+$ appear to be quite similar to those of these metal ions, the rate limiting step in the rearrangement and ion dissociation (Scheme 3) must be substantially slower for V$^+$.

Deuterium isotope effects. It is evident from Figure 3 that an unusually large deuterium isotope effect is observed in the dehydrogenation reactions occurring at V$^+$ centers. As the degree of deuteration is increased, the reaction cross sections are decreased. Much less double dehydrogenation and also less single dehydrogenation are observed for the deuterated alkanes. It is possible that this isotope effect is due to the changes in zero point energy upon deuteration. If the rate limiting step in the reactions of V$^+$ with alkanes is β-H transfer, then there are three factors which may contribute to the overall isotope effect. First, substituting deuterium for hydrogen has the effect of lowering the zero point energy for both the stable intermediates and for the transition states. However, the net zero point energy effect of deuteration is to increase slightly the activation barrier for β-H transfer by the difference in zero point energy. This amounts to approximately 1 kcal/mol higher activation energy for C-D bond breaking relative to C-H bond breaking. Second, C-H bond insertion is more exothermic than C-D

bond insertion due to zero point energy differences. Thus, the C-H bond insertion adduct has more energy available for reaction by 0.4 kcal/mol than does the C-D bond inserted adduct. Both of these factors result in longer lifetimes and slower dissociation rates for the deuterated adducts than for the undeuterated adducts.

A final isotope effect may arise from differences in the zero point energy for the bonds in the molecule which are not directly involved in the reaction. This type of isotope effect has been observed previously. For example, the dissociation rates for $Li(CH_3COCH_3)^+$ and $Li(CD_3COCD_3)^+$ to form Li^+ and acetone were found to show a large isotope effect.[31] The rate of dissociation was approximately five times slower for the deuterated species due to the differences in the total zero point energy of the two molecules. A large isotope effect was also observed in the dissociation reaction of $C_5H_9^+$ and $C_5D_9^+$ to lose H_2 and D_2, respectively.[32] The latter case resulted in a much slower reaction rate due to the longer lifetime of $C_5D_9^+$ by a factor of 5.

It is expected that the deuterium isotope effects observed in our study are also due to an increase in the lifetime of the deuterated adducts. Because the lifetimes of the vanadium adducts are comparable to the ion flight time to the detector, an increase in adduct lifetime would be mirrored by an increase in adduct signal in our experiment. The case for Ti^+, however, is quite different. As mentioned previously, the adduct lifetimes for Ti^+ are much shorter than for V^+. Thus, an increase in the lifetime of the titanium adducts upon deuteration might go

undetected in our experiment. The reactions may still be so fast for Ti^+, even using deuterium labelled alkanes, that they are over before the adducts can reach the detector.

Description of the bonding to V^+ and Ti^+. The ground electronic states of Ti^+ and V^+ are derived from $4s^13d^2$ and $3d^4$ electronic configurations, respectively.[14] Recent calculations have shown that the diatomic metal hydrides of these metal ions utilize metal orbitals which are 40% d in character and 60% s and p in character.[33] Because s-d hybrid orbitals are used in the formation of the first M^+-H bond, to a first approximation, the second M^+-H bond in MH_2^+ will also be an s-d hybrid with an "inherent" bond energy comparable to that of the first. The inherent bond energy is defined here as the actual bond energy plus the promotion energy required to excite the metal ion to a configuration favorable for bonding. The promotion energy includes any exchange energy lost in forming the bond.

The inherent bond energies of MH^+ have been calculated to be 61 kcal/mol for both Ti^+ and V^+, using the simplification that a pure s orbital is used in the formation of the bond.[33] To calculate the promotion energy necessary for MH^+ to bind an additional hydrogen atom, the assumption is made that the second bond uses a pure d metal orbital for bonding. Thus, instead of calculating the bond energies using two s-d hybrid bonds, the bond energies are calculated using one pure s bond and one pure d bond. The inherent strengths of the pure s and d bonds are taken to be equal to the inherent strength of an s-d hybrid bond. To promote TiH^+ from the ground $^3\Phi$ state to a state favorable for

bonding requires the loss of one-half of a d-d exchange term, or 8 kcal/mol.[34] In order to promote VH^+ from the ground $^4\Delta$ state to a state favorable for bonding requires the loss of one d-d exchange term, or 18 kcal/mol.[34] An estimate for the _second_ bond energy, $D(MH^+-H)$, can be obtained from the inherent bond energy, less the promotion energy. This results in a second bond energy of 61-8= 53 kcal/mol for Ti^+ and 61-18 = 43 kcal/mol for V^+. Thus, the sum of the first and second bond energies for MH_2^+ are 108 and 91 kcal/mol for Ti^+ and V^+, respectively. A more useful quantity for C-H bond activation is the sum of the two bonds in $R-M^+-H$. Using the values for M^+-CH_3 in Table 1 results in the sum of the two bonds being 109 kcal/mol and 93 kcal/mol for Ti^+ and V^+, respectively. Note that the estimates for the binding energies to Ti^+ are in excellent agreement with the lower limit $D(Ti^+-2CH_3) \geq 112$ kcal/mol determined from the reaction with n-butane to form $Ti(CH_3)_2^+$.

Typical C-H bond energies for alkanes are in the range 92-98 kcal/mol.[35] It is thus apparent that the bond energies to Ti^+ are more than sufficient to allow for exothermic C-H bond activation. The case for V^+, however, is not so clear. From the estimates made above, it appears that V^+ should be able to activate only tertiary C-H bonds. Assuming that the bond to an alkyl group is stronger than to a methyl group (by 5 kcal/mol) results in V^+ being just barely able to activate secondary C-H bonds. This could explain why V^+ _does not react_ with 2,2-dimethylpropane. Only primary C-H bond insertions or C-C bond insertions are possible with 2,2-dimethylpropane, neither of which may be facile processes for V^+. This is also supported by

the extensive loss of H_2 from n-butane-1,1,1,4,4,4-d_6, perhaps indicating preferential attack at the secondary C-H bonds.

The impact of weak bonds to V^+ on the reactivity of this metal ion can be seen from the qualitative potential energy surface for the 1,2-elimination of H_2 from n-butane illustrated in Figure 4 . This potential energy surface explains the special features of the V^+ reactions observed in this study. The initially formed insertion adduct, 7, is very high in energy. Thus, even fairly small activation barriers for C-H bond insertion or β-H transfer may make the overall reaction energetically unfavorable. This may result in slow reactions and long-lived adduct ions. As discussed previously, the formation of long-lived adduct ions results in the observation of large deuterium isotope effects for the reactions of V^+ with alkanes. If β-methyl transfer has a somewhat higher intrinsic barrier than β-H transfer, then this process would almost certainly be energetically unfeasible. This is indicated by the dashed line in Figure 4 . This may explain the lack of reaction of V^+ with 2,2-dimethylpropane. This also may be partially responsible for the lack of alkane loss products observed in general.

Conclusion

The reactions of Ti^+ and V^+ with alkanes are dominated by the loss of one or more molecules of hydrogen, similar to the reactions observed for Ru^+ and Rh^+. Alkane loss reactions are also observed for Ti^+ but may be due to electronically excited state reactions. It is proposed that both Ti^+ and V^+

Figure 4. A simplified potential energy diagram for the reaction of V^+ with n-butane. The energies of the reaction intermediates were estimated using the values discussed in the text. The strength of the V^+-olefin bonds were taken to be 50 kcal/mol, as suggested for $V-C_2H_4^+$ in Reference 8.
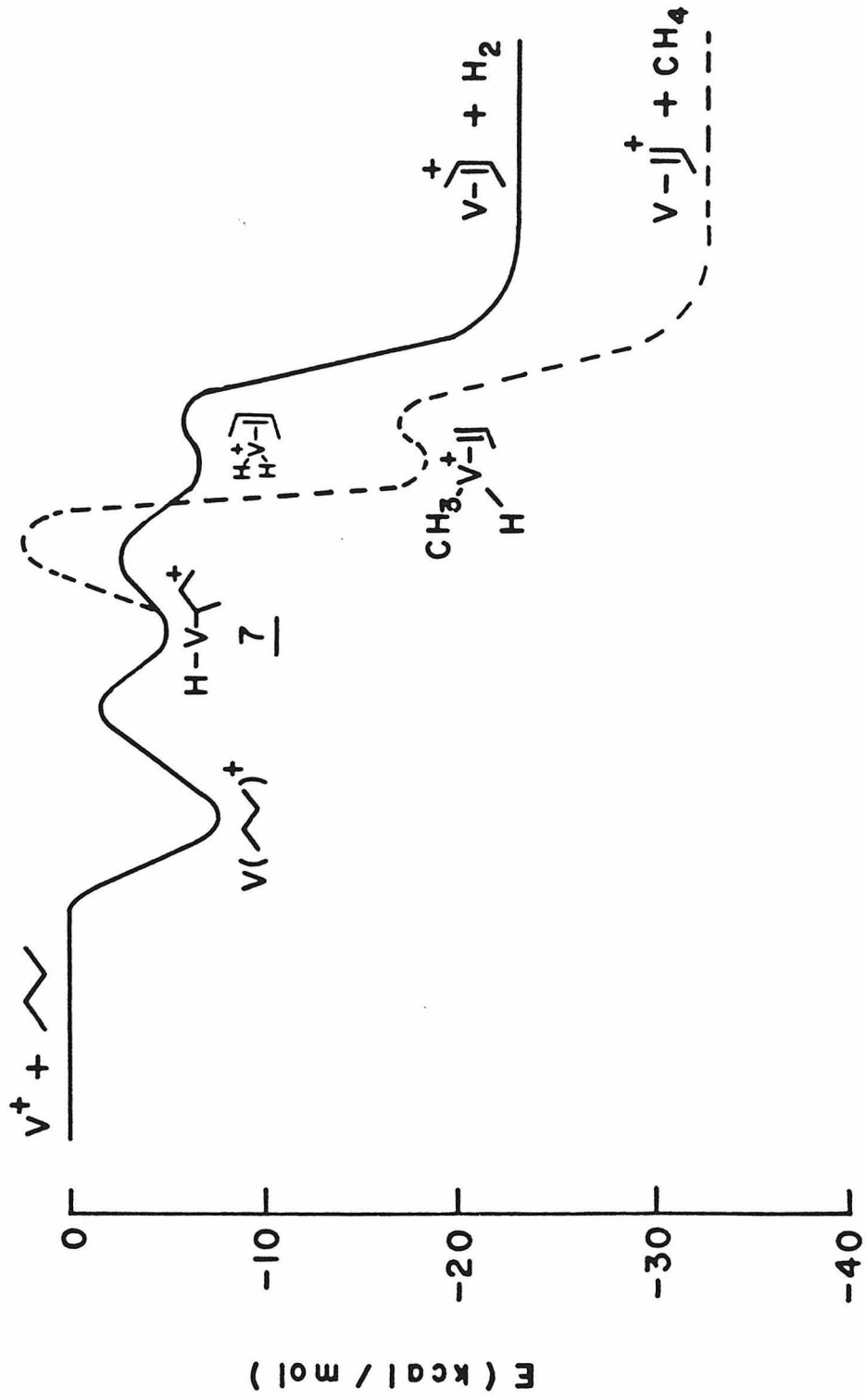
dehydrogenate alkanes by a predominantly 1,2-mechanism, where some 1,3-elimination occurs for the reaction of Ti^+ with n-butane. Although there is much similarity in the reactions of Ti^+ and V^+ with Ru^+ and Rh^+, there are also important differences, especially for V^+. Extensive adduct formation and a large deuterium isotope effect for V^+ are consistent with much slower reaction rates for this metal ion than for Ti^+, Ru^+, and Rh^+. It is suggested that V^+ cannot form two strong sigma bonds due to the $3d^4$ electronic configuration of ground state V^+. This makes insertion into C-H bonds much more difficult than for the other metal ions and may in fact prevent primary C-H bond insertions. This results in higher activation barriers and the formation of relatively long-lived intermediates. Because the lifetime of the adduct ion is comparable to the ion flight time to the detector, a large deuterium isotope effect is observed in the reactions of V^+ with labelled alkanes. These isotope effects are not observed for the reactions of Ti^+ due to the much faster reaction rates for this metal ion.

References

1. (a) Halle, L. F.; Armentrout, P. B.; Beauchamp, J. L. Organometallics 1982, 1, 963.

   (b) Armentrout, P. B.; Beauchamp, J. L. J. Am. Chem. Soc. 1981, 103, 784.

   (c) Houriet, R.; Halle, L. F.; Beauchamp, J. L. Organometallics 1983, 2, 1818.

2. Jacobson, D. B.; Freiser, B. S. J. Am. Chem. Soc. 1983, 105, 5197.

3. Halle, L. F.; Houriet, R.; Kappes, M. M.; Staley, R. H.; Beauchamp, J. L. J. Am Chem. Soc. 1982, 104, 6293.

4. Tolbert, M. A.; Mandich, M. L.; Halle, L. F.; Beauchamp, J. L., to be submitted to J. Am. Chem. Soc.

5. Tolbert, M. A.; Beauchamp, J. L. J. Am. Chem. Soc. 1984, 106, 8117.

6. Byrd, G. D.; Freiser, B. S. J. Am. Chem. Soc. 1982, 104 5944.

7. Elkind, J. L.; Ervin, K. M.; Aristov, N.; Armentrout, P. B., submitted. (Armentrout, P. B., private communication.)

8. Aristov, N.; Armentrout, P. B., submitted.

9. Byrd, G. D.; Burnier, R. C.; Freiser, B. S. J. Am. Chem. Soc. 1982, 104, 3565.

10. Kappes, M. M.; Staley, R. H., unpublished results.

11. Allison, J.; Ridge, D. P. J. Am. Chem. Soc. 1977, 99, 35.

12. Allison, J.; Ridge, D. P. J. Am. Chem. Soc. 1978, 100, 163.

13. (a) Armentrout, P. B.; Beauchamp, J. L. Chem. Phys. 1980, 50, 21.

    (b) Armentrout, P. B.; Beauchamp, J. L. J. Chem. Phys. 1981, 74, 2819.

14. Moore, C. E. Atomic Energy Levels. National Bureau of Standards: Washington D. C., 1949.

15. Garstang, R. H., Monthly Notice Royal Astron. Soc. 1962, 124, 321.

16. Halle, L. F.; Armentrout, P. B.; Beauchamp, J. L. J. Am. Chem. Soc. 1981, 103, 962.

17. Freas, R. B.; Ridge, D. P. J. Am. Chem. Soc. 1980, 102, 7129.

18. Kang, H.; Beauchamp, J. L. J. Phys. Chem. 1985, 89, 3364.

19. Auxiliary heats of formation from Cox, J. D.; Pilcher, G. Thermochemistry of Organic and Organometallic Compounds. Academic Press: New York, 1970. $\Delta H_f(CH_3) = 35.1$ from Reference 35.

20. Jacobson, D. B.; Freiser, B. S. J. Am. Chem. Soc. 1983, 105, 736.

21. Larsen, B. S.; Ridge, D. P. J. Am. Chem. Soc. 1984, 106, 1912.

22. Peake, D. A.; Gross, M. L.; Ridge, D. P. J. Am. Chem. Soc. 1984, 106, 4307.

23. Hanratty, M. A.; Beauchamp, J. L.; Illies, A. J.; Bowers, M. T. J. Am. Chem. Soc. 1985, 107, 1788.

24. Hanratty, M. A.; Beauchamp, J. L.; Illies, A. J.; Bowers, M. T., submitted to J. Am. Chem. Soc.

25. Jacobson, D. B.; Beauchamp, J. L.; Bowers, M. T., to be submitted.

26. The hydride affinity of V^+ is 176 kcal/mol, calculated from the value D(V-H) = 37.9 kcal/mol from: Sallans, L.; Lane, K.; Squires, R. R.; Freiser, B. S. J. Am. Chem. Soc. 1985, 107, 4379.

27. Tolbert, M. A.; Beauchamp, J. L., to be submitted.

28. Uppal, J. S.; Johnson, D. E.; Staley, R. H. J. Am Chem Soc. 1981, 103, 508.

29. Jacobson, D. B.; Freiser, B. S., submitted to J. Am. Chem. Soc.

30. Tonkyn, R.; Weisshaar, J. C. J. Phys. Chem., submitted.

31. Woodin, R. L.; Beauchamp, J. L. Chem. Phys. 1979, 41, 1.

32. Bowers, M. T.; Elleman, D. D.; Beauchamp, J. L. J. Phys. Chem. 1968, 72, 3599.

33. Schilling, J. B.; Goddard, W. A. III.; Beauchamp, J. L. J. Am. Chem. Soc., accepted.

34. The d-d exchange energy for the s^1d^2 configuration of Ti^+ is K_{d-d} = 16.5 kcal/mol. The d-d exchange energy for the s^1d^3 configuration of V^+ is K_{d-d} = 18.2 kcal/mol. Schilling, J. B., work in progress.

35. McMillen, D. F.; Golden, D. M. <u>Ann. Rev. Phys. Chem.</u> 1982, <u>33</u>, 493.

CHAPTER V

ACTIVATION OF CARBON-HYDROGEN AND CARBON-CARBON BONDS
BY TRANSITION-METAL IONS IN THE GAS PHASE.
EXHIBITION OF UNIQUE REACTIVITY BY SCANDIUM IONS

ACTIVATION OF CARBON-HYDROGEN AND CARBON-CARBON BONDS
BY TRANSITION-METAL IONS IN THE GAS PHASE. EXHIBITION
OF UNIQUE REACTIVITY BY SCANDIUM IONS

M.A. Tolbert and J.L. Beauchamp

Abstract: The activation of carbon–carbon and carbon–hydrogen bonds by scandium ions in the gas phase has been studied by using an ion-beam apparatus. Analysis of thresholds for the endothermic reactions of Sc^+ with H_2 and C_2H_6 yields $D°(Sc^+-H)$ $= 54 \pm 4$ kcal/mol and $D°(Sc^+-CH_3) = 65 \pm 5$ kcal/mol, respectively. Results also indicate that Sc^+ forms a *second* strong σ-bond to CH_3 and H, rendering oxidative addition of C–C and C–H bonds an exothermic process. The reactions of Sc^+ with butane and larger alkanes result in the formation of products of the general form $Sc(C_nH_{n+2})^+$, which are not seen in similar reactions with other first-row transition metals. We postulate these products to be dialkylscandium ions. The mechanism proposed for the formation of these products, supported by studies of deuterium-labeled hydrocarbons, invokes β-alkyl transfers and reversible olefin insertions. For the reaction of Sc^+ with n-butane the proposed mechanism involves the formation of an activated scandium dimethylethylene intermediate. Although the reductive elimination of ethane from this intermediate is thermodynamically preferred, the favored decomposition route is observed to be loss of ethylene. This indicates a barrier for reductive elimination of ethane in excess of the endothermicity. In comparison to the first-row group 8 metal ions, another unique process involves selective 1,3-dehydrogenation of alkanes by Sc^+. It is proposed that Sc^+ initially inserts into a C–H bond, followed by addition of a γ-C–H bond across the Sc–H bond, with H_2 being eliminated from this four-center transition state. Two factors are responsible for the unique reactivity of Sc^+ among the first-row transition metal ions. Only two valence electrons are available for the formation of strong σ-bonds, and the formation of more than two such bonds is unlikely. In addition, the absence of additional d electrons on the metal center reduces the binding energy of π-acceptors in scandium(III) intermediates and modifies activation parameters for competitive processes.

Transition-metal ions in the gas phase readily activate the carbon–hydrogen and carbon–carbon bonds of completely saturated hydrocarbons. Extensive studies have probed the mechanism and energetics of these reactions, in which alkanes are dehydrogenated or cleaved to yield smaller alkanes and alkenes.[1-3] Although the available data reveal periodic trends in reactivity, it is recognized that certain processes can be highly metal specific. For example, Ni^+ distinguishes itself in comparison to the remaining first-row group 8 metal ions by dehydrogenating alkanes in a highly selective 1,4-process.[4]

The ability to understand and even predict metal ion reactivity is firmly based on a knowledge of the strengths of particular metal–ligand bonds and the activation parameters for individual reaction steps. These parameters relate to the motion of the system across barriers which interconnect stable configurations assumed by the reaction intermediates. Oxidative addition of C–H and C–C bonds must be an exothermic process in order for hydrocarbons to react readily at transition-metal centers. This requires the formation of relatively strong metal–hydrogen and metal–carbon bonds. On the basis of this consideration alone, what can be predicted for scandium? Scandium is one of the remaining first-row transition metals for which bonding energetics and reactions have not yet been reported.

The low-lying states of Sc^+ are summarized in Table 1.[5] First-row transition metal ions with ground states derived from $3d^n4s^1$ configurations are found to have strong metal–hydrogen and metal–methyl bonds.[6] The σ-bond strengths of metal ions not meeting this requirement decrease with increasing promotion energy from their ground state to the lowest state derived from the $3d^n4s^1$ configuration. Hence we expect scandium ions, with a ^3D ground state derived from the $3d^14s^1$ configuration, to form a strong σ-bond to both H and CH_3. Moreover, there is no electron exchange energy lost in forming a *second* bond to the single d electron. It might therefore be expected that Sc^+ will react readily with hydrocarbons. While our observations generally support this conjecture, there are some surprising features in the reactions of Sc^+. The absence of additional d electrons on the metal center reduces the binding energy of π-acceptors in scandium(III) intermediates and modifies activation parameters for competitive processes. This endows scandium with unique reactivity in comparison to other first-row ions and provides further clues to the enigma of hydrocarbon activation at transition-metal centers.

Table I. Low-Lying States of Sc^+ [a]

| state	configuration	energy,[b] eV	population[c]
a^3D	3d4s	0	85.4%
a^1D	3d4s	0.315	7.0%
a^3F	$3d^2$	0.596	7.5%
b^1D	$3d^2$	1.36	0.1%
a^1S	$4s^2$	1.46	
a^3P	$3d^2$	1.50	
a^1G	$3d^2$	1.77	

[a] Data from ref 5. [b] Listed numbers are the lowest energy J level of that term. [c] Boltzmann population at 2500 K.

Experimental Section

The ion-beam apparatus used in the present study has been described previously.[7] Briefly, singly charged scandium ions are produced by vaporization of anhydrous $ScCl_3$ onto a hot rhenium filament and subsequent surface ionization of the Sc at 2500 K. The estimated beam composition at this temperature is included in Table I. The metal ions are collimated, mass and energy selected, and focused into a collision chamber containing the neutral reactant at ambient temperature. The pressure in the collision chamber is held constant at 1.5 mtorr as measured with a capacitance manometer. Product ions scattered in the forward direction are analyzed by using a quadrupole mass spectrometer. Labeled propane ($2,2-d_2$, 98% D), n-butane ($1,1,1,4,4,4-d_6$, 98% D), and 2-methylpropane ($2-d_1$, 98% D) were obtained from Merck, Sharp and Dohme.

Results

Determination of Sc^+–H and Sc^+–CH_3 Bond Dissociation Energies. The endothermic reaction 1 of Sc^+ with H_2 leads to the formation of ScH^+. The cross section for reaction 1 as a function

$$Sc^+ + H_2 \rightarrow ScH^+ + H \qquad (1)$$
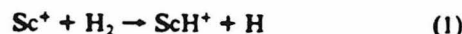
of relative kinetic energy is shown in Figure 1a. The data were fit by using the method described previously to find the reaction threshold, $E_0 = 2.15$ eV.[8] From the threshold value and the H_2 bond energy,[9] a value for $D^\circ(Sc^+-H)$ of 54 ± 4 kcal/mol is determined. The presence of excited-state scandium ions in the beam may be responsible for the low-energy tail in Figure 1a. The quality of the data and the lack of information relating to the excited-state distribution precluded a fit including multiple states. The constants were chosen to fit the major rising part of the curve. The bond energy obtained from this fitting procedure is consistent with the observed reactivity of Sc^+.

The endothermic reactions 2 and 3 of scandium ions with ethane result in the formation of $ScCH_3^+$ and ScH^+, respectively. The

$$Sc^+ + C_2H_6 \rightarrow ScCH_3^+ + CH_3 \qquad (2)$$

$$\rightarrow ScH^+ + C_2H_5 \qquad (3)$$
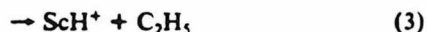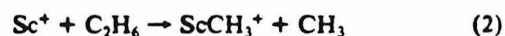
cross section for the formation of $ScCH_3^+$ as a function of relative kinetic energy is shown in Figure 1b. The data are fit as described previously to obtain a threshold for reaction 2 of $E_0 = 1.08$ eV.[10] Combining this value with the C–C bond dissociation energy for ethane, 90.0 kcal/mol, gives $D^\circ(Sc^+-CH_3) = 65 \pm 5$ kcal/mol. Scandium ions dehydrogenate ethane in accordance with reaction 4. The cross section for reaction 4 is 0.74 Å^2 at a relative kinetic

$$Sc^+ + C_2H_6 \rightarrow Sc(C_2H_4)^+ + H_2 \qquad (4)$$

energy of 0.5 eV and decreases with increasing kinetic energy. This behavior suggests that reaction 4 is exothermic and indicates $D^\circ(Sc^+-C_2H_4) \geq 33$ kcal/mol.[11] Very small amounts of $Sc(H_2)^+$ are formed in an endothermic process which has a maximum cross section of less than 0.1 Å^2 at a relative kinetic energy of 2 eV.
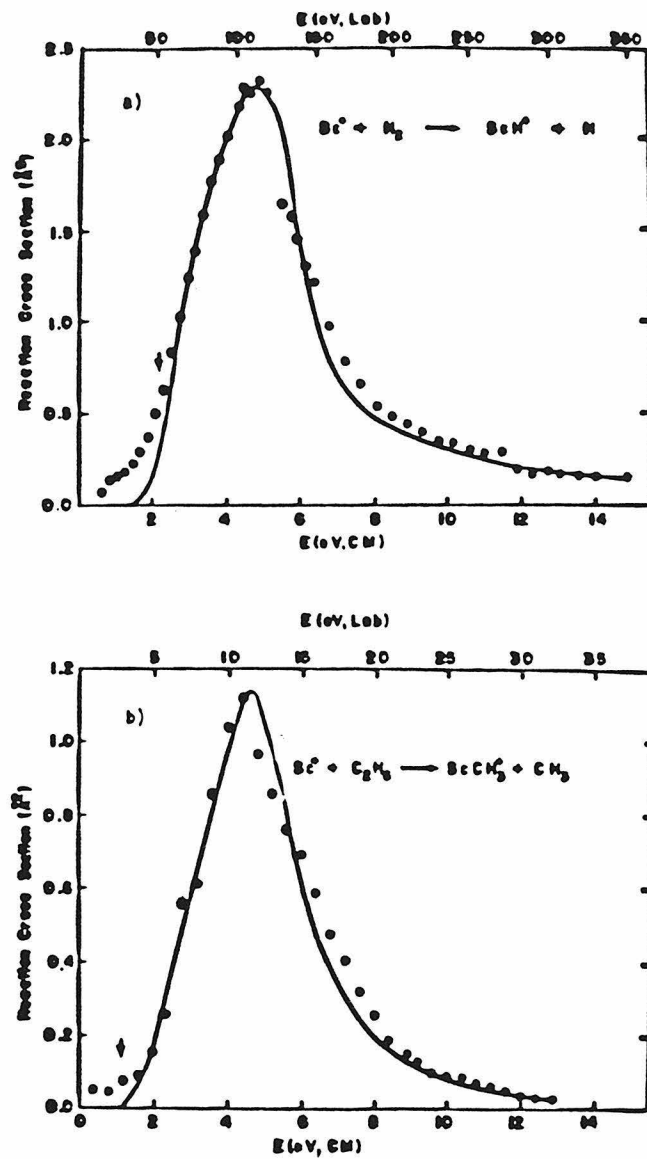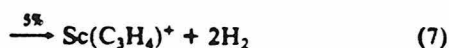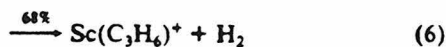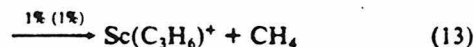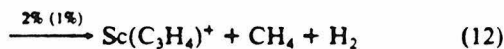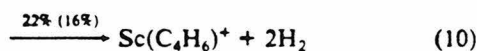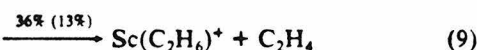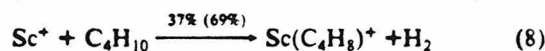
Figure 1. Variation in the experimental cross section with relative kinetic energy for the reaction of Sc^+ with (a) H_2 to form ScH^+ and (b) ethane to form $ScCH_3^+$. The solid lines are fits to the data as described in the text. Arrows indicate the threshold energies at 2.15 eV (for ScH^+) and 1.08 eV (for $ScCH_3^+$).

Reactions of Sc[+] with Alkanes. The exothermic reactions 5–7

$$Sc^+ + C_3H_8 \xrightarrow{27\%} Sc(C_2H_4)^+ + CH_4 \qquad (5)$$

$$\xrightarrow{68\%} Sc(C_3H_6)^+ + H_2 \qquad (6)$$

$$\xrightarrow{5\%} Sc(C_3H_4)^+ + 2H_2 \qquad (7)$$

account for the main products observed when Sc[+] interacts with propane at a relative kinetic energy of 0.5 eV with a total reaction cross section of ~ 7 Å^2 at this energy. At higher energies, ScH[+], ScCH$_3$[+], and Sc(CH$_4$)[+] are formed in endothermic reactions.[12]

The reaction of Sc[+] with n-butane at low energy yields a number of different products, as indicated in reactions 8–13. The product

$$Sc^+ + C_4H_{10} \xrightarrow{37\% \ (69\%)} Sc(C_4H_8)^+ + H_2 \qquad (8)$$

$$\xrightarrow{36\% \ (13\%)} Sc(C_2H_6)^+ + C_2H_4 \qquad (9)$$

$$\xrightarrow{22\% \ (16\%)} Sc(C_4H_6)^+ + 2H_2 \qquad (10)$$

$$\xrightarrow{2\%} Sc(C_2H_4)^+ + C_2H_6 \qquad (11)$$

$$\xrightarrow{2\% \ (1\%)} Sc(C_3H_4)^+ + CH_4 + H_2 \qquad (12)$$

$$\xrightarrow{1\% \ (1\%)} Sc(C_3H_6)^+ + CH_4 \qquad (13)$$

distributions shown were measured at a relative kinetic energy of 0.5 eV. Variation of the cross sections for these reactions with relative kinetic energy is shown in Figure 2. The observed decrease in the cross sections for reactions 8–13 with increasing kinetic energy indicates that all of these processes are exothermic. At higher energies, endothermic reaction pathways primarily result in the formation of ScCH$_3$[+] and Sc(C$_2$H$_5$)[+].[13] Products analogous to those observed with n-butane are also observed with isobutane, with a somewhat different product distribution indicated parenthetically in reactions 8–13, and a total reaction cross section of ~ 43 Å^2 at a relative kinetic energy of 0.5 eV.

Reaction of Sc[+] with alkanes larger than butane results in a large number of products. In contrast to the first-row group 8 metal ions, Sc[+] dehydrogenates neopentane exothermically, a process which accounts for 67% of the total observed product at a relative kinetic energy of 0.5 eV. Processes analogous to reaction 9 result in the formation of Sc(C$_3$H$_8$)[+] and Sc(C$_2$H$_6$)[+] from n-pentane, and Sc(C$_4$H$_{10}$)[+] and Sc(C$_3$H$_8$)[+] from n-hexane. Total reaction cross sections for these larger alkanes are comparable to those observed for n-butane in Figure 2.

Further information about the reaction mechanisms and the structure of reaction products has been obtained by a study using deuterium-labeled compounds. A summary of the reactions of Sc[+] with several labeled alkanes at low energy is given in Table II.
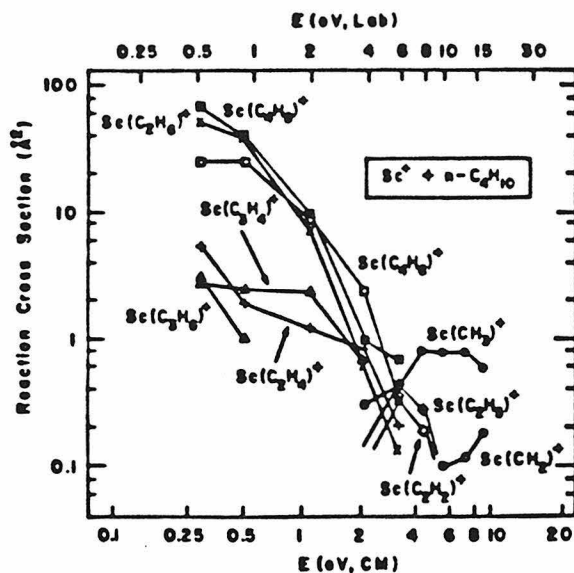
Figure 2. Variation in the experimental cross section for the reactions of Sc$^+$ with n-butane as a function of the relative kinetic energy in the center-of-mass frame (lower scale) and the laboratory frame (upper scale).

Table II. Product Distributions in the Reactions of Sc$^+$ with Deuterium-Labeled Alkanes at a Relative Kinetic Energy of 0.5 eV

neutral lost	alkane		
	propane-2,2-d_2	2-methyl-propane-2-d_1	butane-1,1,1,4,4,4-d_6
H$_2$	0.21	0.41	
HD	0.33	0.27	0.38
D$_2$			0.04[a]
2H$_2$	0.02[a]	0.10	
H$_2$ + HD	0.03	0.06	
2HD (H$_2$ + D$_2$)	0.02		0.13
2D$_2$			
CH$_4$	0.17		
CH$_3$D	0.12		
C$_2$H$_4$		0.05	0.28
C$_2$H$_3$D	0.03	0.11	0.03
C$_2$H$_2$D$_2$	0.07		0.03
C$_2$HD$_3$			0.08
C$_2$D$_4$(C$_2$H$_4$D$_2$)			0.03

[a] This product could correspond to loss of D$_2$ or to loss of 2H$_2$. The masses of the products in either case are identical, and thus the exact formula could not be determined.

Reaction of Sc⁺ with Carbonyl Compounds. First-row group 8 metal ions react with acetone as indicated in equation 14.[14] This

$$M^+ + (CH_3)_2CO \rightarrow M(CH_3)_2^+ + CO \qquad (14)$$

process yields a lower limit for the second metal–methyl bond dissociation energy in the product, a quantity useful in assessing the energetics of alkane reactions with transition-metal ions. This process is *not* observed with Sc⁺. Instead, reaction 15 is observed,

$$Sc^+ + (CH_3)_2CO \rightarrow ScO^+ + C_3H_6 \qquad (15)$$

$$Sc^+ + CH_3CHO \rightarrow ScO^+ + C_2H_4 \qquad (16)$$

and the analogous process 16 occurs with acetaldehyde.[15] Cross sections for both reactions exhibit the characteristic behavior of exothermic processes, with maximum cross sections at low energy. When the known bond energy of ScO⁺, 6.9 ± 0.3 eV,[16] is used, reactions 15 and 16 are exothermic by 43 and 48 kcal/mol, respectively.[17] Formaldehyde reacts with Sc⁺ in an exothermic process to yield the scandium dihydride ion, reaction 17, with a

$$Sc^+ + CH_2O \rightarrow ScH_2^+ + CO \qquad (17)$$
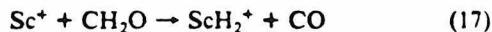
cross section of 1.4 Å² at a relative kinetic energy of 0.5 eV. When the first Sc⁺–H bond dissociation energy determined above (54 kcal/mol) is used, reaction 17 indicates that $D^\circ(ScH^+-H) \geq 50$ kcal/mol.
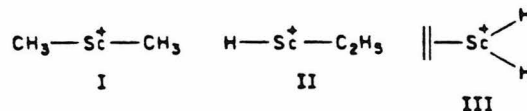
Discussion

Thermochemistry. The measured bond dissociation energies, $D^\circ(Sc^+-H) = 54 \pm 4$ kcal/mol and $D^\circ(Sc^+-CH_3) = 65 \pm 5$ kcal/mol, conform to the expectation that the first metal–ligand σ-bond to Sc⁺ will be strong. The results are in complete accord with similar data for other first-row transition metal ions, including the observation that metal–methyl bonds are stronger than metal–hydrogen bonds.[6,18] Ab initio calculations (generalized valence bond, dissociation consistent, configuration interaction) on the ground $^2\Delta$ state of ScH⁺ yield a value for the bond dissociation enthalpy of $D^\circ(Sc^+-H) = 56$ kcal/mol,[19] in excellent agreement with our measured value. The hybridization of the scandium orbital used for bonding is ~41% 3d and ~59% 4s and 4p. The nonbonding electron on scandium occupies what is predominantly a d orbital. Formation of a second strong bond is thus possible, with a bond angle which may vary reasonably over a wide range (45–135°), depending on which of the d orbitals is used. Since the ground state of ScH⁺ is $^2\Delta$, one would expect the bond angle in ScH₂⁺ to be close to 90°. The angle may open up slightly in order to decrease the interaction between the two Sc⁺–H bonds.

When the measured value of $D^\circ(Sc^+-H)$ is used, the proton affinity of Sc is found to be 217 ± 4 kcal/mol. This is higher than any other first-row transition-metal atom,[20] a factor which can be attributed to the low ionization potential of scandium (6.56 eV).[5]

Since reaction 14 was not observed with Sc^+, we were not able to derive a lower limit for the second bond dissociation energy in $Sc(CH_3)_2^+$. In the case of the dihydride, however, reaction 17 indicates that the strength of the second scandium hydrogen bond is comparable to the first. Interestingly, with the sum of the two bond energies being greater than 104 kcal/mol, ScH_2^+ is predicted to be stable with respect to the reductive elimination of H_2. Since the second metal–hydrogen bond is strong, we surmise that the same will hold for the second metal–methyl bond. Hence, we have confirmed the expectation that both the first and second metal–ligand σ-bonds to Sc^+ are strong. The species formed correspond formally to Sc(III) compounds, which leaves the metal in its favored oxidation state.

Reactions of Sc^+ with Hydrocarbons. Reactions of Sc^+ with alkanes smaller than butane yield results similar to those obtained for the first-row group 8 metal ions.[1b] The first major departure in behavior is observed in the reaction of Sc^+ with n-butane, where a major product with the empirical formula $Sc(C_2H_6)^+$ is observed. This is illustrated by the data in Table III, which summarizes the product distribution for the reactions of first-row transition-metal ions with n-butane. Related products are observed in the reaction of Sc^+ with n-pentane [$Sc(C_3H_8)^+$ and $Sc(C_2H_6)^+$] and n-hexane [$Sc(C_4H_{10})^+$ and $Sc(C_3H_8)^+$]. Again, these products are *not* observed when these alkanes react with other first-row transition-metal ions.

Possible structures of the $Sc(C_2H_6)^+$ product observed in the exothermic reaction of Sc^+ with n-butane are indicated by I–III.

$$CH_3-\overset{+}{Sc}-CH_3 \qquad H-\overset{+}{Sc}-C_2H_5 \qquad \|-\overset{+}{Sc}\!\!<^H_H$$
$$\text{I} \qquad\qquad\qquad \text{II} \qquad\qquad\qquad \text{III}$$

On the basis of thermochemical estimates in the Appendix, the heats of formation of I, II, and III are 189, 205, and 218 kcal/mol, respectively. When these values are used, the reactions of Sc^+ with n-butane to form II and III are predicted to be endothermic by 6 and 19 kcal/mol, respectively. Structure I, however, is formed in a reaction which is estimated to be exothermic by 10 kcal/mol and is therefore the only structure which seems energetically feasible.[21]

Table III. Product Distributions of Exothermic Reactions of First-Row Transition Metal Ions with n-Butane at a Relative Kinetic Energy of 0.5 eV

neutral product lost	metal ion[a]				
	Sc^+	Ti^+[b]	Fe^+[c]	Co^+[c]	Ni^+[c]
H_2	0.37		0.20	0.29	0.48
$2H_2$	0.22	1.0			
CH_4	0.01		0.41	0.12	0.06
$CH_4 + H_2$	0.02				
C_2H_4	0.36				
C_2H_6	0.02		0.39	0.59	0.45

[a] Cr^+ and Mn^+ do not react at all with alkanes. [b] Ion cyclotron resonance data from ref 3a. [c] Data from ref 1c.

The energetics of a proposed mechanism for the formation of $Sc(CH_3)_2^+$ from reaction of Sc^+ with *n*-butane are indicated in Figure 3. The energies of the reaction intermediates were obtained from estimates given in the Appendix. Sc^+ may initially insert into either a C–C or a C–H bond (on energetic grounds). With *n*-butane, the most straightforward route to $Sc(CH_3)_2^+$ involves insertion into a terminal C–C bond, followed by β-methyl transfer and subsequent loss of ethylene. Alternatively, insertion into a secondary C–H bond may be followed by β-methyl transfer and subsequent olefin insertion into the scandium hydrogen bond to give intermediate IV. This sequence also accommodates the formation of $Sc(CH_3)_2^+$ from isobutane. We have previously suggested β-alkyl transfer reactions to explain product distributions for the reactions of Fe^+ with labeled hydrocarbons.[1c] The processes suggested in the above mechanism are well documented in condensed phase studies of organometallic reactions.[22] In particular, facile olefin insertions into Cp_2^*Sc-H have been observed recently.[23]

The mechanism in Figure 3 predicts that $Sc(CD_3)_2^+$ would be the only dimethyl product formed in the reaction of Sc^+ with butane-*1,1,1,4,4,4-d₆*. As seen in Table II, $Sc(CD_3)_2^+$ is indeed the main dimethyl product, but some deuterium scrambling is also observed. This can be explained by assuming that both olefin insertion and β-hydrogen transfer are reversible in the mechanism of Figure 3.
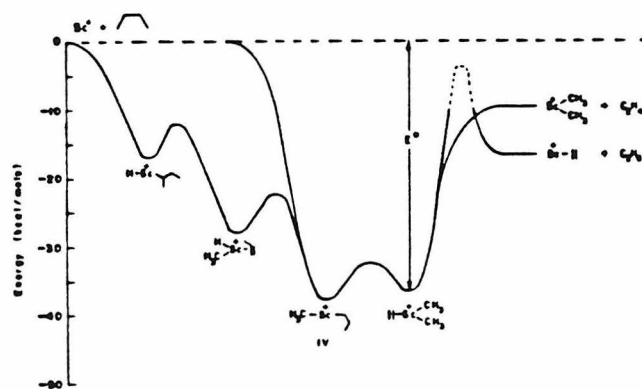

Figure 3. Simplified potential energy diagram for the reaction of Sc^+ with *n*-butane to form the products $Sc(CH_3)_2^+$ and $Sc(C_2H_4)^+$.

An observation deserving attention is the absence of major products analogous to I, namely ScH_2^+ and $HScCH_3^+$, which might be formed in the reaction of Sc^+ with ethane and propane, respectively. A general intermediate (V) for the formation of these three products is $R_1R_2Sc(C_2H_4)^+$, shown in Figure 4. The decomposition products that result from loss of ethylene are shown on the left, and those that result from reductive elimination of R_1R_2 are shown on the right. The energies of these products relative to V are obtained by using the bond energies and heats of formation estimated in the Appendix. The total amount of internal energy available to V for decomposition is indicated by ϵ^* (alkane) for the three cases. With propane and ethane, V does not have sufficient internal energy to lose ethylene in an exothermic process. Therefore, the only exothermic reaction products are those corresponding to reductive elimination of R_1R_2. In the reaction with butane, however, intermediate V has sufficient energy to render the formation of *both* decomposition products exothermic. Although the energy of $Sc(C_2H_4)^+$ is estimated to be lower than the energy of $Sc(CH_3)_2^+$ by 7 kcal/mol, the latter is the favored product by a factor of 20 at low relative kinetic energy. This suggests that there must be an activation barrier of at least 7 kcal/mol for the reverse process (oxidative addition of the C–C bond of ethane by $ScC_2H_4^+$).[24]

It is interesting to note that small amounts of $ScHCH_3^+$ and ScH_2^+ are formed in endothermic reactions of Sc^+ with propane and ethane, respectively. Ther reaction cross sections are too small to determine accurate thresholds for these processes. The formation of $ScHCH_3^+$ from propane appears to be endothermic by approximately 0.5 ± 0.5 eV and the formation of ScH_2^+ from ethane endothermic by 1-2 eV. These results are in qualitative agreement with the potential energy diagram shown in Figure 4.
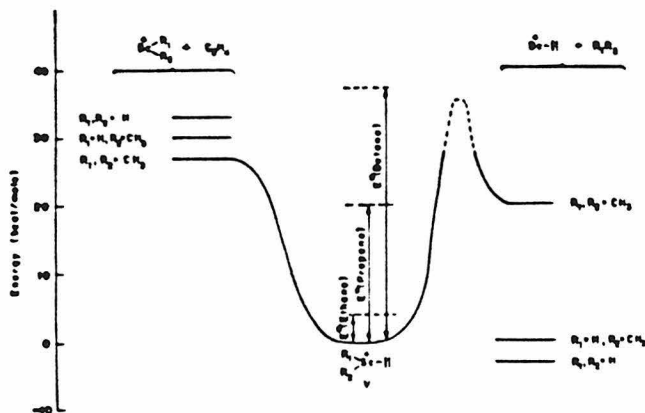

Figure 4. Simplified potential energy diagram for the decomposition of $R_1R_2Sc(C_2H_4)^+$ to form $Sc(R_1R_2)^+$ or $Sc(C_2H_4)^+$. The curve is drawn for the decomposition of $(CH_3)_2Sc(C_2H_4)^+$ formed in the reaction of Sc^+ with *n*-butane.

It is also interesting to note the relative ordering of the activation barriers for reductive elimination of R_1R_2. If the dehydrogenation of ethane proceeds via intermediate V, then the activation energy for reductive elimination of H_2 must be less than 4 kcal/mol.[25] The activation barrier for reductive elimination of CH_4 from V can be bracketed betwen 0 and 20 kcal/mol, whereas that for elimination of C_2H_6 is greater than 27 kcal/mol. This in in qualitative agreement with condensed phase studies of reductive elimination at transition-metal centers, where it has been noted that dialkyl complexes are much more stable than dihydro- and hydridoalkyl complexes.[26,27]

As stated previously, the formation of a dimethyl species is not observed in the reactions of the group 8 transition-metal ions with n-butane. This indicates that the potential energy diagrams for decomposition of intermediates analogous to V must be substantially different than that shown in Figure 4 for Sc^+. There are a number of possible explanations for this behavior. The strength of the second σ-bond in group 8 metals might be less than in Sc^+ due to the electron exchange energy lost in forming a second bond. Reactions with group 8 metal ions which lead to the formation of dialkyl products would therefore be less energetically favorable and perhaps even endothermic. An unusually low olefin bond strength to Sc^+ might also be responsible for the unique behavior observed. The absence of additional d electrons available for back-donation in Sc(III) complexes is probably responsible for a weak scandium–ethylene bond in reaction intermediates such as V. In the reductive-elimination reaction of V, the ethylene bond may remain quite weak until the reaction is near completion. This could be the reason for an activation barrier in the exit channel for reductive elimination of ethane from V as shown in Figure 4. The ethylene bond to Sc(I) may also be weaker than those to other transition metals, rendering reductive elimination of ethane less energetically favorable for V than for the analogous group 8 intermediates.

The reactions of Sc^+ with larger alkanes result in the abundant formation of products of the general composition $Sc(C_nH_{2n+2})^+$. These products are postulated to be dialkyl species which are formed by mechanisms similar to those proposed for the formation of $Sc(CH_3)_2^+$ from n-butane. In intermediates analogous to V the favored decomposition pathway is loss of ethylene to form the dialkyl species, presumably for the same reasons as discussed above for n-butane.

Dehydrogenation of Alkanes by Sc⁺. The first-row group 8 transition-metal ions have been found to dehydrogenate alkanes in a highly specific manner.[1c] Dehydrogenation of small alkanes (propane, isobutane) proceeds exclusively by a 1,2-elimination process at Fe^+, Co^+, and Ni^+ centers. The suggested mechanism involves insertion of M^+ into a C–H bond, followed by β-hydrogen transfer and reductive elimination of H_2. The final product is thus an olefin bound to the metal center. The dehydrogenation of larger linear alkanes by Ni^+ was found to proceed exclusively via a 1,4-elimination,[4] yielding a bis(olefin) complex. Iron and cobalt ions were observed to dehydrogenate larger alkanes by both a 1,2- and 1,4-elimination process.

In marked contrast to the group 8 metal ions, Sc^+ appears to dehydrogenate alkanes via predominantly 1,3-elimination (see Table II). A straightforward explanation for the observed product distributions might simply be that insertion into C–H bonds is relatively nondiscriminatory and a 1,3-elimination process occurs whenever possible. For example, in the reaction of Sc^+ with butane-*1,1,1,4,4,4-d₆*, insertion into any of the C–H (or C–D) bonds can lead to 1,3-elimination due to the availability of γ-hydrogens. In fact, the overwhelming dehydrogenation reaction is loss of HD, supporting this conjecture. However, in the reactions of Sc^+ with propane-*2,2-d₂* and 2-methyl-propane-*2-d₁*, only initial insertion into a terminal C–H bond can lead to 1,3-elimination. Thus, for these cases, both 1,2- and 1,3-elimination processes are observed.[28] Further evidence for a unique 1,3-elimination mechanism is the fact that Sc^+ cleanly dehydrogenates neopentane,[29] a reaction that is not observed for the first-row group 8 metal ions.[1b] Following insertion into a C–H bond in neopentane only α- and γ-hydrogens are available. On the basis of the above results for labeled alkanes, a 1,3-elimination mechanism is likely.

A comparison of the energetics for 1,2- and 1,3-dehydrogenation of *n*-butane is given in Figure 5. A 1,3-mechanism is suggested in which initial insertion into a C–H bond is followed by a four-center process leading to metallacyclobutane[30] formation (Figure 5). A concerted mechanism may be required in order that scandium remains in a favorable oxidation state during the course of the reaction. The thermochemical estimates predict that although both dehydrogenation pathways are exothermic overall, the metallacycle is preferred by $\sim$13 kcal/mol. The failure of 1,2-elimination to compete with the 1,3-process indicates that formation of the metallacycle may also be kinetically preferred. The potential energy curve shown in Figure 5 for 1,2-elimination illustrates a two-step mechanism, where β-hydrogen transfer is followed by reductive elimination of H_2. The activation barrier for reductive elimination of H_2 from intermediate V was previously shown to be quite small. Hence, we suggest that the β-hydrogen transfer process is energetically unfavorable. An alternative mechanism is a one-step β-hydrogen elimination process proceeding via a strained four-center transition state. In either case, a prohibitive activation barrier must exist in order to explain the absence of 1,2-elimination products from reaction with *n*-butane.
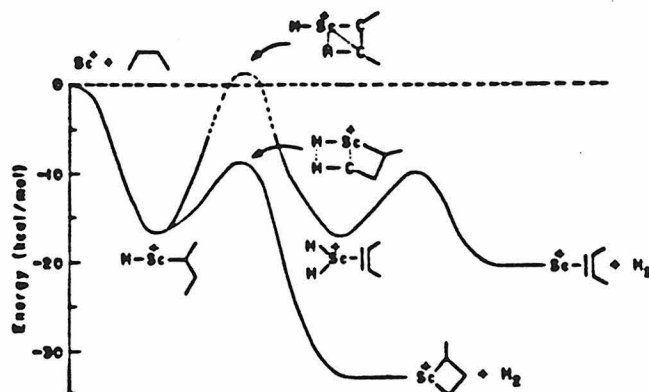
Figure 5. Simplified potential energy diagram for 1,2- and 1,3-dehydrogenation of *n*-butane by Sc⁺.

Appendix

Thermochemical Estimates for Reaction Intermediates and Products. Although we have measured several Sc⁺-ligand bond dissociation energies, there are others which have not been measured. We have estimated these energies by comparison with other systems. The errors that this introduces in the thermochemical estimates probably do not affect the general trends discussed in the text. The thermochemical values used for constructing Figures 3–5 are listed in Table IV. The assumptions that were used in assigning these values are discussed below.

The hydrogen and methyl bond strengths used for the first σ-bond to Sc⁺ are $D^\circ(Sc^+-H) = 54 \pm 4$ kcal/mol and $D^\circ(Sc^+-CH_3) = 65 \pm 5$ kcal/mol. As discussed previously, the second Sc⁺ bond to hydrogen was found to be greater than 50 kcal/mol, and thus we have assigned $D^\circ(ScH^+-H) = 54 \pm 4$ kcal/mol. The second methyl bond in $Sc(CH_3)_2^+$ is known to be greater than 50 kcal/mol because it is formed in an exothermic reaction with isobutane. It is expected that the polarizable first methyl group in $Sc(CH_3)_2^+$ causes a slight delocalization of the charge on Sc⁺, rendering the strength of the second methyl bond less than that of the first. This affect will be less pronounced if the first methyl group is replaced by a hydrogen as in $ScH(CH_3)^+$. Thus, the second σ-methyl bond strengths are estimated to be $D^\circ(ScCH_3^+-CH_3) = 57 \pm 5$ kcal/mol and $D^\circ(ScH^+-CH_3) = 61 \pm 5$ kcal/mol.

The strength of the olefin bond to Sc^+ has not be measured. We have estimated this bond strength by comparison to other metal–olefin bonds. For example, the metal–ethylene bonds in two Ni^+ compounds are estimated to be $D°(CpNi^+–C_2H_4) = 38 \pm 5$ kcal/mol[31] and $D°(Ni^+–C_2H_4) = 50$ kcal/mol,[4] although the latter is probably on the high side. For lithium ions, where no electrons are available for back-donation, the bond to ethylene is much weaker, $D°(Li^+–C_2H_4) = 18 \pm 5$ kcal/mol.[32] The bond to ethylene in Sc(I) was shown above to be greater than 33 kcal/mol from the exothermic reaction of Sc^+ with ethane. Therefore, we have assigned this bond strength a value of $D°(Sc^+–C_2H_4) = 40 \pm 5$ kcal/mol. In Sc(III) complexes where no electrons are available for back-donation, we have assigned $D°(ScR_1R_2^+–C_2H_4) = 30 \pm 5$ kcal/mol for $R_1 = H$, $R_2 = CH_3$. If R_1 and R_2 are both methyl groups, the ethylene bond will be somewhat weaker (as in the case of $CpNi^+$ compared to Ni^+) and, if R_1 and R_2 are hydrogens, the ethylene bond somewhat stronger. We have assigned the olefin bonds to be 3 kcal/mol weaker or stronger for the two cases, respectively.

Table IV. Thermochemical Estimates for Sc^+ Reaction Intermediates and Products

intermediate or product	sum of bond energies[a]	ΔH_f[b]
H—Sc⁺—H	108 ± 7	238 ± 7
H—Sc⁺—CH₃	115 ± 6	214 ± 6
H—Sc⁺—C₂H₅	115 ± 6	205 ± 6
CH₃—Sc⁺—CH₃	122 ± 7	189 ± 7
H—Sc⁺—CH(CH₃)(C₂H₅)	115 ± 6	195 ± 6
CH₃—Sc⁺—C₃H₇	122 ± 7	174 ± 7
‖—Sc⁺(H)(H)	141 ± 8	218 ± 8
‖—Sc⁺(H)(CH₃)	145 ± 8	197 ± 8
‖—Sc⁺(CH₃)(CH₃)	149 ± 9	175 ± 9
(propylene)‖—Sc⁺(CH₃)(H)	150 ± 8[c]	184 ± 8
(butene)‖—Sc⁺(H)(H)	148 ± 9[c]	195 ± 9
Sc⁺—‖	40 ± 5	215 ± 5
Sc⁺—‖ (propylene)	48 ± 5[d]	191 ± 5
Sc⁺ metallacycle	122 ± 7	179 ± 7[e]

[a] All values in kcal/mol. [b] $\Delta H_f(Sc^+) = 242$ kcal/mol from ref 33. $\Delta H_f(CH_3) = 35.1$ kcal/mol and $\Delta H_f(C_2H_5) = 25.9$ kcal/mol from ref 34. Auxiliary heats of formation are taken from ref 11. [c] The strengths of the bonds to propylene and butene in Sc(III) complexes were estimated to be 35 and 40 kcal/mol, respectively, on the basis of trends seen for Li^+ in ref 32. [d] The strength of the Sc^+ bond to butene was estimated to be 48 kcal/mol on the basis of trends seen in ref 31 and 32. [e] The following assumptions were used in estimating the heat of formation of this compound. (1) There is no strain energy involved in forming the metallacycle as suggested in ref 30b. (2) The primary and secondary C–H bond strengths in n-butane are 98 and 95 kcal/mol, respectively.

(1) (a) Armentrout, P. B.; Beauchamp, J. L. *J. Am. Chem. Soc.* **1981**, *103*, 784. (b) Halle, L. F.; Armentrout, P. B.; Beauchamp, J. L. *Organometallics* **1982**, *1*, 963. (c) Houriet, R.; Halle, L. F.; Beauchamp, J. L. *Organometallics* **1983**, *2*, 1818.

(2) (a) Allison, J.; Freas, R. B.; Ridge, D. P. *J. Am. Chem. Soc.* **1979**, *101*, 1332. (b) Freas, R. B.; Ridge, D. P. *J. Am. Chem. Soc.* **1980**, *102*, 7129.

(3) (a) Byrd, G. D.; Burnier, R. C.; Freiser, B. S. *J. Am. Chem. Soc.* **1982**, *104*, 3565. (b) Jacobson, D. B.; Freiser, B. S. *J. Am. Chem. Soc.* **1983**, *105*, 5197.

(4) Halle, L. F.; Houriet, R.; Kappes, M. M.; Staley, R. H.; Beauchamp, J. L. *J. Am. Chem. Soc.* **1982**, *104*, 6293.

(5) Moore, C. E. "Atomic Energy Levels"; National Bureau of Standards: Washington, DC, 1949.

(6) Armentrout, P. B.; Halle, L. F.; Beauchamp, J. L. *J. Am. Chem. Soc.* **1981**, *103*, 6501.

(7) (a) Armentrout, P. B.; Beauchamp, J. L. *Chem. Phys.* **1980**, *50*, 21. (b) Armentrout, P. B.; Beauchamp, J. L. *J. Chem. Phys.* **1981**, *74*, 2819.

(8) (a) Armentrout, P. B.; Beauchamp, J. L. *Chem. Phys.* **1980**, *48*, 315. (b) Armentrout, P. B.; Beauchamp, J. L. *Chem. Phys.* **1980**, *50*, 37. The fitting parameters used in the threshold region as defined in the above references are $E_0 = 2.15$ eV and $\sigma_0 = 4.3$ Å^2.

(9) Darwent, B. de B. *Natl. Stand. Ref. Data Ser. (U.S., Natl. Bur. Stand.)*, **1970**, *NSRDS-NBS 31*.

(10) Armentrout, P. B.; Beauchamp, J. L. *J. Chem. Phys.* **1981**, *74*, 2819. The fitting parameters, defined in the above reference, are $n = 4$, $E_0 = 1.08$, $\sigma_0 = 3.5$ Å^2, and $a = 0.73$. When the parameters $n = 3$ and $n = 5$ were used, the best fit obtained resulted in values for E_0 of 1.3 eV and 0.79 eV, respectively. The curves obtained using $n = 3$ and $n = 5$ clearly did not fit the data. The energies obtained from these fits were used to determine the error estimate for the Sc^+-CH_3 bond energy.

(11) Auxiliary heats of formation are taken from: Cox, J. D.; Pilcher, G. "Thermochemistry of Organic and Organometallic Compounds"; Academic Press: New York, 1970.

(12) The identity of these products was confirmed by using propane-d_8. Although the same products appeared in both cases, the product distributions were somewhat different. For example, the double dehydrogenation product formed in reaction 7 using propane-d_8 constituted 41% of the total observed products.

(13) At high energies, not all of the reaction products were monitored. The products pertinent to the discussion in the text are shown in Figure 2.

(14) (a) Burnier, R. C.; Byrd, G. D.; Freiser, B. S. *J. Am. Chem. Soc.* **1981**, *103*, 4360. (b) Halle, L. F.; Crowe, W. E.; Armentrout, P. B.; Beauchamp, J. L., submitted for publication in *Organometallics*.

(15) The identity of the product formed in reaction 16 was checked by using CD$_3$CDO.

(16) Murad, E. *J. Geophys. Res.* **1978**, *83*, 5525.

(17) Similar processes have been observed for neutral scandium atoms reacting with acetone and acetaldehyde: Liu, K.; Parson, J. M. *J. Phys. Chem.* **1979**, *83*, 970. From the internal state distributions they concluded that the neutrals lost were carbenes. When $\Delta H_f[(CH_3)_2C] = 62.5$ kcal/mol and $\Delta H_f[CH_3CH] = 77.5$ kcal/mol, calculated from this reference, were used, formation of dimethylcarbene and methylcarbene in reactions 15 and 16 would be endothermic by 15 and 18 kcal/mol, respectively.

(18) Mandich, M. L.; Halle, L. F.; Beauchamp, J. L. *J. Am. Chem. Soc.* **1984**, *106*, 4403.

(19) Schilling, J. B.; Goddard, W. A., III, unpublished results.

(20) The proton affinity of metal atoms can be calculated by using the method described in ref 1a, with supplemental data from ref 6. See, also: Stevens, A. E.; Beauchamp, J. L. *Chem. Phys. Lett.* **1981**, *78*, 291.

(21) The formation of a similar product has recently been observed with yttrium, which is a congener of scandium In a study of the collision-induced dissociation of $Y(C_2H_6)^+$, the major reaction seen is loss of methane (Freiser, B. S., private communication). This is a commonly seen product in the dissociation of dimethyl species

(22) (a) Watson, P. L.; Roe, D. C. *J. Am. Chem. Soc.* **1982**, *104*, 6471. (b) McAlister, D. R.; Erwin. D. K.; Bercaw, J. E. *J. Am. Chem. Soc.* **1978**, *100*, 5966 (c) Theoretical study of olefin insertion reactions: Thorn, D. C.; Hoffmann, R. *J. Am. Chem. Soc.* **1978**, *100*, 2079 and references cited therein

(23) Thompson, M. E.; Bercaw, J. E. *Pure Appl. Chem.* **1984**, *56*, 1. The symbol Cp* indicates the pentamethyl cyclopentadienyl ligand.

(24) This does not necessarily imply an activation barrier of 7 kcal/mol for oxidative addition of the C—C bond in ethane by free Sc^+. Addition of ligands such as CO to Fe^+ and Co^+ has been shown to reduce the reactivity of these metal ions with hydrocarbons: Freas, R. B.; Ridge, D. P. *J. Am. Chem. Soc.* **1980**, *102*, 7129.

(25) It is likely that dehydrogenation of ethane does not proceed through intermediate V, but instead occurs directly from the more stable intermediate $HScC_2H_5^+$, via a four-center transition state. If this is the case, then the activation energy for β-hydrogen elimination must be less than 21 kcal/mol.

(26) Norton, J. *Acc. Chem. Res.* **1979**, *12*, 139.

(27) Balazs, A. C.; Johnson, K. H.; Whitesides, G. M. *J. Am. Chem. Soc.* **1982**, *21*, 2162.

(28) More 1,2-elimination is observed than would be predicted by nonselective insertion into any C—H bond. The secondary hydrogens in these compounds are more labile than the terminal hydrogens, leading to the observed nonstatistical behavior.

(29) Titanium ions have also been shown to dehydrogenate neopentane; see ref 3a. Of the second-row transition-metal ions examined thus far, Pd^+, and to a lesser extent Rh^+, also dehydrogenate neopentane (to be submitted for publication).

(30) (a) A similar mechanism has been proposed for the formation of thoracyclobutanes via γ-C—H abstraction: Bruno, J. W.; Marks, T. J. *J. Am. Chem. Soc.* **1982**, *104*, 7357. (b) Recent calculations indicate that a similar molecule, dichlorotitanacyclobutane, is a stable, planar molecule: Rappe, A. K.; Goddard, W. A., III. *J. Am. Chem. Soc.* **1982**, *104*, 297.

(31) This value was obtained by extrapolation of Cp—Ni$^+$—olefin bond strengths from Corderman, F. R. Ph.D Thesis, California Institute of Technology, Pasadena, CA, 1977.

(32) This value was obtained by extrapolation of Li$^+$—olefin bond strengths from Staley, R. H.; Beauchamp, J. L. *J. Am. Chem. Soc.* **1975**, *97*, 5920

(33) Franklin, J. L.; Dillard, J. G; Rosenstock, H. M.; Herron, J. T.; Draxl, K.; Field, F. H. "Ionization Potentials, Appearance Potentials, and Heats of Formation of Gaseous Positive Ions"; (U.S., Natl. Bur. Stand.), *NSRDS-NBS 26*, 1969.

(34) McMillen, D. F.; Golden, D. M. *Annu. Rev. Phys. Chem* **1982**, *33*, 493.